Spring 2021

Removal of Selected Organic Contaminants by Various (Nano) Adsorbent-Ultrafiltration Hybrid Systems

Sewoon Kim

REMOVAL OF SELECTED ORGANIC CONTAMINANTS BY VARIOUS (NANO) ADSORBENT-ULTRAFILTRATION HYBRID SYSTEMS

by

Sewoon Kim

Bachelor of Science
Sejong University, 2014

Master of Science in Engineering
Sejong University, 2016

Submitted in Partial Fulfillment of the Requirements

For the Degree of Doctor of Philosophy in

Civil Engineering

College of Engineering and Computing

University of South Carolina

2021

Accepted by:

Yeomin Yoon, Major Professor

Joseph R.V. Flora, Committee Member

Shamia Hoque, Committee Member

Nader Taheri-Qazvini, Committee Member

Tracey L. Weldon, Interim Vice Provost and Dean of the Graduate School

ABSTRACT

Organic contaminants, which result from overuse and discharge of dyes, pharmaceutically active compounds, personal care products, and endocrine-disrupting compounds, have been received attention as contemporary water issues. However, conventional water and/or wastewater treatment system cannot sufficiently control for these contaminants for their stability and complexity. In this study, combined novel adsorbent with ultrafiltration (UF) hybrid system (termed 'adsorbent-UF') was applied to removal selected organic contaminants. UF with upstream adsorption has positive effects on performance in terms of the removal of selected organic contaminants, separating used adsorbents and reducing foulants. Activated biochar, metal organic frameworks, and $Ti_3C_2T_X$ MXene were used as novel adsorbents for this study. For selected organic contaminants, retention and flux performance were investigated on adsorbent-UF. The adsorbent-UF system was also evaluated under various water quality such as pH, natural organic matter, and background ions for better understanding of behavior in real aquatic environments. Additionally, by comparing the performance of three adsorbent-UF and powdered activated carbon-UF system, feasibility of an adsorbent-UF was investigated as a suitable alternative technology. Consequently, property change of organic contaminants by various water quality are the key to better performance on adsorbent-UF. Also, based on these results, the adsorbent-UF can be a promising advanced water treatment technology and a realistic alternative to conventional systems.

TABLE OF CONTENTS

LIST OF TABLES

LIST OF FIGURES

CHAPTER 1

INTRODUCTION AND MOTIVATION

In recent years, an increasing number of contaminants have been found in water resources due to climate change, population growth and rapid urbanization (Kim et al. 2018). Particularly, various organic contaminants have generated widespread attention because of their potentially harmful impact on both the environment and humans. Pharmaceutically active compounds (PhACs) are one such emerging organic micropollutant, and have been increasingly detected in ground, surface, and wastewater due to discharge and overuse of agricultural applications and according to more stringent standards for human health (Wang and Wang 2018). Although PhACs have been detected at low concentrations, they are potentially very hazardous for human health because they will return to aquatic environments, and then to the water supply, through the water cycle and exert physiologically adverse effects. Natural organic matter (NOM), which is composed of a heterogeneous structural mixture of aromatic and aliphatic compounds with varying molecular sizes, exists in virtually all environmental systems (Lee et al. 2015). The presence of NOM not only results in offensive odors and taste, but also acts as a potential precursor due to complexation with organic chemicals such as PhACs (Jung et al. 2015). Also, dyes released from the textile, paper, leather, plastics, and food industries have been found in increasing concentrations in water streams (Yu et al. 2018). Due to their toxicity and high oxygen demand, residual dyes in water sources can have significant adverse effect

on human life and ecosystems, even at low concentrations. However, conventional water and wastewater treatment processes are not designed to completely degrade most these contaminants (Kim et al. 2018, Joseph et al. 2019). As a result, these can be excreted, and are thus continuously present in the environment. It is therefore necessary to study alternative water treatment systems to improve and enhance conventional technologies.

Among numerous modified processes, adsorption combined with ultrafiltration (UF) is one promising alternative water treatment system. Adsorption by porous materials is considered to be one of the most effective and simple processes for the removal of organic contaminants (Khan et al. 2013, Jiang et al. 2018). However, separating used porous materials remains a technological challenge (Löwenberg et al. 2014). UF is a low-pressure membrane process that has increasingly been applied to the removal of various organic pollutants and particles (Kim et al. 2016). Occasionally, UF exhibits unsatisfactory performance, in terms of the removal of emerging organic pollutants, due to the limited retention ability of UF membranes (Kim, Chu et al. 2018). Furthermore, membrane fouling is often caused by organic contaminants, especially NOM. UF with upstream adsorption has positive effects on performance in terms of the removal of organics, separating used adsorbents and reducing foulants such as NOM. Hence, many scientific studies have focused on UF hybrid systems coupled with adsorption (Stoquart et al. 2012). However, to date, commercialized powdered activated carbon (PAC) has been used as an adsorbent in most hybrid systems (termed a 'PAC-UF' in this paper) and the study of alternative, superior adsorbents is still required to deal with emerging organic contaminants.

Activated biochar (ABC), a promising alternative adsorbent, is derived from pyrolysis of black carbon waste biomass at relatively low temperatures in low oxygen

conditions (Chu et al. 2017, Shankar et al. 2017). ABC effectively removes various pollutants, including nutrients, heavy metals, and various CECs, from aqueous systems due to its high surface area and porous, aromatic structure (Ahmad et al. 2014, Park et al. 2017). Jung et al. reported that seven EDCs/PhACs could be adsorbed to ABC better than to commercially available PAC under various experimental conditions (Jung et al. 2013). Yao et al. found that 2 – 14% of sulfamethoxazole remained in reclaimed water transported to soil with biochar, while 60% of sulfamethoxazole was measured in leachate without biochar (Yao et al. 2012). Studies have reported that the effect of PAC on flux is still unclear in absorbent-membrane hybrid systems (Yu et al. 2014). Most studies of integrated UF and adsorption systems were conducted using PAC as absorbent, resulting in limited information on membrane fouling and water permeability within a combined UF with ABC hybrid system (termed a 'ABC-UF' in this study).

Metal organic frameworks (MOFs) are crystalline porous materials that consist of inorganic components, such as metal ion clusters, and organic components such as ligands. Due to their tunability and high porosity, the presence of coordinatively unsaturated sites, and varying pore architecture and composition, MOFs have an abundance of applications, for example in catalysis (Ma et al. 2010, Huang et al. 2017), separation (Seo et al. 2000, Rodenas et al. 2015), drug delivery (Zheng et al. 2016, Wu and Yang 2017), and gas storage (Xia et al. 2015, Yoo et al. 2020). Furthermore, recently, MOFs have been studied as potential adsorbents for eliminating various water pollutants, such as dyes (Haque et al. 2010, Wang et al. 2015), heavy metals (Ke et al. 2011, Zhu et al. 2012), and organic contaminants (Hasan et al. 2012, Hasan et al. 2016). Nevertheless, research on MOFs lacks diversity. For example, there have been no studies on hybrid MOF systems with UF

(termed 'MOF-UF' in this paper). In particular, there have been no performance evaluations of the retention rates of micropollutants and NOM, or of the permeate flux in MOF-UF hybrid systems.

MXenes are a relatively new family of multilayered two-dimensional transition metal carbides, which have been evaluated for use in a number of applications including energy storage, transparent conductive electrodes, and water purification (Lukatskaya et al. 2013, Jun et al. 2019). In particular, some studies have demonstrated that a range of pollutants for water treatment are effectively removed by MXenes used as adsorbents, because of their excellent stability, superior oxidation resistance, fine structure and high electrical/metallic conductivity (Peng et al. 2019, Wang et al. 2019). For example, Peng et al. reported 95% lead (C_0 = 50 mg/L) removal efficiency using 0.025 g/50 mL of MXene (Peng et al. 2014). Wang et al. (Wang, Song et al. 2019) and Meng et al. (Meng et al. 2018) reported 95% Re(VII) (C_0 = 10 mg/L) and 80% urea (C_0 = 30 mg/L) removal with 8 mg/20 mL and 0.155 g/6 mL of MXene, respectively. Another study indicated that 100 mg/100 mL of MXene resulted in 40% methylene blue (MB) removal (C_0 = 0.05 mg/mL) (Mashtalir et al. 2014). While these reports indicate that MXenes are attractive materials for removal of contaminants in water treatment processes, most studies have focused on the use of MXene in adsorption processes. In addition, although these studies demonstrated high removal rates, the MXene dosages were unrealistically high for use in a real water treatment plant. Therefore, there is still a requirement for study into the application of MXenes in real water treatment systems, such as the potential for combining MXenes with a UF hybrid system (termed 'MXene-UF' in this paper).

Therefore, the main purpose of this study was to investigate the feasibility of ABC-UF, MOF-UF, and MXene-UF to treat organic contaminants. The retention variation and permeate flux were observed under various pH conditions, where the physicochemical properties of those contaminants (*e.g.*, charge and hydrophobicity) vary significantly. Also, for better understanding of its application in a real water treatment system, these three adsorbent-UF were evaluated under a range of conditions with various water qualities with regard to permeate flux and retention rate. Furthermore, these adsorbent-UF compared the results to those obtained with a single UF and with the PAC-UF. Finally, retention and fouling mechanism in the adsorbent-UF were analyzed via a resistance-in-series model, permeate flux modeling, and four conceptual blocking law models.

CHAPTER 2

OBJECTIVES AND SCOPE

Ultrafiltration (UF) has numerous advantages, such as relatively low energy consumption, competitive cost, and ease of operation. However, in UF systems, membrane fouling is still an unresolved problem and the removal efficiency is low in comparison to high-pressure membrane technologies, such as reverse osmosis and nanofiltration. To overcome these disadvantages of UF systems, hybrid system, surface modification, and multi-step membrane processes have been studied. Especially, adsorption is generally applied as a pretreatment to the UF system, due to simple operation, relatively low cost, and effective elimination of organic compounds. The combination of UF with commercial powdered activated carbon (PAC) for removal of CECs has been studied. However, to date, PAC has been used as an adsorbent in most hybrid systems and the study of alternative, superior next generation adsorbents is still required to deal with emerging organic contaminants. Therefore, four objectives were set to this study as follow:

The first objective is to review and summarize the recent progress on the removal of organic contaminants by membrane in water and wastewater. Several key parameters, including the physicochemical properties of organic contaminants, water quality conditions, and membrane properties and operating conditions will be reviewed to address influence the removal of organic contaminants during membrane filtration.

The second objective was to evaluate the removal of selected organic contaminants like PhACs, ibuprofen (IBP), 17α-ethinyl estradiol (EE2), and carbamazepine (CBM) using an activated biochar-ultrafiltration hybrid system (ABC-UF) in presence or absence of natural organic matter (NOM). Also, the performance of ABC-UF was compared with UF only and commercially powdered carbon-ultrafiltration hybrid system (PAC-UF).

The third objective was to investigate the removal of selected organic contaminants like PhACs (IBP and EE2) and natural organic matter (NOM) (humic acid (HA) and tannic acid (TA) in three different ratios) using a metal organic framework-ultrafiltration hybrid system (MOF-UF). The removal and filtration experiments for selected organic contaminants were evaluated and compared the results to those obtained with a single UF, and with the PAC-UF.

The fourth objective of the proposed research was to apply MXene-UF for removal of cationic (methylene blue; MB) and anionic (Methyl orange; MO) dyes as selected organic contaminants. The permeate flux and retention variation was observed as a function of a volume concentration factor (VCF) in the single UF system, MXene-UF, and PAC-UF. Additionally, in hybrid system, whether MXene and PAC can play a role for fouling was studied via resistance-in-series model, flux modeling, and four conceptual blocking law models.

Intellectual merit and major outcome. The proposed research was developed the scientific base for the removal of organic contaminants by adsorbents-UF hybrid system. Determination of the optimum hybrid system condition for each contaminant with different adsorbents allows achievement of higher removal efficiency and flux. These researches

will be more practical with the application of real contaminated water to understand adsorbents-ultrafiltration hybrid system in the real field. The overall research scopes and relationship among each chapter are outlined in Figure 2.1.

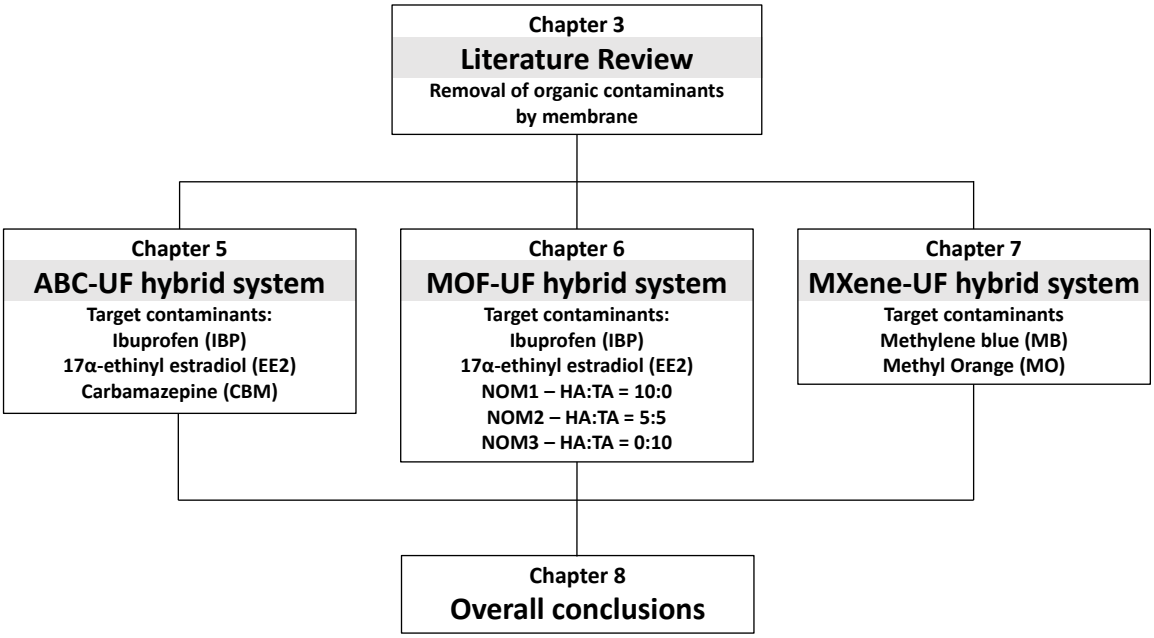

Figure 2.1 The diagram presenting dissertation outline.

CHAPTER 3

REMOVAL OF CONTAMINANTS OF EMERGING CONCERN BY MEMBRANES IN WATER AND WASTEWATER: A REVIEW[1]

Abstract

This review summarizes comprehensive recent studies on the removal of contaminants of emerging concern (CECs) by forward osmosis (FO), reverse osmosis (RO), nanofiltration (NF), and ultrafiltration (UF) membrane treatments, and describes important information on the applications of FO, RO, NF, and UF membranes in water and wastewater (WW) treatment. The main objective of this review was to synthesize findings on membrane treatments of CECs in water and WW, and to highlight upcoming research areas based on knowledge gaps. In particular, this review aimed to address several key parameters, including the physicochemical properties of CECs (solute molecular weight/size/geometry, charge, and hydrophobicity), water quality conditions (pH, solute concentration, temperature, background inorganics, and natural organic matter), and membrane properties and operating conditions (membrane fouling, membrane pore size, porosity, charge, and pressure) that influence the removal of CECs during membrane filtration. Future research directions regarding membrane treatment for the removal of CECs from water and WW are also discussed.

---

[1] Reprinted here with permission of publisher: Sewoon Kim *et al.*, Removal of contaminants of emerging concern by membranes in water and wastewater: A review. Chemical Engineering Journal 335 (2018) 896-914.

3.1 Introduction

To meet the increasing demand for water due to climate change, population growth, and over-consumption, water authorities are considering and implementing water recycling schemes. The fate of contaminants of emerging concern (CECs), such as endocrine-disrupting compounds (EDCs) and pharmaceuticals (PhACs)/personal care products (PPCPs), in water resources is a matter of significant concern according to increases in the consumption of CECs and the intensity of water recycling (Al-Rifai et al. 2011). Stumm-Zollinger and Fair (1965) and Tabak and Bunch (1970) were the first to address concerns regarding the possible adverse effects of PhACs in municipal wastewater (WW), demonstrating that several steroids are unlikely to be removed by conventional WW treatment processes (Stumm-Zollinger and Fair 1965, Tabak and Bunch 1970). The United States Environmental Protection Agency (USEPA) established the Endocrine Disruptor Screening Program for EDCs in 1998, which advised that both human and wildlife influences be evaluated, and estrogen, androgen, and thyroid endpoints be examined (USEPA 2000). There is no current federal regulation for PhACs in drinking or natural water, while assessment of PhACs associated with ecological testing is required by the United States Food and Drug Administration if the environmental concentration in water is anticipated to exceed 1 µg/L (USFDA 1998). Only a few EDCs and PPCPs, including erythromycin (ETM), estrone (E1), 17b-estradiol (E2), 17a-ethinyl estradiol (EE2), and estriol (E3), are currently listed in the USEPA's Drinking Water Contaminant Candidate List 4 (USEPA 2016). The State of California has evaluated the potential influence of EDCs and PPCPs on indirect potable reuse of municipal WW effluent (Snyder et al. 2003).

The potential fate and transport of CECs in typical drinking water treatment and WW treatment processes are described in Fig. 3.1 (Park et al. 2017). Both environmental scientists and engineers need to understand the removal mechanisms of CECs to assess potential human exposure to CECs, and to design more effective and specific water and WW treatment processes. Numerous studies have revealed that conventional water treatment plants (WTPs) (Westerhoff et al. 2005, Yoon et al. 2006, Snyder et al. 2007, Yoon et al. 2007, Benotti et al. 2009) and WW treatment plants (WWTPs) (Andersen et al. 2003, Yoon et al. 2010, Ren et al. 2011, Ryu et al. 2011) incompletely remove many CECs, while advanced technologies involving activated carbon (AC), ozonation, ultraviolet (UV) irradiation, sonodegradation, and membrane filtration enhance the removal of CECs (Westerhoff, Yoon et al. 2005, Yoon, Westerhoff et al. 2006, Han et al. 2012, Jung et al. 2013, Al-Hamadani et al. 2016). Table 3.1 summarizes the estimated performances of different technologies used in both WTPs and WWTPs, based on literature reports of specific classes of compounds or similarities to other CECs that have been examined in detail. In WWTPs, it is fairly complicated to assess the various different removal mechanisms due to the physicochemical properties of CECs (e.g., hydrophobicity, pKa, size, shape, and charge) and factors associated with the WW treatment technology used (e.g., aerobic/anaerobic/anoxic biodegradation, sludge adsorption, and oxidation by O_3/chlorine) (Ryu et al. 2014). Table 3.2 summarizes the removal efficiencies for target CECs in the treatment concept, a representative sample of the existing literature concerning biodegradability, and trends regarding adsorption to sludge and oxidation by chlorination (Ryu, Oh et al. 2014).

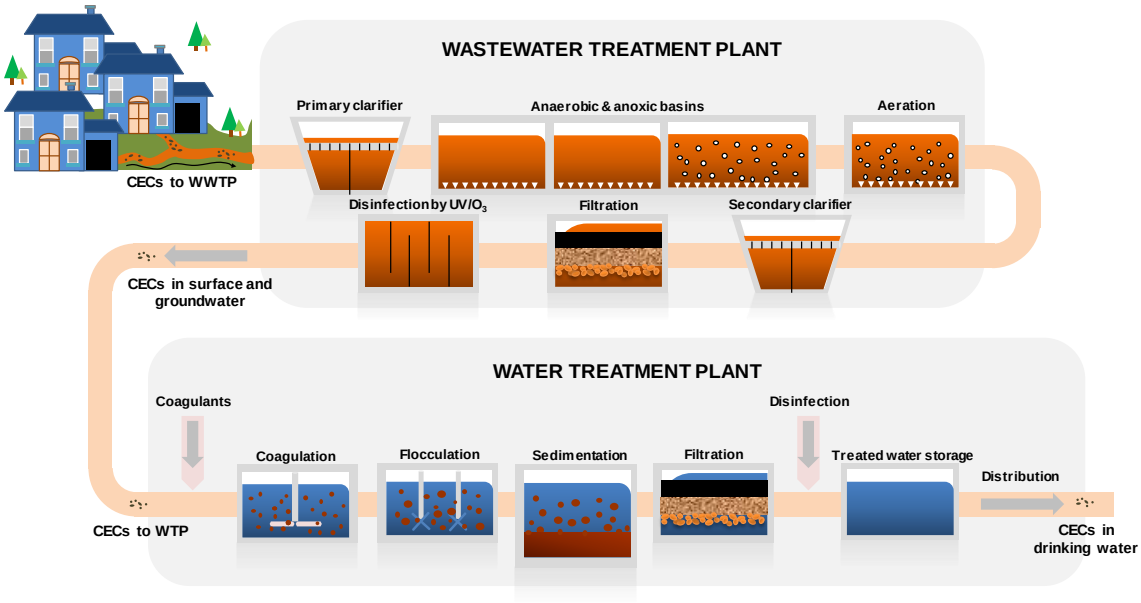

Figure 3.1 Possible fate and transport of CECs in typical drinking water treatment and WW treatment processes adopted from (Park, Chu et al. 2017).

Table 3.1 Unit processes and operations used for CEC removal.

Group	Classification	AC	BAC	O_3/ AOPs	UV	Cl_2/ ClO_2	Coagulation/ flocculation	FO	RO	NF	UF	Degradation {B/P/AS}c*
EDCs	Pesticides	E	E	L-E	E	P-E	P	F-E	E	G	P-F	E {P}
	Industrial chemicals	E	E	F-G	E	P	P-L	F-E	E	E	P-F	G- E {B}
	Steroids	E	E	E	E	E	P	F-E	E	G	P-F	L-E {B}
	Metals	G	G	P	P	P	F-G	F-E	E	G	P-F	P {B}, E {AS}
	Inorganics	P-L	F	P	P	P	P	F-E	E	G	P-F	P-L
PhACs	Antibiotics	F-G	E	L-E	F-G	P-G	P-L	F-E	E	E	P-F	E {B} G-E {P}
	Antidepressants	G-E	G-E	L-E	F-G	P-F	P-L	F-E	E	G-E	P-F	G-E
	Anti-inflammatories	E	G-E	E	E	P-F	P	F-E	E	G-E	P-F	E {B}
	Lipid regulators	E	E	E	F-G	P-F	P	F-E	E	G-E	P-F	P {B}
	X-Ray contrast media	G-E	G-E	L-E	F-G	P-F	P-L	F-E	E	G-E	P-F	E {B and P}
	Psychiatric control	G-E	G-E	L-E	F-G	P-F	P-L	F-E	E	G-E	P-F	G-E
PCPs	Synthetic scents	G-E	G-E	L-E	E	P-F	P-L	F-E	E	G-E	P-F	E {B}
	Sunscreens	G-E	G-E	L-E	F-G	P-F	P-L	F-E	E	G-E	P-F	G-E
	Antimicrobials	G-E	G-E	L-E	F-G	P-F	P-L	F-E	E	G-E	P-F	F {P}
	Surfactants/detergents	E	E	F-G	F-G	P	P-L	F-E	E	E	P-F	L-E {B}

Source: Modified from (Snyder, Westerhoff et al. 2003).
BAC = biological activated carbon; AOPs = advanced oxidation processes; *B = biodegradation, P = photodegradation, AS = activated sludge; (solar); E = excellent (> 90%), G = good (70-90%), F = fair (40-70%), L = low (20-40%), P = poor (< 20%).

Table 3.2 Removal efficiencies of selected CECs in order by log K_{OW} at WWTP under dry weather conditions with examples of previously published literature related to biodegradability, tendency of adsorption to sludge, and tendency of oxidation by chlorination.

Compound	Use	MW (g/mol)	pK_a[b]	log K_{OW}[c]	Inf. (ng/L)	Eff. (ng/L)	Rem (%)	Bio.	Ads	Oxi	Ref.
Triclocarban	Antibiotic	315.6	NA	4.90	198	33	83	L	H	NF	(Heidler et al. 2006)[B]; (Hyland et al. 2012)[A]
Gemfibrozil	Antichol-esterol	250.2	4.7	4.72	45	33	27	H	M	H	(Snyder et al. 2004)[B,A]; (Westerhoff, Yoon et al. 2005)[O]
Triclosan	Antibiotic	289.6	8 (7.9)	4.76	190	63	67	L	H	H	(Snyder, Leising et al. 2004)[B,A]; (Westerhoff, Yoon et al. 2005)[O]
Ibuprofen	Analgesic	206.1	4.5 (4.9)	3.97	2724	241	91	H	M	M	(Buser et al. 1999)[B]; (Carballa et al. 2008)[A]; (Lei and Snyder 2007)[O]
Diphenhy dramine	Antihist-amine	255.5	9.0	3.27	171	142	17	L	M	NF	(Wu et al. 2010)[B]; (Hyland, Dickenson et al. 2012)[A]
Naproxen	Analgesic	230.1	4.5 (4.2)	3.18	5113	482	91	M	M	H	(Snyder, Leising et al. 2004)[B]; (Hyland, Dickenson et al. 2012)[A]; (Lei and Snyder 2007)[O]
Benzophenone	Ultraviolet blocker	182.2	<2	3.18	88	47	47	L	M	L	(Kasprzyk-Hordern et al. 2009)[B]; (Zhang et al. 2011)[A]; (Stackelberg et al. 2007)[O]
E1	Steroid	270.4	10.3 (10.5)	3.13	ND	ND	NA	H	M	H	(Snyder, Leising et al. 2004)[B,A]; (Westerhoff, Yoon et al. 2005)[O]

Propylparaben	Preservative	180.2	8.5	3.04	520	7	99	H	H	H	(Kasprzyk-Hordern, Dinsdale et al. 2009) [B,A]; (Andersen et al. 2007)[O]
TCPP	Fire retardant	327.6	NA	2.89	585	434	26	L	L	L	(Meyer and Bester 2004)[B,A]; (Stackelberg, Gibs et al. 2007)[O]
Diltiazem	Calcium channel blockers	414.5	12.9	2.79	ND	ND	NA	M	M	L	(Domenech et al. 2011)[B]; (Blair et al. 2013)[A]; (Huerta-Fontela et al. 2011)[O]
Atrazine	Herbicide	215.1	<2 (1.6)	2.61	ND	ND	NA	L	M	L	(Snyder, Leising et al. 2004)[B,A]; (Lei and Snyder 2007)[O]
Carbamazepine	Analgesic	236.3	<2	2.45	188	156	17	L	L	H	(Clara et al. 2004)[B]; (Carballa, Fink et al. 2008)[A]; (Westerhoff, Yoon et al. 2005)[O]
DEET	Insect repellent	191.3	<2	2.18	47	46	2	M	L	L	(Snyder, Leising et al. 2004)[B,A]; (Westerhoff, Yoon et al. 2005)[O]
Simazine	Herbicide	201.7	1.62	2.18	ND	ND	NA	H	M	M	(Bueno et al. 2012)[B,A]; (Ormad et al. 2008)[O]
TCEP	Fire retardant	285.5	NA	1.44	439	348	21	L	M	L	(Meyer and Bester 2004)[B,A]; (Snyder, Leising et al. 2004)[A]; (Lei and Snyder 2007)[O]
Benzotriazole	Heterocyclic	119.2	8.2	1.44	88	47	47	M	L	L	(Reemtsma et al. 2010)[B,A]; (Sichel et al. 2011)[O]

Trimethoprim	Antibiotic	290.1	6.3, 4.0, <2 (7.1)	0.91	150	118	21	L	L	H	(Alexy et al. 2004)[B]; (Kim et al. 2005)[A]; (Westerhoff, Yoon et al. 2005)[O]
Sulfamethoxazole	Antibiotic	253.1	2.1 & <2 (5.7)	0.89	400	117	71	L	H	H	(Snyder, Leising et al. 2004)[B,A]; (Westerhoff, Yoon et al. 2005)[O]
Primidone	Anticonvulsant	218.3	11.5	0.73	100	40	60	M	L	H	(Kim et al. 2012)[B]; (Ternes et al. 2002)[A]; (Huerta-Fontela, Galceran et al. 2011)[O]
Meprobamate	Anti-anxiety	218.3	<2	0.70	ND	ND	NA	M	L	L	(Snyder, Leising et al. 2004)[B,A]; (Lei and Snyder 2007)[O]
Diclofenac	Arthritis	318.1	(4.2)	0.7	6897	359	95	L	L	H	(Buser et al. 1998)[B]; (Carballa, Fink et al. 2008)[A]; (Westerhoff, Yoon et al. 2005)[O]
Atenolol	Oral beta blocker	266.3	9.6	-0.03	1040	529	49	M	L	L	(Bueno, Gomez et al. 2012) [B,A]; (Huerta-Fontela, Galceran et al. 2011)[O]
Caffeine	Stimulant	194.2	6.1	-0.07	8810	236	97	H	H	M	(Snyder, Leising et al. 2004)[B]; (Blair, Crago et al. 2013)[A]; (Westerhoff, Yoon et al. 2005)[O]
Sucralose	Sweetener	397.6	NA	-1.00	5289	4043	24	L	L	L	(Torres et al. 2011)[B,A,O]
Acesulfame	Sugar substitute	201.2	2.0	-1.33	3863	3705	4	L	L	L	(Buerge et al. 2009) [B,A]; (Mawhinney et al. 2011)[O]

Iopromide	Contrast agent	790.9	<2 and >13	-2.10	11133	12895	-16	L	L	L	(Snyder, Leising et al. 2004)[B,A]; (Lei and Snyder 2007)[O]
Iopamidol	Contrast agent	777.1	10.7	-2.42	8518	10091	-18	L	L	NF	(Deblonde et al. 2011)[B,A]
Iohexol	Contrast agent	821. 1	11.7	-3.05	14432	16008	-11	L	L	L	(Deblonde, Cossu-Leguille et al. 2011)[B,A]

Source: Modified from (Ryu, Oh et al. 2014).

Inf. = influent; Eff. = effluent; Rem. = overall removal; Bio. = biodegradation ([B]); Ads. = adsorption to sludge ([A]); Oxi. = oxidation by chlorine ([O]); Ref. = references; H = high; M = medium; L = low; ND = not determined because under detection limit (ND values = 15 ng/L for E1, 50 ng/L for diltiazem, 5 ng/L for atrazine, 1.5 ng/L for simazine, and 0.5 ng/L for meprobamate) ; NA = not available or not applicable; NF = not found.

Membrane processes, including forward osmosis (FO), reverse osmosis (RO), nanofiltration (NF), and ultrafiltration (UF), have been widely used in water and WW treatment processes (Al-Obaidi et al. 2017, Corzo et al. 2017, Lee et al. 2017, Soriano et al. 2017). The main advantages of FO are the production of high-quality permeate due to a high removal of various CECs and the ability to operate under an osmotic driving force without requiring a hydraulic pressure difference (Cartinella et al. 2006). The permeation of CECs through RO membranes involves adsorption of the CECs onto the membrane surfaces, dissolution of the CECs into the membrane, and subsequent diffusive transport of dissolved CEC molecules through the membrane matrix (Steinle-Darling et al. 2007). While complete or near-complete removal of a wide range of CECs can also be predicted by NF membranes, the retention of CECs by NF membranes greatly depends on the physicochemical properties of CECs, which can be affected by solution chemistry (i.e., mainly by the solution pH) (Nghiem et al. 2005). UF membrane processes, used in WW reclamation and drinking water to remove CECs, were investigated via existing separation mechanisms (e.g., size/steric exclusion, hydrophobic adsorption, and electrostatic repulsion) (Yoon, Westerhoff et al. 2006, Rodriguez et al. 2016). While the majority of CECs are organic compounds, several studies have examined the transport mechanisms of toxic ions of inorganic CECs (e.g., chromate, arsenate, and perchlorate) through membranes (Yoon et al. 2009, Sanyal et al. 2015). Unlike organic CECs, the degree of removal of inorganic CECs is mainly governed by both size exclusion and electrostatic exclusion, while adsorption plays a minimal role in their removal.

While numerous studies have reported the removal of both inorganic and organic CECs by membrane treatments, a systematic understanding of the removal mechanisms

and effects of operating conditions on the transport of CECs through FO, RO, NF, and UF membranes is lacking. Therefore, a broad review of CEC removal by membrane treatment is important, since the transport of both inorganic and organic CECs by membranes is significantly affected by the unique properties of CECs, as well as water quality conditions and membrane type. The main objective of this review was to combine present findings on membrane treatments of CECs in water and WW and to highlight upcoming research areas according to knowledge gap. Particularly, this review aimed to address several key parameters, including the physicochemical properties of CECs (e.g., solute molecular weight (MW)/size/geometry, charge, and hydrophobicity), water quality conditions (e.g., pH, solute concentration, temperature, background inorganics, and natural organic matter (NOM)), and membrane properties and operating conditions (e.g., membrane fouling, membrane pore size, porosity, charge, and pressure) that influence the removal of CECs during membrane filtration.

3.2 Membrane treatment of various CECs

3.2.1 Removal by FO membranes

3.2.1.1 Effect of the physicochemical properties of CECs

The FO process uses an osmotic pressure difference caused by the concentrated draw solution (DS) to permeate water from the feed solution to the DS across the membrane, whereas RO, NF, and UF processes use a hydraulic pressure difference as the driving force to transport water through a semipermeable membrane (Cartinella, Cath et al. 2006). Thus, the transport of water through the membrane in FO is coupled with the transport of the draw solute in the opposite direction (Xie et al. 2012). The transport of 20

PhACs assessed in closed-loop FO systems weakly correlated with retention and size/MW, suggesting that, aside from steric hindrance, solute-membrane interactions also affect retention (D'Haese et al. 2013). While CEC transport and retention in FO likely share many characteristics (e.g., membrane material and pore size) with the RO and NF processes, the reverse permeation of the draw solute and high salinity of the DS may affect the retention of diverse solutes and transport mechanisms (Xie, Nghiem et al. 2012).

The bench-scale FO retention of 23 nonionic and ionic EDCs and PPCPs was 40–98%, which depended primarily on size and charge (80–98% for positively and negatively charged compounds and 40–90% for nonionic compounds) (Hancock et al. 2011), and gave rise to the following general observations: (i) relatively small compounds are able to partition into the relatively hydrophilic FO membrane and diffuse through the membrane active layer; (ii) a membrane surface fouling layer separates and hinders the interaction between hydrophobic compounds, which consequently increases retention (Nghiem et al. 2008); and (iii) the retention of charged compounds is usually high due to electrostatic interactions (i.e., repulsion) arising from the negative surface charge of the FO membrane (Verliefde et al. 2007). While the mechanism underlying the retention of positively charged compounds is somewhat unclear, a high retention of > 90% is promising (Nghiem, Schafer et al. 2005). The retention of four PhACs (carbamazepine (CBM), diclofenac (DCF), ibuprofen (IBP), and naproxen (NPX)) by FO membranes increased with increasing hydrophobicity (Jin et al. 2012), indicating that hydrophobic interactions between selected PhACs and cellulose tri-acetate (CTA) membranes may represent the dominant short-term removal mechanism (Bellona and Drewes 2005). Therefore, the relatively poor retention of NPX by FO membranes may be due to its lower affinity (lower log *D* value at pH 6 =

1.37) to the membrane polymer. However, the retention of CBM (MW = 236 g/mol) is significantly greater than that of IBP (MW = 206 g/mol) due to its relatively larger MW, while they share similar hydrophobicity (log *D* at pH 6 = 2.45 for CBM and 2.43 for IBP); this suggests that size exclusion also contributes to the retention of PhACs and that the MW of IBP may be close to the MW cut-off (MWCO) of CTA-based FO membranes.

For selected organic compounds, the average retention by FO membranes followed the order: sulfamethoxazole (SMX, 67–90%) ≈ CBM, 68–83%) >> atrazine (ATZ, 34–49%) > 4-chloraphenol (4CP, 28–39%) > phenol (PHN, 21–22%) (Heo et al. 2013). The retention of relatively large MW and negatively charged dominant compounds (CBM = 236.3 g/mol, neutral; SMX = 253.3 g/mol, negative at pH = 7.0) was approximately 70%, while that of the relatively small MW and nonionic compounds (PHN = 94.1 g/mol and 4CP = 128.6 g/mol) was inconsistent, ranging from ~20 to 35%. This is presumably due to the combined effects of the relatively small MW and low hydrophobicity of PHN and 4CP, which allow them to readily diffuse through the active layer in osmotically driven processes. In addition, the small retention of ATZ by FO membranes (vs. CBM and SMX) could be attributed to its lower affinity for the membrane polymer and size exclusion contributions, because the MW of ATZ (215.7 g/mol) is relatively less than that of CBM, while they are comparably hydrophobic (Heo, Boateng et al. 2013).

Retention of > 99% was achieved for various heavy metal ions (e.g., As, Cd, Cr, Cu, Hg, and Pb) under FO processes (Cui et al. 2014). The very high retention of heavy metal ions under FO could be attributed to several factors: (i) the key mechanism for heavy metal transport across the FO membrane is solution-diffusion, since the influence of convective flow is minor for heavy metal transport in the FO process; therefore, heavy

metal ions with larger hydration radii are removed readily because diffusivity decreases with increasing hydrated radius and (ii) the Donnan equilibrium effect could hinder the degree of ionic permeation of the feed ions due to the presence of highly concentrated bulk DSs across the active layer (Hancock et al. 2011).

3.2.1.2 Effect of water quality conditions

The retention of tract PhACs (metoprolol (MTP), SMX, and triclosan (TCS)) is pH-independent of the modified FO membrane by integrating nano-TiO_2 (Huang et al. 2015), as follows: (i) the degree of retention of MTP (positively charged) is lower than that of TCS (neutral) and SMX (negatively charged), mainly due to electrostatic interactions between the compounds and the negatively charged membrane; (ii) the retention of SMX increased with increasing pH, since the speciation of SMX from a neutral species at $pKa_1 < pH < pKa_2$ to a negatively charged entity at $pH > pKa_2$ results in pH-dependent behavior; and (iii) upon comparing the performance of pristine and modified membranes at an average retention value, the performance of the modified membrane was better than that of the pristine membrane. The negatively charged/ relatively hydrophilic FO CTA membrane enhanced the retention of E1 and E2 (i.e., undissociated/uncharged hormones at the feed solution pH 6.5) in the presence of an anionic surfactant (sodium cocoyl N-methyl taurate) (Cartinella, Cath et al. 2006). Given these conditions and properties, it is hypothesized that hydrophobic attractions occur between the surfactant tail and the membrane surface, resulting in adsorption of individual surfactant molecules to the membrane (Childress and Elimelech 2000). Two mechanisms may enhance hormone transport by the FO membrane in the presence of anionic surfactants: (i) a small amount of hormones are available for adsorption onto the membrane because they are adsorbed onto the hydrocarbon chains of

the micelles in the bulk feed solution, and (ii) the anionic surfactant adsorbs to the membrane surface due to hydrophobic interactions and enhances resistance to hormone transport by hindering hormone adsorption to the membrane (Cartinella, Cath et al. 2006).

The effects of organic fouling on CEC retention depend on the foulants. When the FO membrane was fouled by alginate, the retention of some PhACs (e.g., SMX and NPX) was significantly lower, whereas the change in retention was negligible for the majority of the 20 tested PhACs (D'Haese, Le-Clech et al. 2013). This result is presumably due to alginate forming a cake that is somewhat porous in comparison with the FO membrane, therefore only slightly contributing to PhAC retention. Hindered PhAC diffusion back to the bulk feed solution within the foulant layer results in cake-enhanced concentration polarization, which causes low apparent retention (Ng and Elimelech 2004). Therefore, decreases in the retention of CECs by fouled FO membranes could exert a substantial influence in closed-loop FO applications. In a separate study, the presence of humic acid (HA) increased the retention of SMX for pristine and modified FO-TiO_2 membranes (Huang, Chen et al. 2015), by shielding the membrane surface charge (Xie et al. 2013). However, no substantial effect on the retention of TCS was observed for neutral TCS, since the degree of permeation of TCS was considered in the absence of electrostatic interactions. The presence of HA resulted in a decrease in the retention of MTP for both pristine and modified FO membranes (Huang, Chen et al. 2015), since positively charged MTP at pH 7 was enriched on the HA layer and readily diffused through the membrane barrier to the permeate side (Yangali-Quintanilla et al. 2009). In a separate study on 32 EDCs and PPCPs, the retention of negatively charged EDCs and PPCPs positively correlated with increasing MW and retention, as shown in Fig. 3.2 (Coday et al. 2014). Negatively charged

compounds were also more easily retained by the FO membrane due to electrostatic repulsion by the negatively charged membrane surface. The retention of nonionic compounds decreased in all but two cases, as proposed by Linares et al. (Linares et al. 2011), while the retention of hydrophobic nonionic compounds varied significantly.

A lab-scale FO system was employed to evaluate the performances of thin-film inorganic FO membranes for the retention of several heavy metals (Cd, Cu, Pb, and Zn) at a range of DS concentrations (0.5–2.0 mol/L NaCl) and initial FS concentrations (50–1,000 mg/L) of heavy metal ions (You et al. 2017). The thin-film inorganic membrane was proficient at removing heavy metal ions, with an average retention efficiency of approximately 95%. The retention of heavy metals was less dependent on the DS concentration applied. The retention efficiency decreased from 95% to less than 85% with an increase in the initial concentration of the heavy metal (50–1,000 mg/L), which was likely because the increasing FS concentration enhanced the diffusion of heavy metal ions across the membrane (You, Lu et al. 2017).

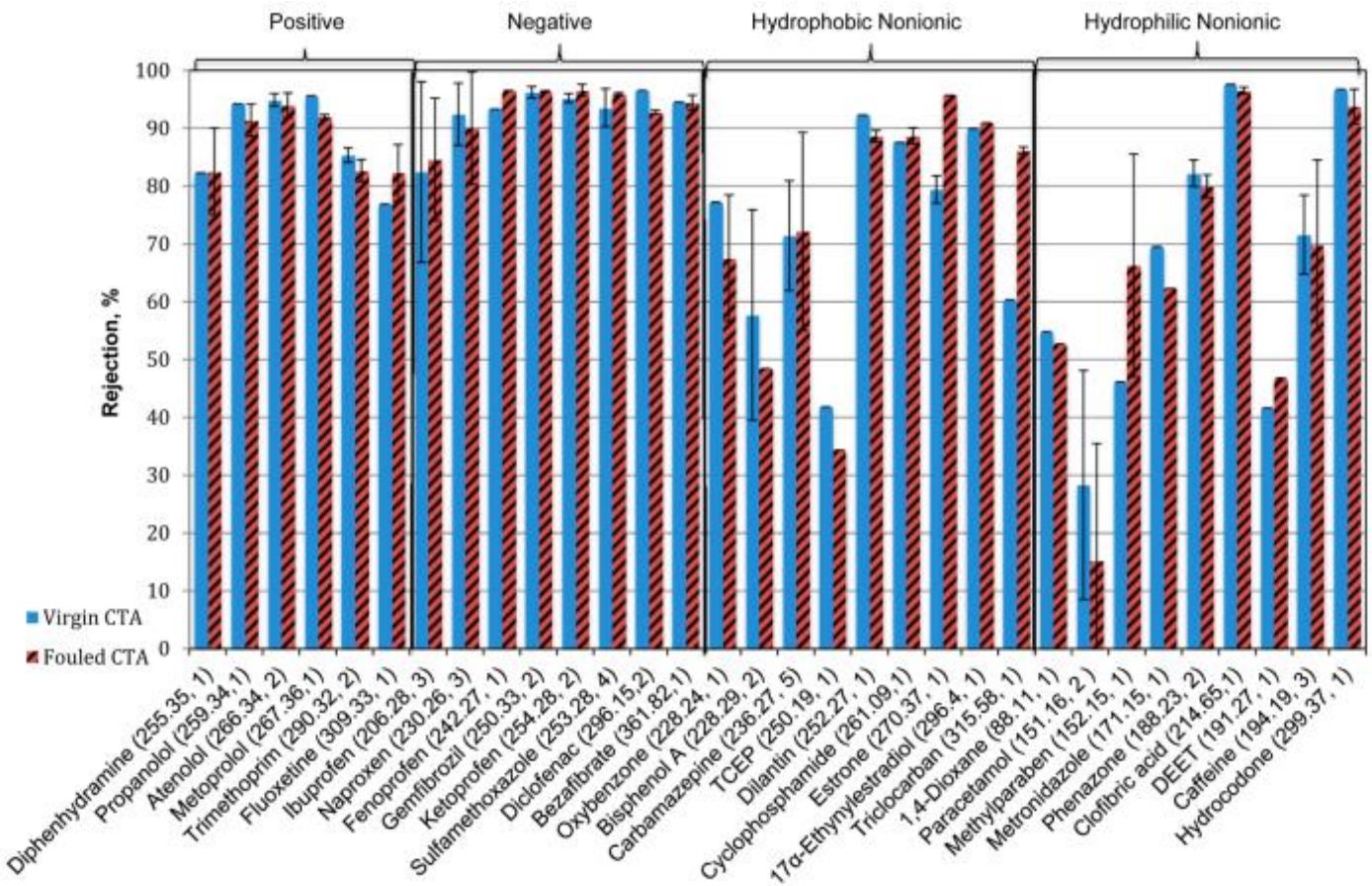

Figure. 3.2 Average retention of EDCs and PPCPs by virgin and fouled FO CTA membranes tested at the bench scale adopted from (Coday, Yaffe et al. 2014).

3.2.1.3 Effect of membrane properties and operating conditions

In addition to the physicochemical characteristics of CECs and water chemistry conditions, CEC retention is also influenced by membrane properties (e.g., charge, hydrophobicity, structure, and pore size) and operating conditions (e.g., pressure, dead-end/cross-flow, and bench-/pilot scale). For all selected PhACs, the thin-film composite (TFC) polyamide membranes showed greater retention than the CTA membranes (Jin, Shan et al. 2012), whereas for CBM and DCF, the effects of membrane properties on their removal performance was somewhat insignificant. For NPX and IBP, the degree of retention was clearly higher with TFC polyamide membranes than with CTA-based FO membranes considering the water flux effect. The greater retention by TFC polyamide membranes is presumably due to: (i) the higher size exclusion effect indicated by the higher degree of glucose retention of TFC membranes and (ii) the electrostatic interactions (i.e., repulsion) between the deprotonated (negatively charged) NPX/IBP and the negatively charged surface of the TFC polyamide membranes at pH 6 (Jin, Shan et al. 2012). Bench- and pilot-scale FO experiments revealed the different retention trends of 23 EDCs and PPCPs; the retention of EDCs and PPCPs during pilot-scale experiments (80–>99%) was significantly higher than those for bench-scale experiments (40–98%) under all conditions tested (Hancock, Xu et al. 2011). Although the reason for this difference is somewhat unclear, it is presumably due to the formation of a fouling layer, membrane compaction, and the enhanced hydrodynamic conditions used in the pilot-scale system.

Active layer structures of the CTA and TFC FO membranes differed considerably, which could play a significant role in the retention of PPCPs (Xie et al. 2014). The TFC membrane exhibits greater hindrance to PPCP diffusion compared to the CTA membrane

(Hancock, Phillip et al. 2011). The TFC membrane showed a greater PPCP retention than the CTA membrane due to its relatively high membrane surface charge, in association with the pore hydration that is manifested by a layer of water molecules permanently attached to the negatively charged membrane surface via hydrogen bonds (Raghunathan and Aluru 2006). The CTA membrane possessed relatively less surface charge since its pore hydration was significantly inhibited due to the higher ionic strength in the membrane pore (Nghiem et al. 2006), whereas TFC membrane pores remained hydrated in FO mode, resulting in greater PPCP retention compared to the CTA membrane. Therefore, the retention performance of FO membranes could be enhanced significantly by modifying the surface charge associated with the active layer structure (Xie, Nghiem et al. 2014).

Since the membranes were rapidly saturated and adsorption decreased over long-term operation, the initial membrane adsorption of CECs may be insignificant. Nevertheless, it is important to evaluate the impact of initial adsorption and predict the CEC retention accurately to determine the correlations between membrane and CEC properties (Comerton et al. 2007). The compounds showed the following adsorption trend at equilibrium with a contact time of 96 h: EE2 (91.7%) >> 4CP (39.4%) > CBM (31.2%) > SMX (27.7%) > ATZ (22.8%) >> PHN (6.9%) (Heo, Boateng et al. 2013). The relatively hydrophilic CECs (SMX, CBM, and ATZ) showed lower adsorption affinities on the FO membrane than EE2, while SMX, CBM, and ATZ showed no correlation based on the log K_{OW} values. Phenolic compounds such as PHN and 4CP (i.e., relatively low MWs compared with the other compounds used) showed different adsorption trends (6.9% for PHN and 39.4% for 4CP) due to variation in their physicochemical properties (i.e., PHN is highly soluble in water vs. 4CP). The adsorption of 4CP (log K_{OW} = 2.39) was greater

than that of PHN (log KOW = 1.67), as anticipated based on the hydrophobicities of these two compounds (Heo, Boateng et al. 2013). The electrostatic repulsion caused by de-protonation, which occurred because the solution pH was higher than the compound dissociation constant (pKa), did not significantly influence the adsorption process in either membrane compared with log K_{OW}. In a separate study, the retention of E1 and E2 was greater than 99% until 20% recovery was reached for FO experiments involving simulated WW feed solutions (Cartinella, Cath et al. 2006). From 20 to 45% recovery, the retention decreased slowly to 95–96%, while from 45% recovery to the end of the experiments (70% recovery), the retention increased slowly to 96–97%.

Cross-flow velocities (CFVs) are one of the key membrane operating conditions that significantly affect the transport of CECs during FO membrane filtration. A previous study showed that SMX retention was higher with a CFV of 58.8 cm/s than 9.8 cm/s, since SMX transport associated with diffusion was influenced more by higher water flux states (i.e., a CFV of 58.8 cm/s) when the FO membrane was negatively charged (Heo, Boateng et al. 2013). In addition, these findings agreed well with previous studies (Hancock, Xu et al. 2011, Huang, Chen et al. 2015), indicating that the increase in concurrent CFVs has a significant effect on diffusive movement (hindered diffusion of compounds) and increases solute retention in the FO process by decreasing concentration polarization effects. Solute retention is comparatively constant regardless of CFV in the solute retention performance of the membrane, while water flux depends on the osmotic driving force, which also contributes to the increased compound retention under high CFV operating conditions. In addition, it has been reported that reverse salt flux influences the increase in organic compound retention in osmotically driven processes, because the retarded forward

diffusion phenomenon from reverse salt flux hinders the diffusive transport of organic compounds (Xie, Nghiem et al. 2012).

3.2.2 Removal by RO membranes

3.2.2.1 Effect of the physicochemical properties of CECs

While high pressure-driven separation of RO membranes is being increasingly used in water and WW treatments and reclamation, solute–membrane interactions, such as steric exclusion (sieving effect), electrostatic interactions (charge effect), and hydrophobic/adsorptive interactions, should be evaluated for CECs varying in size, charge, and hydrophobicity (Bellona et al. 2004). In the RO membrane (BW30; Dow FilmTech), the average retention followed the order: ATZ (93.7%) > CBM (84.3%) > SMX (75.2%) > 4CP (60.9%) > PHN (47.3%) (Heo, Boateng et al. 2013). In that study, in general, the RO membrane had a greater retention efficiency than the FO membrane (CTA; Hydration Technologies). The higher retention efficiency of the RO membrane could be attributed to the positively coupled effects arising from size exclusion, electrostatic repulsion (Donnan exclusion), and hydrophobic/supramolecular interactions (i.e., hydrogen bonding and π-π stacking) of the RO membrane polymer, which mainly consists of an aromatic polyamide, whereas the relatively small water flux in the RO membrane negatively affects target compound retention (Heo, Boateng et al. 2013). The retention of the relatively large MW compounds (CBM, SMX, and ATZ) was > 75%, while the retention of the nonionic and small MW compounds (PHN and 4CP) ranged from 45 to 60%. Among similarly sized compounds, the lower log K_{OW} of SMX showed a weak influence on its lower retention; an increase in retention with increasing log KOW was observed in the cases of CBM and

ATZ. This phenomenon is in agreement with a previous study (Kiso et al. 2001), which reported that the retention of most hydrophobic molecules by an aromatic polyamide membrane material was enhanced with increasing affinity of the solute for the membrane.

E1 and E2 are currently listed in the USEPA Drinking Water Contaminant Candidate List 4. While there are fairly insignificant differences between E1 and E2 retention (> 85%) by RO membranes, the variance shows a small experimental error (~3%) (Nghiem et al. 2004). Although E1 and E2 contain a 17-keto group and a 17-hydroxyl group, respectively, they share similar molecular structures. These results suggest that the 3-oxygen atoms of the first ring of E1 and E2 may participate in hydrogen bonding with the membrane polymer. This is somewhat consistent with the findings of Le Questel et al. (Le Questel et al. 2000) in their study of the hydrogen bond formation between progesterone and its human receptor. The findings in that study suggested that the 3-oxygen atom of progesterone was the key hydrogen bonding acceptor. In a separate study, an examination of PhAC (SMX, sulfamethazine, trimethoprim, clarithromycin, and roxithromycin) retention rates by RO revealed that this filtration technique removes antibiotics at a very high rate, because the results from all of the applied fluxes were below the limits of quantification (Sahar et al. 2011). Regardless of their high degree of retention, however, antibiotic concentrations exceed the limits of detection in most cases. These findings indicate that several molecules of antibiotics penetrate the RO membrane, and thus it can be concluded that RO cannot serve as an absolute barrier to antibiotics.

The RO process combined with a membrane bioreactor (MBR) has been effectively applied for the treatment of raw sewage and secondary effluent (Tam et al. 2007, Dialynas and Diamadopoulos 2009). An RO-MBR system showed that the overall retention rates of

20 PhACs studied in the influent were greater than 99% (Dolar et al. 2012), while RO alone showed a very effective degree of retention of numerous micropollutants (e.g., atenolol, clarithromycin, ETM, and MTP) to below the detection limit (≤ 10 ng/L) (Joss et al. 2011): CBM (> 99%) (Gur-Reznik et al. 2011), SMX, MTP, and sotalol (> 98%) (Radjenovic et al. 2008), and antibiotics, psychiatric control, and anti-inflammatories (> 90%) (Snyder, Westerhoff et al. 2003). The retention of CECs by RO is determined by somewhat complex interactions of electrostatic and other physical forces between the target solute, the solution and the membrane itself. In particular, key retention mechanisms in RO membranes include steric hindrance, electrostatic interactions (repulsion), and hydrophobic interactions (adsorption) between the CECs and the membrane (Bellona, Drewes et al. 2004). The retention of relatively hydrophilic PhACs (log $K_{OW} < 3$) is also very high (> 99%), whereas hydrophilic compounds do not adsorb to the membrane polymeric matrix (Alturki et al. 2010). Since the MWCO of the RO membrane (TR70-4021-HF) is approximately 100 Da, one of the potential removal mechanisms involved is steric hindrance (size exclusion). In addition, electrostatic interactions (attraction or repulsion) may affect the retention of some PhACs in an RO membrane due to their charge (e.g., positive charge of macrolide antibiotics and negative charge of SMX) (Dolar, Gros et al. 2012).

3.2.2.2 Effects of water quality conditions

The presence of NOM and colloidal particles could significantly affect membrane performance. The E1-binding ability of hydrophobic HA is the key contributor to its significant enhancement of E1 retention by RO membranes (DL and CK, Osmonics) (Jin et al. 2010). It is widely known that divalent cations (e.g., Ca^{2+}) affect the binding of trace CECs by humic substances (Schlautman and Morgan 1993). Therefore, the Ca^{2+}

concentration in a feed solution is believed to affect the E1 retention in HA-containing solutions. Although the presence of HA could enhance the retention of E1, a higher Ca^{2+} concentration tends to reverse this effect (Jin, Hu et al. 2010). Particularly, the addition of 0.3 mM Ca^{2+} in feed solution enhanced the effect of HA on E1 retention by the membrane, decreasing to 180% compared to an enhancement of 30% in the absence of Ca^{2+}. When the Ca^{2+} concentration was increased to 0.6 mM, HA showed no noticeable improvement in E1 retention. In another study, the pH dependence of E1 speciation closely mirrored the pH dependence of E1 retention, with the retention decreasing noticeably at high pH for the RO membrane (Schafer et al. 2003). This decrease was not the result of changes in membrane characteristics due to high pH, because the flux was largely constant over the entire pH range examined. This finding corroborates the earlier suggestion that adsorptive effects (presumably mediated by hydrogen bonds between the hydroxyl and/or carbonyl groups of E1 and the membrane) are major contributors to the retention of E1 on these membranes; it is to be expected that adsorption would be highest under conditions where charge repulsion is lowest. At high pH, adsorption would decrease and, depending on the pore size, retention would decrease as charge repulsion increases (Schafer, Nghiem et al. 2003). In the absence of colloidal silica particles, the decrease in E2 retention appeared to be linear, whereas for the case with colloidal fouling, the retention decreased severely initially, followed by a moderate linear decline (Ng and Elimelech 2004). However, unlike E2, progesterone retention decreased severely initially but gradually slowed down until the end of the experiment. These findings suggest that the formation of a colloidal cake layer on the membrane surface restricts back diffusion of the compounds, causing a significant reduction in their retention.

The concentrations of CECs found in sewage are in the order of ng/L to μg/L. Therefore, the effect of initial CEC concentration on removal reflects the behaviors of the CECs. The effect of initial concentration (ranging from 1 to 1,000 ng/L) on the retention of E1 by several RO membranes is insignificant, which is presumably due to the constant partition coefficient for E1 at high concentrations between the membrane and bulk solution (Schafer, Nghiem et al. 2003), indicating that the membrane surface sites may not become saturated. A similar finding, in which the retention of several pesticides was somewhat independent of the initial feed concentration, was also reported (Van der Bruggen et al. 1998).

The pH of the feed water influences the membrane surface charge, the characteristics of the solutes in the feed water, and the membrane separation performance for solutes (Qin et al. 2003). Variations in Ni^{2+} retention during RO filtration at varying pH conditions are somewhat insignificant. While the Ni^{2+} concentrations in the influent varied between 8.22 and 10.29 mg/L, its concentrations in the pretreatment effluent decreased to between 4.07 and 6.56 mg/L. However, the Ni^{2+} concentrations in pretreatment + RO were below the detection limit. While the feed exhibited high Ni^{2+} concentrations at pH 5.5–7, Ni^{2+} showed much larger decreases under other pH conditions in the permeate from pretreatment. For Zn^{2+}, the same effects were also observed at pH = 6. Zn^{2+} concentrations in the feed ranged between 10.7 and 13.7 mg/L, and its concentrations in permeate pretreatment decreased to between 7.14 and 9.56 mg/L. Zn^{2+} concentrations in the permeate did not change much with pH (mostly less than 0.88 mg/L) (Qin, Oo et al. 2003).

3.2.2.3 Effects of membrane properties and operating conditions

For RO membranes, the retention governed by the adsorption affinity of compounds correlates with their hydrophobicity, except for phenolic compounds, which have different characteristics (the adsorption affinity of 4CP to the RO membrane was remarkably higher, and 4CP reached a pseudo-equilibrium state faster than the other compounds examined) (Heo, Boateng et al. 2013). The compound adsorption affinities on the RO membrane showed the following order (% removal): 4CP (93.8%) > EE2 (89.9%) >> PHN (69.8%) > ATZ (55.2%) > CBM (31.8%) >> SMX (6.2%). For phenolic compounds, the greater retention by the polyamide RO membrane was caused by the following aspects (Ahmad and Tan 2004, Kimura et al. 2004, Yuan and Lu 2005, Hughes and Gale 2012): (i) the retention is depending on physicochemical properties, including the functional groups (−OH and −Cl), solubility, and hydrophobicity, which impart high affinity for polyamide materials; (ii) the chlorine functional group of 4CP is an electron-withdrawing group; therefore, the reaction affinity with the membrane polymer may dominate; (iii) water solubility generally correlates with log KOW, indicating that the adsorption capacity of 4CP to the RO membrane increased with lower solubility; and (iv) many studies of membrane adsorption have reported that organic compound adsorption onto membranes is influenced by the membrane surface, as well as by the support layer and membrane pores. In addition, Yoon et al. (Yoon et al. 2004) reported that adsorption was related to the membrane pore radius, consequently allowing relatively low MW organic compounds (e.g., PHN and 4CP) to access and diffuse into the membrane's internal adsorption sites. Therefore, from these results, we conclude that a weak correlation exists

between all CECs. Moreover, regarding phenolic compounds and other CECs, a strong correlation between hydrophobicity and adsorption capacity was observed.

Understanding the influence of operating variables on the retention of CECs is very significant from a design, as well as an operational, perspective. In general, retention by the RO membrane increases with increasing CFV, since an increase in CFV decreases the concentration polarization at the membrane–bulk solution interface. However, no CFV effects on E1 retention were observed (Nghiem, Manis et al. 2004) since the E1 concentration within the membrane could be higher than that of the polarization layer due to E1 adsorption onto the membrane surface. Therefore, the concentration polarization effect appears to be minimal in this case. Generally, solute retention increases with pressure up to an asymptotic value. However, E1 retention decreases by 15% with increasing pressure (10 to 25 bar) (Nghiem, Manis et al. 2004), which is presumably due to the strong interaction with membrane polymers for organic compounds (Nghiem et al. 2004, Johnson et al. 2015). Solute-membrane interactions can be supported by friction associated with hydrodynamic conditions and diffusion associated with a chemical concentration gradient. Because the RO membrane has an average pore radius of 0.7 nm (Nghiem, Schafer et al. 2004), those interactions are critical since it is in the same order of magnitude as the molecular size of E1. The drag force within the membrane pores increases, since an increase in pressure causes an increase in permeate flux. Therefore, the desorption of E1 improves, or the time for adsorption decreases due to the lower residence time in the membrane, which may contribute to the reduction in retention (Nghiem, Manis et al. 2004). A low-pressure RO membrane is a pressure-driven membrane dominated by an increase in permeate flux against increasing transmembrane pressure. The retention of several heavy

metals increased with an increase in transmembrane pressure (Ozaki et al. 2002), which may be due to a decrease in the average pore size on the membrane surface and an increase in the favored sorption of pure water at a higher pressure (e.g., solvent permeability increases compared with solute at a high pressure, causing increased retention) (Sourirajan 1970). Retention is also dependent on the valency of the metal ion. Cr(IV) was removed (99.9%) more than Ni^{2+} and Cu^{2+} (both > 99.5%) at 500 kPa pressure (Ozaki, Sharma et al. 2002).

3.2.3 Removal by NF membranes

3.2.3.1 Effect of the physicochemical properties of CECs

Similar to FO and RO membranes, the influence of the physicochemical properties of CECs on retention by NF membranes is also significant. The retention of BPA by an NF membrane (NE4040-70; Saehan, MWCO = approximately 200 Da) was much lower (74.1%) than that of IBP or salicylic acid (98.1 and 97.0%, respectively), quickly decreasing with operation time and reaching an asymptote (Kim et al. 2008). BPA (pKa = 9.6-10.2) remains as an uncharged species at the tested pH 7, while IBP (pKa = 4.9) and salicylic acid (pKa = 2.9) should be mostly deprotonated, resulting in a negative charge. Therefore, the sieving effect (size exclusion) is the dominant mechanism of BPA retention, while the low BPA retention could be attributed to the absence of electrostatic interactions (repulsion) between the membrane surface and BPA. However, while IBP (MW = 206 g/mol) and salicylic acid (MW = 138 g/mol) have smaller MWs than BPA (MW = 228 g/mol), IBP and salicylic acid exhibited much greater retention than BPA due to both size exclusion and electrostatic repulsion. In addition, the fast decrease in BPA retention with

operation time is presumably because hydrophobic and uncharged BPA readily adsorbs to the hydrophobic membrane surface until saturation. However, IBP and salicylic acid exhibited minor decreases in retention with operation time, although these compounds have higher log K_{ow} values than BPA, presumably due to electrical repulsion between the compounds and the membrane (Kim, Park et al. 2008).

In addition to the chemical speciation of CECs governed by solution pH and pKa, the physicochemical activities of CECs for their retention are significantly influenced by their functional groups (Bellona, Drewes et al. 2004). The degree of retention of three PhACs (CBM, SMX, IBP) by two NF membranes (NF-90 and NF-270; FilmTech) varied significantly due to their different physicochemical properties (Nghiem, Schafer et al. 2005). The retention of neutrally charged CBM (pKa = 2.3) by both the NF-90 and NF-270 membranes was relatively constant, since retention is exclusively governed by steric (size) exclusion in the absence of charged functional groups. In the absence of electrostatic interactions (repulsion), the compound physicochemical properties can influence retention performance. SMX, which contains two functional moieties at both sides of the sulfonamide linkage, shows two dissociation constants: one involving the protonation of the primary aromatic amine -NH2 and the other corresponding to the deprotonation of the sulfonamide –NH. The retention of the neutral SMX by the loose NF-270 membrane was significantly lower than that of CBM, despite the higher MW of SMX compared to CBM, since SMX has a higher polarity (dipole moment) than CBM. Organic molecules with high dipole moments (above 3 D) can show lower retention than molecules with a similar MW but with a lower dipole moment (Van der Bruggen et al. 1999). This finding suggests that

the compound dipole moment plays a significant role in the retention by NF membranes, via affecting molecule orientation as it approaches the membrane pores.

3.2.3.2 Effects of water quality conditions

The effects of seasonal changes, ionic strength, and spiked concentration on the retention of CBZ by an NF membrane (NF270) were examined with MBR effluents (Gur-Reznik, Koren-Menashe et al. 2011). The removal of CBZ from the effluents was seasonally dependent despite a spiked concentration (3, 600, and 1,000 μg/L), with a higher retention in the summer (approximately 85–90%) compared to the winter (approximately 50–55%). Variations in the effluent organic matter seasonally produced during the biological stage could describe this phenomenon. In addition, metabolic rate changes due to low temperature were reported to influence organic matter degradation, particularly hydrolysis yields (Lew et al. 2009). In another study, it was reported that solute–solute interactions in tertiary effluent significantly improved the retention of PhACs for the NF membrane (NF-270) due to the association between PhACs and organic macromolecules in the effluents (Azais et al. 2014). Therefore, bound PhACs are rejected by NF membranes more readily by size exclusion and/or electrostatic interactions (repulsion) occurring between the complexes and the membrane surface, as previously reported for various contaminants (Zazouli et al. 2009). The association between organic PhACs and organic macromolecules is believed to be a result of hydrogen bonding and hydrophobic interactions (Plakas et al. 2006). It was also observed that PhAC binding by effluent organic matter was favored in WW effluent, presumably due to higher biopolymers (soluble microbial polymers) (Kimura et al. 2009).

The presence of calcium in the feed water reduces the removal of organic EDCs and PhACs in NF membranes (Devitt et al. 1998), whereas the removal of PhACs with NF membranes was noticeably increased in the presence of a high calcium concentration (Azais, Mendret et al. 2014). Comerton et al. observed that the retention of hydrophilic PhACs (log $K_{OW} < 4$) by NF in MBR effluent decreased significantly when cations were doubled (Comerton et al. 2009). Increases in ionic strength and divalent cation concentrations result in changes in effluent organic matter conformation, which may alter the presentation of sites for compound association, leading to a decrease in organic matter-compound complexation (Devitt, Ducellier et al. 1998). This phenomenon could be explained by the fact that NOM has a stretched and linear configuration in low ionic strength solutions and in the absence of divalent cations, while NOM has a more inflexible, compact and coiled configuration in high ionic strength solutions and in the presence of divalent cations (Hong and Elimelech 1997). The presence of NaCl in the deionized (DI) water matrix had a minimal effect on the overall retention of CBZ by NF270 (MWCO = 155 Da), while the fluctuations in CBZ retention can be attributed to the dehydration of CBZ in the presence of 5 g/L NaCl, which produces a smaller molecule that can more easily leak through the membrane pores (Gur-Reznik, Koren-Menashe et al. 2011). Schäfer et al. also observed only a negligible effect for NaCl (0–100 mM) and CaCl2 (0–5 mM) on the retention of E1 by the TFC-SR2 (Koch) membrane from DI water (Schafer, Nghiem et al. 2003). It was hypothesized that ionic strength affects solute retention by two integrated and comparable effects: (i) the presence of salt could screen the charge associated with the polar functional groups of PhACs and decrease the apparent size of the molecule, and (ii) it can shield the electrostatic potential of the membrane surface and reduce electrostatic

interactions (repulsion). The reduction of IBP by an NF membrane (MWCO = 150–300 Da) was reported with increasing ionic strength with MBR effluents (Park et al. 2004), while divalent salt ($CaCl_2$ and $CaSO_4$) had an insignificant effect on pesticide retention by an NF-Desal DK membrane (Osmonics, MWCO=150–300 Da), which was presumably due to blockage of membrane pores as a result of divalent ion retention (Boussahel et al. 2000).

A fouled NF membrane (UTC-60; Toray) was used to evaluate the degree of retention of several PhACs in WW effluent and DI water (Kimura, Iwase et al. 2009). In that study, the effect of the association between the PhACs and organic macromolecules in WW effluents was likely significant in the case of MBR effluent, particularly for primidone and CBM. Organic macromolecules in MBR effluent appeared to increase the removal of PhACs by the NF membrane due to their association. After silica fouling, the retention of PPCPs was increased by the tight NF90 membrane (MWCO = 200 Da), but decreased by the loose NF270 membrane (MWCO = 270 Da) (Lin et al. 2014). With or without silica fouling, the solution pH negligibly influenced the retention of both relatively hydrophilic and hydrophobic compounds by NF90, but significantly influenced the retention of those compounds by NF270. PPCP retention was enhanced after silica fouling due to the additional steric hindrance effect provided by the fouling layer, thus decreasing the permeation of PPCPs across the membrane surface. For NF90, both steric exclusion and electrostatic interactions (repulsion) occurred synergistically to enhance the retention of PPCPs after fouling and with an increase in pH. However, for NF270, electrostatic repulsion was the mechanism governing the transport of PPCPs as the pH increased, with or without silica fouling. Although a fouling layer may provide additional steric hindrance

for loose NF270, its influence was overwhelmed by the accompanied cake-enhanced concentration polarization phenomenon. The cake-enhanced concentration polarization phenomenon hindered the back-diffusion of PPCPs into the feed solution, and trapped and accumulated PPCPs on the membrane surface to enhance their diffusion across the membrane (Vogel et al. 2010).

3.2.3.3 Effects of membrane properties and operating conditions

As described earlier, CEC adsorption onto the membrane is the main removal mechanism at the initial stage of filtration while, at the later stage, the retention of CECs is less than expected based only on a steric/size exclusion mechanism. While size exclusion is the main retention mechanism at the later stages of membrane filtration, it was proposed that partitioning and subsequent diffusion through the membrane polymer matrix causes a fairly lower rate of retention (Nghiem, Schafer et al. 2004). In that study, a clear deviation of retention based on size exclusion was observed, while the diffusive transport of hormones (E1, E2, progesterone, and testosterone) was slow through the polyamide skin layer (15–40 nm) of the NF-270 membrane. In addition, although the “tight” NF-90 and “loose” NF-270 membranes have different membrane pore sizes based on their MWCOs, the similar retention rates of natural hormones by those membranes may be explained by their comparable active layer thicknesses that influence the diffusion behaviors of hormones (Couarraze et al. 1989), as follows: (i) although the contribution of convective flow to the transport of hormones across the membrane is somewhat small, the presence of water plays a significant role in allowing the diffusion process (Freger et al. 2002) and (ii) hormone diffusion in the dense polymeric phase occurs, which can be caused by switching

between two bonding sites ,or from a hydrophobic bond to a substrate and a hydrogen bond to water (Cohen 1975).

A chemically modified NF via graft polymerization significantly improved BPA retention (74.1% (raw membrane) to 96.9% for the polymerized membrane) (Kim, Park et al. 2008). Since BPA is an uncharged species at the tested pH 7.2, the enhanced retention was attributed to the steric hindrance associated with the polymer chains. Greater steric hindrance was achieved for the membrane polymerized for 60 min compared to that polymerized for 15 min, since the longer polymerization time produced longer polymer chains. In addition, BPA retention by the polymerized NF membrane decreased more slowly versus that by the raw membrane, which was presumably due to the increased adsorption of BPA associated with the relatively hydrophilic polymerized membrane. The retention of IBP and salicylic acid (negatively charged solutes) by the polymerized NF membrane improved from 98.1% to 99.7% and from 97.0% to 99.1%, respectively, indicating that the increased negative surface charge and increased steric hindrance of the polymerized NF membranes were directly responsible for the enhanced retention (Kim, Park et al. 2008).

3.2.4 Removal by UF membranes

3.2.4.1 Effect of the physicochemical properties of CECs

The retention of seven different PhACs by a UF membrane (pore size = 0.1 μm) was investigated using the pilot-scale municipal WW reclamation system (Chon et al. 2013). In that study, MW, log *D*, and charge at a neutral pH of the PhACs were considered major parameters affecting their retention by the UF membrane. Most of the target PhACs

were not effectively removed using the UF membrane (< 35%), with the exception of DCF and SMX. However, there was no significant relationship between the retention of target PhACs by the UF membrane and their MW, log *D*, or charge at neutral pH. In a separate study, inconsistent degrees of retention for 16 PhACs by a UF membrane (MWCO = 100 kDa) were obtained with municipal WW, while a somewhat small overall retention (< 29%) was achieved (Sheng et al. 2016). In particular, acetaminophen, caffeine, IBP, and NPX remained unchanged at the membrane permeate since the UF membrane has a much larger pore size than the target PhACs (< 400 g/mol). In addition to size exclusion, membrane surface adsorption associated with compound hydrophobicity (log K_{OW}) is another key mechanism by which UF removes PhACs. It is believed that PhACs are unlikely to be adsorbed on the membrane surface when PhACs have high hydrophilicity (log K_{OW} = < 2.6), while the opposite effect of PhACs adsorbed onto membrane surfaces is obtained for highly hydrophobic PhACs (log K_{OW} = > 4.5) (Fernandez et al. 2014), consistent with the finding that the high retention of TCS was due to its very high log *K*ow value (4.76, the highest among all target PhACs) (Sheng, Nnanna et al. 2016). Although DCF, IBP, and NPX have relatively high log *K*ow values (4.4, 3.97, and 3.3, respectively), both the retention and adsorption caused by the membrane were almost negligible, presumably due to the reduced hydrophobicity of these PhACs once they are deprotonated (Yoon, Westerhoff et al. 2007).

For dead-end stirred-cell experiments, the sulfonated polyethersulfone UF membrane (nominal MWCO = 8 kDa) showed a fluoranthene (FRT) retention of > 95% in the absence of NOM, presumably due to hydrophobic adsorption (Yoon, Westerhoff et al. 2004). FRT adsorption (15–25% for the UF membrane) was lost in the presence of NOM,

presumably due to competition for adsorption sites and pore blockage by NOM. In that study, E2 retention by the UF membrane was reduced from 60 to > 95% in the absence of NOM, and to 10–20% in the presence of NOM due to competition for adsorption sites. A model species (parachlorobenzoic acid, PCBA) was employed to verify that hydrophobic interactions (attraction) occurred between a hydrophobic compound and the hydrophobic membrane. A PCBA retention of approximately 30% in the presence of NOM, and 50% in the absence of NOM, was obtained by the UF membrane, while PCBA is less hydrophobic. These findings indicate that an electrostatic exclusion mechanism could be more dominant than hydrophobic adsorption for PCBA retention (Yoon, Westerhoff et al. 2004). In a separate study, the concentrations of 52 CECs and conventional contaminants were lower in the permeate than those in initial feed samples. The feed concentrations of the compounds ranged from 16 to 234 ng/L (Yoon, Westerhoff et al. 2006). Numerous permeate concentrations of both CECs and conventional contaminants were below the limit of detection, indicating a high degree of retention by the UF membrane (MWCO = 8 kDa), except for a few compounds (e.g., α- and β-BHC, FRT, hydrocodone, metolachlor, and musk ketone) that were poorly removed. In most cases, the concentrations of EDC/PPCPs followed the order: initial feed > retentate > permeate, except for a few compounds (e.g., DCF, ETM, E3, gemfibrozil, IBP α-chlordane, and dieldrin). Because the retentate concentration was lower than the initial concentration, these findings indicate that significant amounts of compounds in the retentate were adsorbed in the test. Assuming negligible loss due to degradation and/or adsorption onto the glassware, this could be due to adsorption to the membrane surface and into membrane pores. Previous studies have shown that the retention of relatively hydrophobic compounds and hormones/steroids (e.g.,

log K_{OW} > 3.0) by RO, NF, and UF membranes is governed significantly by adsorption (Kimura et al. 2003, Nghiem et al. 2004, Nghiem et al. 2004, Yoon et al. 2004). In these studies, some polar and less hydrophobic compounds were also adsorbed onto the membrane surface, which was dependent on the membrane material and feed solution pH.

A polymer (carboxymethyl cellulose, CMC)-enhanced UF (polyethersulfone, MWCO = 10 kDa) process was used to evaluate the removal of toxic heavy metals, such as Cu(II), Ni(II), and Cr(III), from synthetic WW solutions (Barakat and Schmidt 2010). Comparable retention effects were obtained for both Cu(II) and Cr(III) ions from a mixed solution versus the single solutions. Upon increasing the metal ion concentration from 10 to 100 mg/L, the metal retention rates varied from 98 to 98.5% and from 99 to 97.1% for Cu(II) and Cr(III), respectively. However, a higher separation effect was observed for Ni(II) ions from the mixed solution versus the single solution. Increasing the initial Ni(II) ion concentration from 10 to 100 mg/L caused the metal retention rates to vary from 99 to 76.4% in the mixed solution, and from 99.1 to 57% in the single solution. The higher retention efficiency of Ni(II) ions in the simultaneous solution could be attributed to the association of the Ni-CMC complex with the other two complexes of Cu(II) and Cr(III) with CMC (Barakat and Schmidt 2010).

3.2.4.2 Effects of water quality conditions

Similar to FO, RO, and NF membranes, CEC retention by UF membranes can also vary depending on feed water chemistry, as previously shown (Adams et al. 2002, Nghiem, Manis et al. 2004). Because four feed waters having diverse water chemistry conditions were employed to evaluate the retention of 52 CECs and conventional contaminants with

UF membranes, it is somewhat difficult to compare the retention trends for each compound (Yoon, Westerhoff et al. 2006). Therefore, in that study, compound retention was compared to several major parameters, including dissolved organic carbon (DOC), specific UV absorbance (SUVA), conductivity, and pH. For more polar and hydrophilic compounds, the retention for the UF membrane followed this order (MWCO = 8 kDa): Passaic Valley water (PVW, relatively low pH and high conductivity) > Ohio River water (ORW, relatively low SUVA and low conductivity) ≈ Colorado River water (CRW, relatively low SUVA and high conductivity) > Suwanee River RO isolate NOM water (SRW, relatively high DOC and high SUVA). However, for less polar and highly hydrophobic compounds, the UF membrane retained these compounds somewhat more from ORW and CRW than from SRW and PVW, which could be due to more competition between the NOM in SRW and PVW and compounds for the membrane adsorption sites than ORW and CRW. The SRW contained the most DOC with the highest SUVA, usually indicating more hydrophobic and larger-MW NOM than the other waters with lower SUVA values. In addition, SRW contained the lowest total CEC spiked concentration (1,789 ng/L) compared to ORW (6,586 ng/L), CRW (5,670 ng/L), and PVW (5,849 ng/L). Therefore, SRW had the lowest competition among those compounds for membrane adsorption sites (Yoon, Westerhoff et al. 2006).

The retention (5–34%) of five EDCs (E1, E2, E3, EE2, and BPA) by a fouled UF membrane was higher than those (10–76%) of a clean membrane (MWCO = 100 kDa), indicating that membrane fouling may influence EDC removal (Hu et al. 2014). For the fouled membrane, BPA had the highest removal degree (64–76%), followed by EE2 (42–53%), E1 (28–46%), E2 (24–63%), and E3 (10–17%). Fouling reduced membrane pore

size (Sutzkover-Gutman et al. 2010), which enhanced the retention of EDCs due to size exclusion. In addition, EDCs–HA sodium matrix forms as EDCs adsorb to humic particles, which were then co-rejected by the membrane (Devitt, Ducellier et al. 1998). While the BPA molecule was the smallest, it showed the highest retention efficiency, presumably because BPA exhibits the strongest electropositivity, resulting in its tight bond with humic particles (Hu, Si et al. 2014). EE2 had comparable electro positivity with E1, E2, and E3; however, it is larger than the others and therefore had a higher retention rate. In addition, cake layers formed under different pressures had differing abilities to retain different EDCs (Bellona, Drewes et al. 2004). The cake formed at 50 kPa showed the best effect on EDC retention, while cakes formed at 25, 30, and 75 kPa exerted a relatively insignificant effect on EDC retention (Hu, Si et al. 2014). After fouling, membranes with cakes formed under different pressures still presented electronegativity, which differed from the clean membrane, where there were adsorptive sites not only on the membranes but also on the cakes. Therefore, adsorption still contributes to the retention of EDCs. In addition, membrane fouling significantly influences membrane characters, such as porosity and hydrophilicity. Lower porosity and stronger hydrophilicity were favored for EDC retention by a fouled membrane (Hu, Si et al. 2014). This is presumably because the cake with a lower porosity underwent additional severe compression and had a greater number of small pores, so that the EDCs were more difficult to penetrate through. Furthermore, hydrophobic EDCs were more repulsive to more hydrophilic cake, consistent with previous findings (Yoon, Westerhoff et al. 2007).

The retention of inorganic CECs (Cr(VI), As(V), and ClO_4^-) by the UF membrane (MWCO = 8 kDa): (i) decreased with increasing solution conductivity due to the

decreasing negative membrane charge; (ii) increased with pH due to the increasing negative membrane charge; and (iii) decreased in the presence of divalent counter ions (Ca^{2+}) due to a less negative membrane charge (Yoon, Amy et al. 2009). In addition, a general trend in which the retention of these toxic ions increased as the solution pH increased from 4 to 10 was also observed. These findings can be explained by electrostatic exclusion, since the membrane charge became more negative with increasing pH, resulting in increased electrostatic repulsion between the target ions and the membranes, thus increasing ion retention. However, for As(III), the retention by the UF membrane only varied marginally over a range of pHs below 10, because As(III) exists mostly as an uncharged species below pH 9.13 (i.e., its pKa). In contrast, As(III) retention increased considerably at pH 10, when it became anionic, indicating that steric/size exclusion was the mechanism determining the uncharged As(III) species until it became anionic at pH > 9.13, where an electrostatic exclusion mechanism began to play an important role (Yoon, Amy et al. 2009).

3.2.4.3 Effects of membrane properties and operating conditions

The minimal retention of steroidal hormones (e.g., E1, E2, progesterone, and testosterone) by UF membranes in the absence of organic matter was predicted due to the small size of the hormones relative to the membrane pore sizes of 0.8–0.9 and 1.6–18.2 nm (MWCO = 10 and 100 kDa, respectively) (Neale and Schafer 2012). However, up to 28% retention was observed, with retention increasing with a decreasing membrane MWCO (1 kDa) influencing size exclusion. Retention was also related to membrane adsorption, with higher retention by lower MWCO membranes due to longer experimental durations. In addition, an increase in organic matter concentration was anticipated to enhance E1

retention due to greater partitioning with the higher organic matter mass. These results indicate an increase in E1 retention as organic matter concentration increases from 12.5 to 125 mg/L for both 10 and 100 kDa membranes (Neale and Schafer 2012). In a separate study, the retention of 16 EDCs and PPCPs was evaluated during UF of natural surface waters at four different surface shear stress regimes: no shear stress, low peak shear stress associated with continuous coarse bubble sparging, sustained peak shear stress associated with intermittent coarse bubble sparging, and high peak shear stress associated with large pulse bubble sparging (Wray et al. 2014). Overall, surface shear stress conditions somewhat influenced compound retention, while the average retention for all EDCs and PPCPs under the conditions tested (no shear stress, continuous coarse, intermittent coarse, and pulse bubble sparging) was 32, 18, 22, and 34%, respectively.

The effects of membrane type were investigated at fixed heavy metal ion (Zn and Cd) concentrations of 50 mg/L (Trivunac and Stevanovic 2006). For both metals, the flux of treated water decreased, as expected, with decreasing membrane pore diameter, having very small values for the UF membrane. Therefore, polysulfonamide membranes are not recommended for most applications, although they provide very high retention coefficients. Due to the small differences in pore size of Versapor membranes, the retention coefficients were very similar. The lowest retention coefficient of Zn was obtained using dextrin as a complexing agent due to its low MW. Polyethylene glycol and diethylaminomethyl cellulose were more effective complexing agents, with constant retention coefficients with all three membranes (Trivunac and Stevanovic 2006). For the UF (MWCO = 8 kDa) membrane, As(III) retention was fairly constant over the entire pH range (7–11%) (Yoon, Amy et al. 2009), presumably because steric/size exclusion was

dominant for the UF membrane. While the retention of uncharged As(III) was the lowest among the ions tested, ClO_4^- retention was significantly lower than Cr(VI) and As(V) for the UF membrane, presumably because the hydrated divalent ions have a larger size (0.27 nm for $HAsO_4^{2-}$) and/or a greater charge than the hydrated monovalent perchlorate ion (ClO_4^-, 0.14 nm). The solute radii were calculated using the Stokes–Einstein equation (Bowen and Mohammad 1998). For target toxic ions, the RO membrane with a small pore size (the measurement of which was discussed in a previous report (Yoon and Lueptow 2005) exhibited the highest retention (> 90%), indicating that size exclusion was at least partially responsible for retention. However, the UF membrane with a relatively large pore size exhibited the lowest retention, ranging from 7% to 43% (Yoon, Amy et al. 2009). Table 3.3 summarizes the removal efficiencies of selected CECs by FO, RO, NF, and UF membranes under various experimental conditions and water types. In addition, a retention diagram of organic CECs during membrane treatments based on solute and membrane properties is presented in Fig. 3.3.

3.3 Conclusions and areas of future research

Overall, the general CEC removal trend was as follows: (i) the removal efficiency for the membranes follows the declining order: RO ≥ FO > NF > UF; (ii) the retention of CECs by RO and FO membranes is mainly governed by size/steric exclusion, while high retention can still be achieved due to hydrophobic (adsorption) and electrostatic (attraction) interactions for NF and UF membranes; (iii) more polar, less volatile, and less hydrophobic organic CECs have less retention than less polar, more volatile, and more hydrophobic organic CECs; (iv) while, in general, FO and RO membranes show significant metal/toxic anion retention (> 95%) regardless of water quality and operating conditions, metal/toxic

anion retention by NF and UF membranes is more efficient at neutral and alkaline conditions than at acidic values; and (v) while UF alone may not effectively remove CECs, it can be employed as a pretreatment step prior to FO and RO.

However, numerous studies were limited to a few membranes (e.g., FO, RO, NF, or UF), focused on synthetic solutions, or examined only a few compounds under limited solution pH/ conductivity ranges and operating conditions. Thus, a systematic retention assessment of various CECs is necessary for the following reasons: (i) to investigate the removal mechanisms of FO, RO, NF, and UF membranes in the presence of co- and counter- ions in natural source waters; (ii) to systematically evaluate the influence of DS type, concentration, and reverse permeation rate on CEC retention for FO membranes; (iii) to better understand water conditions in the presence of various NOMs that improve removal, and those for which specific target compounds favor the formation of bound complexes (since determining the optimal solute–solute interactions with organic matter and fouling is critical when designing membrane operations); (iv) to determine whether the accumulation of foulants and retarded diffusion influence the retention of CECs by membranes having varying fouling degrees in various waters; and (v) to evaluate larger-scale processes because, unfortunately, insufficient information is currently available about FO, RO, NF, and UF membrane processes to allow full-scale implementation.

Table 3.3 Summary of selected CEC and heavy metal removal by FO, RO, NF, and UF membranes.

Membrane class	CEC class	Experimental condition	C_o and water type	Key removal (%)	Key finding	Ref.
FO	PHN, 4CP, ATZ, CBM, SMX	Cross-flow HTI-CTA CFV=58.8 cm/s	2 μM SDW	SMT (89.7), CBM (82.6), ATZ (48.7), 4CP (38.6), PHN (21.9)	Compared to the polyamide-based RO membrane, the CTA-based FO membrane exhibited superior water flux performance due to the optimized properties of its active and support layers in FO-mode.	(Heo, Boateng et al. 2013)
	E1 E2	Cross-flow CTA, DS=NaCl Recovery = 0-70%	1,000 ng/L SDW	>95 (E1) 75-95 (E2)	Experiments revealed that membrane consistently retains both E1 and E2 at or above 99.5%, independent of feed composition.	(Cartinella, Cath et al. 2006)
	Twelve EDCs PPCPs	Cross-flow, CTA DS = NaCl, $MgSO_4$, glucose CFV=9 cm/s	2,000 ng/L SDW	30-90	The pore hindrance transport model can be used to describe the retention of organics by the FO process. Retention of charged organics by the CTA membrane was generally high and was governed by both electrostatic interaction and steric hindrance.	(Xie, Nghiem et al. 2014)
	Eighteen PPCPs charged (positive, neutral, and negative)	Cross-flow HTI-CTA DS = NaCl	2,000 ng/L SDW	80-90 (positive) 50-85 (neutral) >95 (negative)	Fouling by long-term biofilm growth caused FO retention to vary in function of biofilm age, although overall biofilm influence was limited.	(D'Haese, Le-Clech et al. 2013)
	Twenty three EDCs and PPCPs	Bench scale Pilot scale	0.63-388 ng/L WWE	70-95 (positive)	Retention of EDCs and PPCPs during pilot-scale experiments was significantly greater	(Hancock, Xu et al. 2011)

(positive, negative, hydrophobic nonionic, nonionic)	DS = NaCl		60-95 (negative) 40-90 (hydrophobic nonionic) 40-95 (nonionic)	than observed for bench-scale experiments under all conditions evaluated.	
MTP, SMX, TCS	Cross-flow TiO_2 modified FO DS = NaCl	500 μg/L SDW	>99 (MTP) >99 (SMX) >97 (TCS)	The retentions of triclosan and sulfamethoxazole were higher than metoprolol in the FO mode due to their different speciation characteristics and membrane surface charges at different pH values.	(Huang, Chen et al. 2015)
CBM, DCF, IBP, NPX	Cross-flow Cellulose acetate Polyamide TFC DS = NaCl	250 μg/L SDW	65->95 (CBM > DCF>IBP > NPX)	For commercial cellulose acetate based FO membranes, size exclusion and hydrophobic interaction between the compounds and membrane dominate their retention under acidic conditions.	(Jin, Shan et al. 2012)
Twenty four PhACs	Cross-flow DS = NaCl CFV = 20.4 cm/s	100 μg/L SDW	>60 (retention increases with increasing water flux)	For all PhACs, the retention ratio increased with the increase of the draw solute concentration, although the increase became marginal when the draw solute concentration was higher than 1 M.	(Kong et al. 2015)
SMX, trimethoprim, norfloxacin, roxithromycin	FO+electro chemical oxidation DS = NaCl CFV = 8 cm/s	200 μg/L SWW	50-90 (facing DS mode) 90-95 (facing feed solution mode)	The FO process with function of electrochemical oxidation has the capability to thoroughly remove trace antibiotics from wastewater.	(Liu et al. 2015)

	BPA, TCS, DCF	Cross-flow FO/RO mode DS = NaCl, $MgSO_4$	500 □g/L SWW	>80 (BPA) >95 (TCS) >90 (DCF)	The difference in the separation behavior of these hydrophobic trace organics in the FO (when NaCl was used as the draw solute) and RO modes could be explained by the retarded forward diffusion of feed solutes within the membrane pore.	(Xie, Nghiem et al. 2012)
	Zn, Cu, Cd	Cross-flow COD	20-500 μg/L Landfill leachate	48-59 (Zn) 63-86 (Cu) >99.5 (Cd)	Among the investigated metals, Cu and Zn exhibit a significant removal, while Cd removal seems not to be affected by the presence of organic compounds in the leachate.	(Chianese et al. 1999)
	Cr, As, Pb, Cd, Cu, Hg	Cross-flow DS= NaCl, $Na_4[Co(C_6H_4O_7)_2$	1,000-5,000 mg/L SWW	99.87 (Cr), 99.74 (As), >99.9 (Pb), 99.78 (Cd), 99.77 (Hg)	The proposed FO process maintains high retentions under high concentrations of heavy metal ions. Even when 5,000 mg/L feed solution was used, the retentions were maintained at 99.5%.	(Cui, Ge et al. 2014)
	Cd, Pb, Cu, Zn	Cross-flow, TFI DS = NaCl	200 mg/L SWW	>94 (Cu>Cd>Zn>Pb)	The retention efficiency reached 94% on average for four typical divalent heavy metals as investigated herein when their massive concentration was below 200 mg/L.	(You, Lu et al. 2017)
	Ni	Cross-flow CTA, TFC DS = NaCl	100 mg/L SWW	>96 (CTA≥TFC)	Heavy metals Ni^{2+} promoted the formation of concentration polarization, and then decreased the water flux. However, this effect decreased with the increase of FS salinity and membrane hydrophilicity.	(Zhao et al. 2016)
RO	PHN, 4CP, ATZ, CBM, SMX	Cross-flow Dow Filmtec-BW-30	2 μM SDW	ATZ (93.7), CBM (84.3), SMT (75.2), 4CP (60.9), PHN (47.3)	For the RO membrane in FO-mode, internal concentration polarization was severe and attributed to the lower porosity of the support layer of the RO membrane. The lower porosity played a dominant role in the reduction of water and/or reverse salt flux.	(Heo, Boateng et al. 2013)

Twenty six EDCs and PPCPs	Spiral wound Sahan-RE4040-FL	10-11,500 ng/L WWE	>90-99	In order to efficiently remove micro-contaminants, processes including granular AC and MF with RO are suggested due to their high removal rates. Ultimately, a multi-barrier approach using MBR followed by RO could prove the most effective in contaminant removal.	(Kim et al. 2007)
E1	Cross-flow Polyamide Cellulose acetate	100 ng/L WWE	>90 (polyamide) 30-90 (cellulose acetate)	The removal efficiency can be enhanced significantly in the presence of effluent organic matter in feed solution. The hydrophobic fraction played a paramount role in the 'enhancement effect.	(Jin, Hu et al. 2010)
E2 E3	Cross-flow Dead-end	100 ng/L SDW WWE	>85 (E2) >80 (E3) Cross-flow> dead-end	The presence of organic matter appears to enhance hormone retention. This enhancement is apparently stronger in natural water, in which organic matter generally has larger molecular weight, than that in secondary effluent.	(Nghiem, Manis et al. 2004)
E1	Dead-end Four RO membranes	100 ng/L SDW	>95	It appears that both size exclusion and adsorptive effects are instrumental in maintaining high retention of E1 on a variety of RO membranes over a range of solution conditions.	(Schafer, Nghiem et al. 2003)
Six antibiotics/three pharmaceuticals/ BPA/cholesterol	Spiral wound MBR+RO pilot	<1,500 ng/L WWE	>93	The RO removal mechanism is based on the characteristics of the membrane, the molecule being removed, and the background fluid. Despite significant differences between the tested membrane pressures, all were removed at high rates.	(Sahar, David et al. 2011)

Twelve EDCs PPCPs	Cross-flow, CTA DS = NaCl, $MgSO_4$, glucose CFV=9 cm/s	2,000 ng/L SDW	~60->95	The observed higher retention of neutral organics by the TFC membrane to a more favorable active layer structure as indicated by the larger active layer thickness to porosity ratio parameter, l/ε, and the negative membrane surface charge that induced pore hydration.	(Xie, Nghiem et al. 2014)
Thirteen EDCs and PhACs	Full-scale WW recycling plant MF+RO	1-4,000 ng/L WWE	<detection limit to <500 ng/L	The activated sludge, MF and RO processes proved to be a reliable combination for the removal of the whole range of physicochemical parameters considered.	(Al-Rifai, Khabbaz et al. 2011)
Ten EDCs and PPCPs	Pilot MBR-flat sheet MBR-hollow fiber MBR-RO	0.06-59.5 □g/L WWE	4.2->99 (MBR-RO > MBR-flat sheet/hollow fiber)	High water quality was obtained using the combined treatments MBR-RO, with removal efficiencies higher than >90% for salinity and NO3-. Therefore, the requirements for the reuse of WW can be fulfilled.	(Cartagena et al. 2013)
Atenolol, dilatin, CBM, caffeine, DCF, SMX	Pilot Polyamide TFC	54.1-206.6 ng/L WWE	<85-95 for all compounds excluding caffeine (~60)	The removal of micropollutants by the RO membrane could be predicted by their molecular weight, Log *D*, and charge characteristics.	(Chon, Cho et al. 2013)
Eighteen PPCPs charged (positive, neutral, and negative)	Cross-flow ESPA4 Polyamide TFC	2,000 ng/L SDW	>95 (positive) >95 (neutral) >99 (negative)	Model foulants caused a slight decrease in retention for most compounds, while the retention of some were significantly negatively impacted. The water flux decreased by 10%.	(D'Haese, Le-Clech et al. 2013)

Twenty PhACs	Pilot MBR+RO	17-2,020 ng/L WWE	50-95 (MBR) >99 (RO)	Size exclusion and electrostatic attraction or repulsion are supposed to be the main mechanisms involved in the removal of target compounds with RO membranes.	(Dolar, Gros et al. 2012)
Sixteen EDCs and PPCPs	Cross-flow Polyamide	0.55-610 µg/L NSW	92.5-99.9 for all the compounds excluding trimethoprim (87.1)	While CECs with low pKa and high log Kow values usually had greater removal than others, RO filtration, removed more than 90% of most CECs.	(Huang et al. 2011)
Eleven EDCs and PPCPs	Cross-flow Polyamide Cellulose acetate	100 µg/L SDW	57-91 (polyamide) <1-85 (cellulose acetate)	The dominant retention mechanism for RO membranes would be different depending on membrane material and the physicochemical properties of CECs.	(Kimura, Toshima et al. 2004)
Ten PCPs	Cross-flow TFC on polyester	1-150 ng/L WWE	<19-99	RO polished water could be used for environmental use, in aquaculture or even for industrial cooling.	(Krzeminski et al. 2017)
Ni, Zn	Cross-flow GAC+RO 1,100 kPa	44-169 mg/L (Ni) 64-170 mg/L (Zn) SDW	>98.5 (Ni) >90 (Zn)	The metal retentions seem not to be greatly affected by different conductivity and pH. EDTA increased Zn^{2+} and Ni^{2+} removal, but the effluent conductivity also increased, especially in Zn^{2+} removal.	(Ipek 2005)
Ni, Cr, Cu	Cross-flow Nitto Denko-ES20	50 mg/L SWW IWW	>98.5 (Cr>Cu>Ni)	The pH is found to influence the retention and flux of heavy metals since the charge property of surface material of polyamide low pressure RO membranes changes with pH.	(Ozaki, Sharma et al. 2002)
Ni	Cross-flow 75-300 psi	21 mg/L SWW	93.9, 95.1, 96.7,96.8 (75, 140, 220, 300 psi)	An appropriate UF pretreatment could be beneficial for reducing the fouling of RO membrane and increased the flux of RO membrane by 30–50%.	(Qin et al. 2002)

	Cr, As,	Cross-flow Polyamide TFC	100 µg/L SDW NSW	>90 (SDW > NSW)	The Cr. As, and ClO_4^- retentions by the negatively charged RO membranes are significantly greater than expected based exclusively on steric/size exclusion due to electrostatic repulsion.	(Yoon, Amy et al. 2009)
	ClO_4	Cross-flow, ultrathin nanostructured polyelectrolyted-based	10 mg/L SDW	75-95	As for retention, the highest increase was seen on going from the bare membrane to 1 bilayer and after that there was only a slight increase till 3 bilayers.	(Sanyal, Sommerfeld et al. 2015)
NF	Eleven EDCs and PPCPs	Cross-flow TFC or CA MWCOs = 15-300 Da	500 µg/L SDW/WWE	>70 excluding acetaminophen (<40)	The effect of pH on the retention of negatively charged compounds was slightly positive for NF membranes due to electrostatic repulsion at high pH.	(Acero et al. 2010)
	E1	Cross-flow MWCO = 490, 560 Da	100 ng/L SDW	10-40 after 10 hr filtration time	The presence of HA in feed solution appeared to improve E1 adsorption on membrane significantly as well as E1 retention.	(Hu et al. 2007)
	Acetaminophen, amoxicillin, cephalexin, indomethacin, tetracycline	Cross-flow TFC Varying pH and pressure	500 µg/L SDW	35->99 w/ and w/o alginate	The PhACs retention was influenced by pH, ionic strength, and transmembrane pressure, and those effects were a function of structure and property of the PhACs and properties of the membrane.	(Zazouli, Susanto et al. 2009)
	CBM, acetaminophen, atenolol, diatrozate	Cross-flow Polypierazine Pore radius = 0.128-0.258 nm	750 µg/L WWE	90-95 by 0.128 nm pore radius 20-90 by 0.258 nm pore radius	The study of the retention of neutral compounds by virgin and pre-fouled membrane demonstrated that the retention was governed by steric hindrance and then was poorly influenced by fouling.	(Azais, Mendret et al. 2014)

Organic acids including ibuprofen, glutaric acid, acetic acid	Cross-flow TFC polyamide MWCO = 200-300 Da	1.5-13.2 mg/L SDW	~30-70 (IBP) ~20-<95 (glutaric acid) ~10-80 (acetic acid)	The retention of negatively charged organic acids by NF membranes resulted in a larger retention than expected based on steric/size exclusions due to electrostatic repulsion between solute and membrane as driving factor for retention.	(Bellona and Drewes 2005)
Ten EDCs and PPCPs	Pilot MBR-flat sheet MBR-hollow fiber MBR-NF	0.06-59.5 µg/L WWE	4.2->99 (MBR-NF > MBR-flat sheet/hollow fiber)	While using MBR treatment alone cannot completely remove all the contaminants studied. nicotine, caffeine, ibuprofen and acetaminophen were completely removed from the liquid fraction by this treatment.	(Cartagena, El Kaddouri et al. 2013)
Acetaminophen, SMX, TCS	Cross-flow MWCO = 300-550 Da	500 µg/L SDW NOM/calcium ions	<10 (acetaminophen) 35-80 (SMX) 80-95 (TCS)	For small and neutral-charged target compounds such as acetaminophen, the presence of humic acid and calcium ions increased retention due to an extra hindrance layer provided by the foulants.	(Chang et al. 2012)
Eleven EDCs and PPCPs	MBR-NF Cross-flow MWCO = 210 Da	26.2-433.9 ng/L WWE	<1-80 (MBR alone) 78->99 (MBR-NF)	The most important factor influencing fouling formation was the characteristics of the dissolved organic matter in the feed water rather than membrane properties.	(Chon et al. 2011)
Eighteen PPCPs charged (positive, neutral, and negative)	Cross-flow NF270 Polyamide TFC	2,000 ng/L SDW	60-90 (positive) 75-95 (neutral) 85->99 (negative)	For positively charged or neutral compounds, the NF retention is more variable and lower. The relatively low retention by NF is likely caused by decreased steric hindrance in NF due to larger pore size.	(D'Haese, Le-Clech et al. 2013)
Twelve PhACs	Pilot scale MWCO = 200 Da	<1-58.8 ng/L NSW	<1-76 (conventional treatment)	The use of this kind of containerized pilot plant, powered exclusively by a hybrid renewable energy system, allows treating	(Garcia-Vaquero

			24->99 (NF)	efficiently and sustainably drinking water resources.	et al. 2014)
CBM, diatrizoate	Cross-flow Polyamide TFC	800 µg/L SDW WWE	53-92 (CBM) 96-98 (diatrizoate)	Both season and water matrix influence the dissolved organic matter composition and consequently retention of low molecular weight compounds with medium hydrophobicity by loose membranes.	(Gur-Reznik, Koren-Menashe et al. 2011)
BPA, IBP	Cross-flow Surface modified NF	1000 µg/L SDW	75-95 (BPA) >95 (IBP)	Graft polymerization on the raw NF membrane increased the hydrophilicity and negative surface charge of the membrane in proportion to the amount of carboxylic acid in the grafted polymer chains.	(Kim, Park et al. 2008)
Clofibric acid, DCF, ketoprofen, CBM, primidone	Cross-flow MWCO = 150 Da	100 ng/L SDW WWE	50-70 (deionized water) 90-95 (MBR effluent) 70-95 (tertiary effluent)	Two mechanisms for the increase in PhAC removal of caused by macromolecules remaining in the WW effluents: modification of the membrane surface due to membrane fouling and association between the macromolecules and the pharmaceuticals.	(Kimura, Iwase et al. 2009)
Eight PhACs	Cross-flow TFC	10 mg/L SWW	99-99.4	Relating the solute retentions to membranes' porosity has shown that the dominant retention mechanism of the examined unionazable antibiotics by all the membranes was the size exclusion effect.	(Kosutic et al. 2007)
Ten PCPs	Cross-flow Polyamide TFC	1-150 ng/L WWE	13-99	Membrane filtration provides sufficient removal of chemical contaminants and a potent hygienic barrier for bacteria.	(Krzeminski, Schwerm

		MWCO = 150-400 Da				er et al. 2017)
	Seventeen PhACs	Dead-end, NF200 MWCO = 200-300 Da	10 µg/L SDW	35-99 depending on water chemistry conditions	The solution chemistry, organic matter and salinity affect the retention of tetracycline's and sulfanamides and selected hormones by NF membranes.	(Koyuncu et al. 2008)
	ClO_4	Cross-flow MWCO = 200, 210, 350 Da	100 µg/L SDW	<5-50 (350 Da) >90 (200, 210 Da)	The results suggest that the solution chemistry condition of feed water affects perchlorate removal efficiency.	(Lee et al. 2008)
	ClO_4	Cross-flow, ultrathin nanostructured polyelectrolyted-based	10 mg/L SDW	70-90	The modified membrane had higher permeability, while the perchlorate retention was not significantly enhanced at the same conditions of feed concentration and pressure.	(Sanyal, Sommerfeld et al. 2015)
	Cr, As, ClO_4	Cross-flow Polyamide TFC MWCO = 200, 400 Da	100 µg/L SDW NSW	45-75 (ClO_4) 75-95 (Cr, As)	The results also show that retention of ions by negatively charged NF membranes is significantly influenced by solution pH.	(Yoon, Amy et al. 2009)
UF	Herbicides (chlortoluron, isoproturon, diuron, linuron)	Cross-flow Polyamide TFC MWCOs = 2–20 kDa	5-50 µM SDW	35-85 w/ NOM 40-90 w/o NOM	The retention efficiency of the tested UF membranes followed the sequence linuron > diuron > chlortoluron > isoproturon and agreed well with their values of log Kow and with the sequence of adsorbed mass of herbicide on the membrane.	(Acero et al. 2009)

Benzotriazole, DEET, 3-methylindole, chlorophene, nortriptyline	Cross-flow Hollow fiber cellulose acetate MWCO = 100 kDa	1 μM SDW WWE	<5	Effluent organic matter competitive effect was more noticeable for the PPCPs less amenable to adsorption; the less hydrophobic compounds, benzotriazole, DEET and methylindole.	(Rodriguez, Campinas et al. 2016)
Sixteen PhACs	Cross-flow MWCO = 100 kDa	<10-2,500 ng/L SDW	<5-95 (UF) 20-95 (PAC+UF)	The combination of PAC and UF in-line treatment yielded an average removal efficiency of 90.3% that tailors the strengths of and eliminates the flaws of the two (PAC and UF) individual techniques.	(Sheng, Nnanna et al. 2016)
Sixteen EDCs and PPCPs	Hollow fiber Pore size = 0.04 Outside-in	1,000 ng/L Three NSW	<5-40 (Lake Ontario) 10-90 (Lake Simcoe) 30-90 (Otonabee River)	The results indicated that retention was influenced by the specific water matrix characteristics, with increased retention in waters with higher concentrations of organic matter, including biopolymers.	(Wray, Andrews et al. 2014)
Eleven EDCs and PPCP	Cross-flow Polyamide TFC MWCOs = 2-20 kDa	500 μg/L SDW/WWE	<60 excluding hydroxybiphenyl (>90)	The effect of pH on the retention of negatively charged compounds was negative for UF membranes due to the decrease of adsorption at high pH.	(Acero, Benitez et al. 2010)
E2	Dead-end Sulfonated PES MWCO = 8 kDa	0.1, 0.5 μM SDW	10-20 w/ NOM 60-95 w/o NOM	E2 removal by UF membranes is clearly governed by hydrophobic adsorption during initial operation due to the hydrophobicity of the compound. However, size exclusion can be a very significant removal mechanism once steady-state operation is achieved.	(Yoon, Westerhoff et al. 2004)

Fifty two EDCs and PPCPs	Dead-end Sulfonated PES MWCO = 8 kDa	2-250 ng/L RO isolate NOM water Three different NSW	<10 (Group I compounds) 30-80 (Group II compounds)	More polar, less volatile, and less hydrophobic Group I compounds had less retention than less polar, more volatile, and more hydrophobic Group II compounds, indicating that retention by UF is clearly governed by hydrophobic adsorption.	(Yoon, Westerhoff et al. 2006)
E2, E3, progesterone, testosterone	Dead-end MWCOs = 1 -100 kDa	100 ng/L SDW	20-50 (E2) 15-40 (E3) 35-65 (progesterone) 5-30 (testosterone)	While UF would not be applied to remove micropollutants alone, it can be used as a pre-treatment step prior to RO or as a separation stage in a membrane bioreactor or hybrid process, such as powdered activated carbon-UF.	(Neale and Schafer 2012)
Amoxicillin, cefuroxime axetil	Hollow fiber Spiral wound	20 mg/L WWE	70-71 (hollow fiber) 90-91 (spiral wound)	UF was not sufficient for removing either amoxicillin trihydrate or cefuroxime axetil to a safe level.	(Awwad et al. 2015)
Atenolol, dilatin, CBM, caffeine, DCF, SMX	Pilot Hollow fiber Polyvinylidene fluoride	54.1-206.6 ng/L WWE	<40 (DCF > SMX > caffeine > others)	Most of the micropolluants were not effectively removed using the UF membrane (<17%), with the exception of diclofenac and sulfamethoxazole.	(Chon, Cho et al. 2013)
E1, E2, E3, EE2, BPA	Dead-end MWCO = 100 kDa	100 µg/L WWE	10-90 (BPA > EE2 ≥ E2 ≥ E1 > E3)	Membrane fouling improved EDCs removal by 0%–58.3% and different enhancements were owing to the different porosity and hydrophilicity of cakes that grew under different pressures.	(Hu, Si et al. 2014)

Ten PCPs	Cross-flow MWCO = 1k, 10 kDa	1-150 ng/L WWE	<1-99	Since the nominal pore sizes of the applied UF membranes are in range of 1-10 kDa, the size exclusion was not a major mechanism in removal of CECs having molecular sizes in range of 200–400 Da.	(Krzeminski, Schwermer et al. 2017)
SMX, CBM, carbamazepine, mecoprop, DCF, benzotriazole	Pilot PAC-UF Pore size = 20, 40 nm	200-4,300 µg/L WWE	35-95	Both UF membrane systems proved to be well compatible with the application of PAC showing no sign of abrasion, pore blockage or other negative impacts.	(Lowenberg et al. 2014)
Cr, As, ClO_4	Cross-flow MWCO = 8 kDa	100 µg/L SDW NSW	30-60 (ClO_4) 40-70 (Cr) 7-90 (As)	The retention of the target toxic ions decreases with increasing solution conductivity for the membrane due to a reduction of electrostatic repulsion with increasing conductivity.	(Yoon, Amy et al. 2009)
Cu, Ni, Cr	Polymer-enhanced polyethersulfone Hollow fiber UF (10 kDa)	10-100 mg/L IWW	94.4-95.1 (Ni(II)) 98-98.6 (Cu(II)) 98.3-99.1 (Cr(III))	The complexation and filtration processes are pH dependent, the metal retention was more efficient at neutral and alkaline conditions than at acidic one.	(Barakat and Schmidt 2010)
Cd, Zn	Dead-end MWCO = 13 kDa Complexation-assisted UF	50 mg/L SDW	>95 (Cd) >99 (Zn)	At varying pH values, it is possible to perform the removal of metals obtaining high retention coefficients resulting in recovery of the concentrated metal present in feed and regeneration of the complexing agent applied.	(Trivunac and Stevanovic 2006)
ClO_4	Dead-end	1 mM NGW	10-90	The polyelectrolyte enhanced UF can be an extremely effective alternative to the ion-	(Huq et al. 2007)

	MWCO = 3 and 10 kDa			exchange method if applied with proper engineering skills focusing on environmental aspects.	
ClO_4	Dead-end Adsorption -UF MWCO = 3k-100 kDa	10 mg/L SDW	35-95 (increased with increasing chitosan dosage)	Due to the electrostatic attraction between positively charged chitosan surfaces and negatively charged ClO4 ions, ClO4 was trapped by chitosan molecule and then concentrated by UF process.	(Xie et al. 2011)
ClO_4	Cross-flow Surfactant modified MWCO = 8 kDa	100 μg/L SDW NSW	80 (SDW) >5-80 (NSW)	ClO_4 retention by a UF membrane modified with cationic surfactant was greater than expected, based mostly on steric/size exclusion as a result of a decrease of the membrane pore size.	(Yoon et al. 2003)

CA = cellulose acetate; C_0 = CEC initial concentration; GAC = granular activated carbon; NOM = natural organic matter; COD = chemical oxygen demand; PAC = powdered activated carbon; SDW = synthetic drinking water; NSW = natural surface water; IWW; industrial wastewater; NGW = natural groundwater; SWW = synthetic wastewater; WWE: WW effluent.

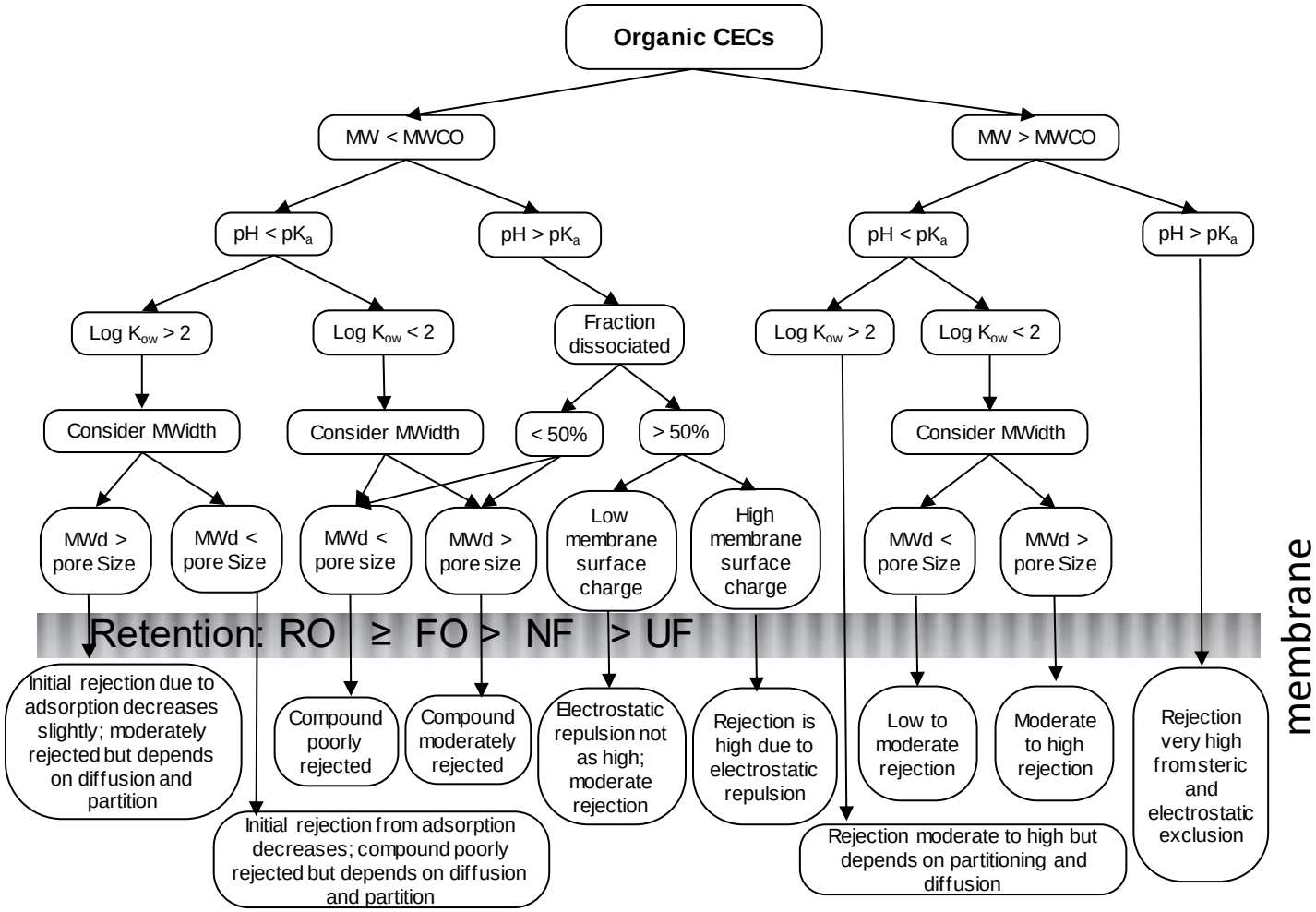

Figure 3.3 Retention diagram for organic CECs during membrane treatment based on solute and membrane properties adopted from (Bellona, Drewes et al. 2004).

CHAPTER 4

MATERIALS AND METHODS

4.1 Preparation of adsorbents

A sample of ABC was prepared in the laboratory. A loblolly pine sample with bark (15 mm × 6 mm) was dried at 300°C for 15 min in a bath-type tube-furnace to produce ABC. A gas of 7% oxygen and 93% nitrogen was used in the experiments, as described elsewhere (Jung, Park et al. 2013). The biochar was activated with 4 M NaOH for 2 h and dried overnight at 105°C. Then the ABC was separated from the NaOH solution using a Buchner filter funnel, heated at 800°C for 2 h under a 2 L/min nitrogen gas flow, and cooled at a rate of 10°C/min. The dried ABC was rinsed alternately with deionized (DI) water and 0.1 M HCl to obtain pH 7 and dried again at 105°C. Finally, the ABC was milled and passed through a 74-µm sieve.

To prepare two MOFs in our laboratory, iron chips (99.98%), and trimesic acid (BTC, 95%) for MIL-100(Fe), and chrome(III) nitrate nonahydrate ($Cr(NO_3)_3 \cdot 9H_2O$, 99%), and terephthalic acid (TPA, 98%) for MIL-101(Cr), were purchased from Sigma-Aldrich. Nitric acid (HNO_3, 60%), hydrofluoric acid (HF, 40%), and reagent alcohol (CH_3CH_2OH, ≤ 0.003%) were also obtained from Sigma-Aldrich. MIL-100(Fe) (Horcajada et al. 2007) and MIL-101(Cr) (Férey et al. 2005) were synthesized by the solvothermal method following protocols reported in the literature with some modifications. Briefly, for the MIL-100(Fe), 1.0 Fe^0:0.67 BTC:1.2 HNO_3:2.0 HF:280 DI

water was placed in a Teflon-lined steel autoclave. The autoclave was then placed in an electric oven at 150°C for 12 h. After cooling, the solid orange products were recovered by filtration using a 10 µm glass filter. The as-synthesized MIL-100(Fe) was purified in two steps using DI water at 90°C for 3 h, and reagent alcohol at 65°C for 5 h. After filtration, the purified MIL-100(Fe) was dried at 100°C overnight and stored in a desiccator. The reactant composition for the MIL-101(Cr) was 1.0 $Cr(NO_3)_3 \cdot 9H_2O$:1.0 TPA:1.0 HF:300 DI water, which was loaded in a Teflon-lined autoclave and placed in an electric oven at 210°C for 8 h. After cooling to room temperature, the green-colored solids in the solution were filtered twice consecutively using 25 and 10 µm glass filters. Then, to further purify the products, the as-synthesized MIL-101(Cr) was treated with reagent alcohol at 100°C for 20 h, filtered off, and dried overnight at 100°C. The purified MIL-101(Cr) was stored in a desiccator.

$Ti_3C_2T_x$ MXene was purchased from the Advanced Materials Development Expert Store (Hangzhou, Zhejiang, China). Furthermore, two kinds of commercially available PAC were purchased from Sigma-Aldrich (Darco-KB-G; St. Louis, MO, USA) for chapter 5, and from Evoque Water Technologies (Randolph, MA, USA) for chapter 6 and 7.

4.2 Characterization

The ABC was characterized via an elemental analysis (2400 Series II elemental analyzer; PerkinElmer, Waltham, MA, USA). In addition, the Brunauer-Emmett-Teller (BET) specific surface area (SSA) and Barrett-Joyner-Halenda (BJH) pore volume (N_2 at $P/P_0 = 0.95$) were measured using a surface analyzer (Germini VII 2390; Micromeritics, Norcross, GA, USA).

The structure of the MOFs was confirmed by X-ray diffraction (XRD) patterns, which were collected on an UTIMA III X-ray diffractometer (Rigaku, Tokyo, Japan) using Cu Kα radiation (λ = 1.5418 Å) while operating at 40 kV and 44 mA. The Fourier transform-infrared (FT-IR) spectra were obtained using a Frontier spectrometer (PerkinElmer, Waltham, MA, USA), following the KBr pellet technique to detect the presence of functional groups. The morphology and element distribution of the MOFs was analyzed by transmission electron microscopy coupled with energy-dispersive spectroscopy (TEM-EDS) using a Titan G2 ChemiSTEM Cs Probe (FEI, Eindhoven, The Netherlands). X-ray photoelectron spectroscopy (XPS) measurements were carried out on a Quantera SXM (Physical Electronics, Inc., Chanhassen, MN, USA) with Al Kα X-ray as the excitation source, to confirm the surface electronic states of the synthesized MOFs. Nitrogen adsorption and desorption equilibrium data were gathered at -196˚C using a Micromeritics ASAP 2020 static volumetric adsorption unit (Micromeritics Inc., Norcross, GA, USA). These data were used to estimate the materials textural properties. Prior to each analysis, MOFs were degassed at 150˚C under high vacuum for 12 hours. Surface area was estimated using Brunauer-Emmett-Teller (BET) and Langmuir models. Pore diameter and pore volume were evaluated using the Barrett-Joyner-Halenda (BJH) method, and we obtained pore size distributions (PSDs) using Horvath-Kawazoe (H-K) and BJH analyses methods and to cover micropore and mesopore regions, respectively (Rege and Yang 2000, Lowell et al. 2012).

The physicochemical properties of the MXene were analyzed using several instruments. SEM (S-4200; Hitachi, Tokyo, Japan) and TEM (Titan G2; FEI, Hillsboro, OR, USA) were used for surface morphology characterization, and the structure of the

MXene was confirmed by XRD (D/max-2500; Rigaku, Tokyo, Japan). Surface charge was measured using a zeta potential analyzer (ZetaPals; Brookhaven Instruments Corporation, Holtsville, NY, USA). Finally, a Micromeritics ASAP 2020 static volumetric adsorption unit (Micromeritics Inc., Norcross, GA, USA) was used to obtain nitrogen adsorption and desorption equilibrium data at -196°C. The surface area of the MXene was estimated based on these data using Brunauer-Emmett-Teller (BET) models.

4.3 Target organic contaminants and analytical method

4.3.1 Selected PhACs for chapter 5

The three PhACs (IBP, EE2, and CBM) selected for chapter 5 were purchased from Sigma-Aldrich. Ibuprofen (IBP) is pain killer PhAC that is used globally as a nonsteroidal anti-inflammatory drug (Essandoh et al. 2015). The synthetic hormone, 17 α-ethinyl estradiol (EE2) has become a widespread problem because it readily accumulates in sediment and is highly resistant to decomposition (He et al. 2018). Carbamazepine (CBM) is the most widely prescribed pharmaceutical for epilepsy and readily bioaccumulates in the aquatic environment (Monteagudo et al. 2015). Detailed physicochemical properties are summarized in Table 4.1. These compounds have different characteristics, such as molar weight, acid dissociation constant (pK_a), and octanol-water partition coefficient (K_{OW}). The 10 mM stock solutions of IBP, EE2, and CBM were prepared in methanol to achieve a cosolvent effect. Each solution of 10 µM concentration was placed in a separate beaker and the methanol was evaporated, before dilution with ultra-pure DI water. To ensure the same level of methanol evaporation, each beaker was under a fume hood at room temperature for 2 h.

The pH and conductivity were adjusted to desired values (*e.g.*, pH 3.5, 7, and 10.5; conductivity 300 µS/cm) using 1 M HCl or NaOH with 1 mM phosphate buffer solution and 0.1 M NaCl, respectively. Humic acid (HA), one of the most commonly dissolved NOM compounds, was purchased from Sigma-Aldrich. First, 1,000 mg/L of HA stock solution was prepared in DI water and filtered sequentially through a 0.45 µm filter. This HA stock solution was then further diluted with DI water to 5 mg/L and dissolved organic carbon (DOC) was added in several separate experiments.

The concentrations of IBP, EE2, and CBM were analyzed using high-performance liquid chromatography with UV detection (100 Series; Agilent, Santa Clara, CA, USA). Compounds were placed in a 2 mL amber vial. A 5 µm column (Atlantis T3; Waters, Milford, MA, USA) was used at a flow rate of 1.2 mL/min. The mobile phase was a 60:40 (v/v) mixture of acetonitrile and phosphoric acid (5 mM). The concentration of HA was measured using UV-vis spectroscopy (8453; Agilent) at a wavelength of 254 nm. A ZetaPALS Analyzer (Brookhaven, USA) was used to determine the zeta potential of ABC and PAC.

4.3.2 Selected PhACs and three ratios of NOM for chapter 6

Two PhACs, IBP and EE2, were purchased from Sigma-Aldrich (St. Louis, MO, USA). Their detailed physicochemical properties are summarized in Table 4.1. The 10 mM stock solution of IBP and EE2, which were prepared in methanol, was placed in a separate beaker and diluted with deionized (DI) water to achieve an initial concentration of 10 µM. HA and TA were purchased from Sigma-Aldrich. Three different HA:TA ratios were used, all with total dissolved organic carbon concentrations (DOCs) of 10 mg/L. NOM 1, NOM

Table 4.1 Physicochemical properties of the selected PhACs and dyes.

Compound (Formula) [ID]	Structure	MW (g/mol)	log D_{OW}[a] pH 3.5	pH 7.0	pH 10.5	Log K_{OW}	pK_a[a]	Mol. Dimension (Å)[b]	Vol[a] (Å^3)	Mol. Polarity[a]	π Energy[a]
Ibuprofen ($C_{13}H_{18}O_2$) [IBP]	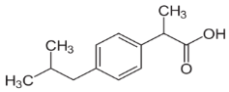	206.3	3.84	1.82	0.60	3.84	4.52	L: 10.98 H: 4.33 W: 5.31	211.8	23.7	15.7
17 α-ethinylestradiol ($C_{20}H_{24}O_2$) [EE2]	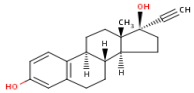	296.4	3.90	3.90	3.57	3.90	10.47	L: 12.28 H: 6.23 W: 3.77	291.7	33.9	18.5
Carbamazepine ($C_{15}H_{12}N_2O$) [CBM]	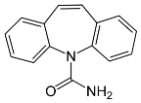	236.3	2.77	2.77	2.77	2.77	13.96	L: 9.43 H: 5.92 W: 7.38	210.3	27.0	29.1
Methylene blue ($C_{16}H_{18}ClN_3S$) [MB]		319.9	2.58	2.60	2.60	0.75	3.14	L: 14.2 H: 6.20 W: 1.60	262.1	N/A	N/A
Methyl orange ($C_{14}H_{14}N_3NaO_3S$) [MO]		327.3	2.38	1.29	1.29	N/A	3.58	L: 16.1 H: 6.10 W: 5.20	258.9	N/A	N/A

[a]chemicalize.org by ChemAxon; [b]Molecular dimensions calculated using MacMolPlt v.7.4

2, and NOM 3 correspond to 10:0, 5:5, 0:10 (HA:TA), respectively. In order to achieve the desired pH and background conductivity, each feed solution was adjusted by 1 M HCl or NaOH, and 0.1 M NaCl, respectively. Commercially available PAC (Evoqua Water Technologies, Pittsburgh, PA, USA) was used as a control group for the MOF.

The selected PhACs were collected into a 2 mL amber vial, and the concentrations of the compounds were measured by high-performance liquid chromatography with an ultraviolet (UV) detector (1200 Series; Agilent, Santa Clara, CA, USA). The single NOM (HA or TA) solutions were analyzed using a total organic carbon analyzer (Shimadzu, Kyoto, Japan) to determine the DOC concentration, and by an UV-visible (UV-Vis) spectrometer (DR-6000; Hach, Loveland, CO, USA). To obtain mixed NOM solutions, because HA is precipitated, whereas TA is stable under acidic conditions, we separated them by precipitation using a 5 M HCl at a pH value of 1.5. After the mixed sample had been separated over 24 h, we filtered it and then performed the DOC and UV-vis analyses.

4.3.3 Selected dyes for chapter 7

MB and MO, as target dye contaminants, were purchased from Sigma-Aldrich (St. Louis, MO, USA). The concentration of these compounds was determined using UV-vis spectrophotometer (Agilent Technologies, Santa Clara, CA, USA) based on absorbance at 464 and 665 nm, respectively. A commercial flat sheet polyamide membrane was acquired from GE Osmonics Inc. (Minnetonka, MN, USA). The physicochemical properties of the target compounds are summarized in Tables 4.1. To evaluate the effect of a range of water conditions on the treatment system, humic acid (HA) was used as the most dissolved NOM compound, HCl and NaOH were used to evaluate the effect of pH, and NaCl, $CaCl_2$, and

Na_2SO_4 were used to investigate the effect of background ions (all purchased from Sigma-Aldrich).

4.4 Operation of the adsorbent-UF system

A commercial flat sheet polyamide UF membrane was purchased from GE Osmonics Inc. (Minnetonka, MN, USA). The membrane properties are described in Table 4.2. The pure water permeability (PWP) test and hybrid system test were conducted in a dead-end cell filtration system (HP4750; Sterlitech Co., Kent, WA, USA) with a 14.6 cm^2 active membrane area and 300 mL total feed volume. The dead-end cell filtration system was described in Figure 4.1. Only membranes with ≤ 10% permeability change, based on the PWP test, were used for this study. The UF membrane was washed at least three times with DI water and stored by soaking in DI water at 4°C, away from direct light, prior to use. A mixed compound solution was used for the adsorbent-UF system experiment.

The membrane experiments were conducted with the transmembrane pressure and stirring speed set to 520 kPa (75 psi) and 300 rpm, respectively. To analyze the retention rate of selected compounds, permeate samples were obtained every 20 mL until a permeate volume of 240 mL and retentate volume of 60 mL was reached, corresponding to a volume concentration factor (VCF) of 5. The VCF (ratio of initial feed volume to concentrate volume) was calculated using Eq. (4.1) (Naidu et al. 2017):

$$VCF = \frac{V_F}{V_R} = 1 + \frac{V_P}{V_R} \tag{4.1}$$

where V_F (mL), V_P (mL), and V_R (mL) are the initial volume of feed, volume of permeate, and volume of retentate, respectively.

Table 4.2 Specifications of UF membrane used in this study.

Parameter	Value
Manufacturer/product name	GE Osmonics/GK
Material[a]	Polyamide thin film composite
MWCO (Da)[a]	3,000
Pore size (Å)	26-30
Zeta potential at pH 7 (mV)	-32.6
PWP (L/d/m^2/kPa)	1.06

[a]Data obtained from the manufacturer.

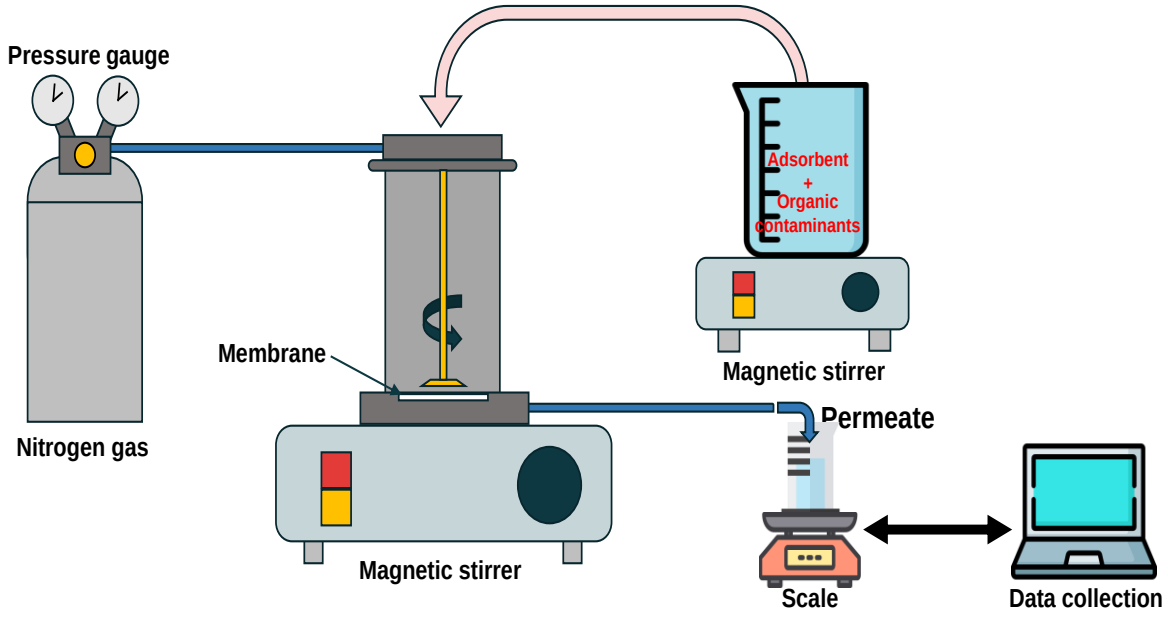

Figure 4.1 Overall schematic of dead-cell filtration system.

4.4.1 Operation of the adsorbent-UF system for chapter 5

Each 10 μM of the initial concentration of IBP, EE2, and CBM was blended in the presence and absence of 10 mg/L of ABC and 5 mg/L of HA for 4 h at 300 rpm before the membrane experiments. In many water treatment plants, the adsorption process is generally applied at 5–50 mg/L with contact times of 1–5 h (Yoon et al. 2003).

4.4.2 Operation of the adsorbent-UF system for chapter 6

Both the PhACs and NOM in three different ratios, were mixed with 20 mg/L of MOF for 2 h at 200 rpm for upstream adsorption. The adsorption conditions generally applied in water treatment plants (*i.e.*, 5–50 mg/L with contact time of 1–5 h) were used (Yoon et al. 2003, Kim et al. 2019).

4.4.2 Operation of the adsorbent-UF system for chapter 7

As the pretreatment, adsorption was performed with 2 mg/L of the selected dye and 20 mg/L of adsorbent for 2 h at 200 rpm. Generally, 5–50 mg/L of adsorbent and a contact time of 1–5 h are used in water treatment plants (Kim et al. 2020).

4.5 Evaluation of adsorbent-UF performance

In the membrane experiments, the retention rate of selected PhACs and flux decline were investigated to evaluate the UF-ABC system. The retention rate is defined by Eq. (4.2):

$$Retention\ (\%) = \left(1 - \frac{C_{p,VCF}}{C_{f,0}}\right) \times 100 \tag{4.2}$$

where $C_{f,0}$ (mg/L) is the initial concentration of selected pharmaceuticals in feed, $C_{p,VCF}$ (mg/L) is the concentration in permeate at corresponding VCF. The dominant mechanism of compound removal was analyzed based on retention rate, obtained via a mass balance. For the UF membrane process, there are various removal mechanisms, including those based on size/steric exclusion, adsorption, and charge effect. However, the rate of removal of IBP, EE2, and CBM is mainly determined by both adsorption and charge effect, while size/steric exclusion plays a negligible role because the compounds are too small relative to the membrane pore. Therefore, retention of mass is equal to the sum of retention of adsorption and charge effect, as quantified by Eq. (4.3):

$$Retention_{mass}\ (\%) = Retention_{adsorption}\ (\%) + Retention_{charge}\ (\%) \qquad (4.3)$$

An electronic balance (AV8101C; Ohaus, Parsippany, NJ, USA) was used to determine the permeate mass, and the flux decline was calculated using Eq. (4.4):

$$\mathrm{J} = \frac{d_m}{\rho A_m d_t} \qquad (4.4)$$

where J is the permeate flux (L/m^2/h), m is the mass of permeate (kg), ρ is the density of permeate solution at 20°C, A_m is the active membrane area (m^2), and t is the sampling time (h). The obtained permeate fluxes were converted to normalized fluxes, which is the flux at the VCF divided by the corresponding initial flux; these fluxes were used to evaluate the membrane fouling of each system. Furthermore, a resistance-in-series model was used to predict the solute molecule transportation mechanisms in the UF-only and hybrid systems. In membrane filtration, Darcy's expression is commonly used to evaluate the permeate flux (Crittenden et al. 2012, Mulder 2012):

$$J = \frac{\Delta P}{\eta(R_m + R_f)} = \frac{\Delta P}{\eta(R_m + R_{re} + R_{irr})} = \frac{\Delta P}{\eta(R_m + R_c + R_{ad})} \quad (4.4)$$

where ΔP is the pressure drop across the membrane (kPa), η is the dynamic viscosity of the solvent (kg/m/s), and Rm is the hydrodynamic membrane resistance (1/m). The membrane fouling resistance (R_f) is subdivided into reversible resistance (R_{re}), and irreversible resistance (R_{irr}), corresponding to the cake layer resistance (R_c) and adsorptive fouling resistance (R_{ad}), respectively. We used the previously defined equations to evaluate the proportions of these different resistance types.

The cake filtration model represents one method for evaluating the fouling mechanism. This model is widely applied to assess the membrane filtration index (MFI) under constant pressure filtration. The MFI is determined as the second linear slope line obtained from plotting *t/V* against *V* (Mulder 2012, Dhakal et al. 2018).

$$\frac{t}{V} = \frac{\eta\, R_m}{A\, \Delta P} t + \frac{\eta\, \alpha\, C_f}{2\, \Delta P} V == \frac{\eta\, R_m}{A\, \Delta P} t + MFI \cdot V \quad (4.5)$$

Where *t* is the filtration time (h), *V* is the permeate volume (m^3), *A* is the effective membrane area (m^2), C_f is the dye concentration in the feed (mg/L), and α is the specific cake resistance for each cake layer (m/g). Permeate flux modeling can also be used to calculate the MFI, as a quarter of the β constant in Eq. (4.6), which can be simply expressed in the form $J^2 = (\alpha + \beta t)^{-1}$ (Danis and Aydiner 2009).

$$J^2 = \left[\left(\frac{\eta\, R_m}{\Delta P}\right)^2 + \left(\frac{2\, \eta\, \alpha\, C_f}{\Delta P}\right) t\right]^{-1} \quad (4.6)$$

The model constants α and β were obtained using SigmaPlot 12.3 software (Systat Software, Inc., San Jose, CA, USA) to allow performance of a non-linear regression analysis.

Finally, four conceptual blocking law models incorporating specific operating conditions, including constant pressure, a cylindrical membrane pore, and non-Newtonian fluids were used to explain the fouling mechanisms, as shown in as Eq. (4.7) (Hermia 1982, Aslam et al. 2015).

$$\frac{\mathrm{d}^2 t}{dV^2} = \mathrm{k}(\frac{dt}{dV})^n \tag{4.7}$$

where n is the blocking index, set at 2, 1.5, 1 and 0 for complete blocking, standard blocking, intermediate blocking, and cake filtration, respectively.

CHAPTER 5

REMOVAL OF SELECTED PHARMACEUTICALS IN AN ULTRAFILTRATION-ACTIVATED BIOCHAR HYBRID SYSTEM[2]

5.1 Characterization of ABC and PAC

The elemental compositions, specific surface area (SSA), and pore volume of ABC and PAC were characterized and quantified by an elemental analysis and a surface analyzer, respectively; the results are shown in Table 5.1. ABC has a higher oxygen content (13%) than PAC (7.7%), because ABC with pyrolysis in the presence of oxygen was partly combusted. While the carbon content of ABC (83.8%) was higher than that of PAC (79.1%), the ash content of ABC (2.7%) was lower than that of PAC (9.8%). In addition, the polarities [(O+N)/C] of PAC (0.07) were lower than those of ABC (0.12), indicating that PAC has a slightly higher hydrophobicity compared to ABC (Chun et al. 2004, Martín-González et al. 2014). On the other hand, the H/C ratios of 0.03 for ABC and 0.52 for PAC indicated that ABC was carbonized to a greater extent, and had a higher degree of aromatization, compared to PAC (Bagreev et al. 2004, Santamaria et al. 2010). The SSA and pore volume of the adsorbents were quantified by N_2 adsorption experiments (Table 5.1). PAC had a slightly larger specific surface and pore volume (1,264 m^2/g and 0.93 $cm^3/$

[2] Reprinted here with permission of publisher: Sewoon Kim *et al*., Removal of selected pharmaceuticals in an ultrafiltration-activated biochar hybrid system. Journal of Membrane Science 570-571 (2019) 77-84.

g, respectively) compared to lab-made ABC (1,151 m^2/g and 0.63 cm^3/g, respectively). It is notable that, although the SSA and pore volume of ABC are lower than activated carbon. Aromatic structures may inhibit the development of SSA and the porous structure of ABC (Jung, Park et al. 2013, Park et al. 2013, Shankar, Heo et al. 2017). For superior adsorption capacity, effective SSA, pore volume, and absolute aromaticity are important. Therefore, given its high degree of aromatization and porous properties, ABC made from renewable biomass is a promising adsorbent.

5.2 Retention of selected PhACs by the ABC-UF

The ABC-UF were used to evaluate the retention of selected PhACs under different pH conditions in the presence or absence of HA, as a function of the VCF (Figure 5.1). VCF is a more practical value for evaluation of retention rate and flux decline than permeate volume or time, because the physical and chemical properties of the membrane, as well as the solute retention, were significantly affected by the concentration of PhACs and HA retained at the membrane surface during membrane filtration (Lee et al. 2005, Yoon and Lueptow 2005). The average retention rates over the entire pH range were observed for UF only (24.4, 14.8, and 7.0%), ABC-UF without HA (41.8, 53.0, and 40.9%), and ABC-UF with HA (36.9, 42.5, and 23.9%) for IBP, EE2, and CBM, respectively. The average retention rates were thus in the order: IBP > EE2 > CBM in the single UF. However, EE2 had a higher retention rate than IBP and CBM in the ABC-UF.

Previous studies have shown that the retention mechanism of the UF membrane system is based on interaction between the membrane and organic compounds, and on size/

Table 5.1 Characteristics of ABC and PAC based on elemental composition, BET-N_2- surface area (SA-N_2), and cumulative pore volume.

Adsorbent	C (%)	H (%)	N (%)	O (%)	Ash (%)	H/C	Polarity index [(O+N)/C]	SSA-N_2[a] (m^2/g)	Pore volume[b] (cm^3/g)
ABC	83.8	0.2	0.3	13.0	2.7	0.03	0.12	1,151	0.63
PAC	79.1	3.4	$\leq$ 0.1	7.7	9.8	0.52	0.07	1,264	0.93

[a]Calculated using the Brunauer-Emmett-Teller (BET) equation for data in the range less than 0.1 of relative pressure.
[b]Calculated from the adsorbed quantity of N_2 at P/P_0 = 0.95 with t-plot mod.

steric exclusion (Löwenberg et al. 2014, Kim et al. 2018). Even though selected compounds are mainly found in neutral ionic forms under acidic conditions, increasing the pH converts ionic forms from neutral to negative species depending on the p*Ka* value (Jung, Park et al. 2013). This change of ionic form leads to increasing electrostatic repulsion between the membrane and compounds. Regarding the molecular weight of selected compounds (206-294 g/mol), size/static exclusion is a negligible mechanism because the used membrane pore size (1.03 nm) and nominal molecular weight cutoff (MWCO = 3,000 Da) are much larger than the compound molecules (Galanakis 2015, Castro-Muñoz et al. 2016, Castro-Muñoz et al. 2017, Cassano et al. 2018). For the ABC-UF, the following represent additional possible retention mechanisms for PhACs: π-π electron donor-acceptor (EDA), electrostatic interactions, and hydrophobic adsorption between ABC and selected compounds (Löwenberg, Zenker et al. 2014). Among these retention mechanisms, the π-π EDA interactions between ABC and selected PhACs were not considered in this study. Although π-π EDA interaction between ABC and compounds can be highly affected by the π energy level of individual compounds (Nam et al. 2015), the retention rate in this study did not suggest a strong relationship between adsorbents and adsorbates. It has been reported that hydrophobic adsorption by absorbents is primary mechanism of adsorbents-UF system (Löwenberg, Zenker et al. 2014, Secondes et al. 2014). Furthermore, our findings showed that the sharp improvement in the retention rate of ABC-UF compared to UF only can explain the effect of adsorption on ABC (Figure 5.1). Although IBP has a lower octanol-water distribution coefficient (log D_{OW} = 1.82 at pH 7, which represents hydrophobicity), above pH 7 the average retention rate of IBP is similar to or slightly higher than that of CBM. These results suggest that retention in ABC-UF is affected by both

charge effect (*i.e.*, electrostatic repulsion) and hydrophobic adsorption among compounds, ABC, and the membrane affect retention in ABC-UF.

5.3 Retention mechanism of the ABC-UF

In the UF only and ABC-UF, the retention behavior described above is affected by the coupled influence of the ionic speciation and hydrophobicity of compounds, depending on the solution pH, compound p*Ka* value, and log D_{OW}. Figure 5.2 describes in more detail the retention-based adsorption and charge effect and Figure 5.3 shows the average retention rate of target compounds at various pH conditions as log D_{OW} was changed. Despite the significant effect of solution pH on the speciation and hydrophobicity of chemicals, hydrophobic adsorption is the dominant mechanism over the entire pH range in both systems, with the exception of IBP above pH 7. The retention of IBP by charge effect increased with increasing solution pH, because the PhACs chemicals were deprived of their proton at pH values above each p*Ka* value, resulting in negative charge. This mechanism indicates that electrostatic repulsion between each compound and the membrane, as well as ABC, improved when the pH value was greater than the p*Ka* value, particularly for IBP (p*Ka* = 4.52) which has a relatively lower p*Ka* value compared to EE2 (10.47) and CBM (13.96). However, the ionized IBP is barely adsorbed on aromatic adsorbents (Jung, Park et al. 2013), resulting in sharply decreasing hydrophobicity (log D_{OW} = 3.84 at pH 3.5, log D_{OW} = 1.82 at pH 7, log D_{OW} = 0.60 at pH 10.5). Additionally, among the three PhACs, IBP is most affected by solution pH due to great variation in ionic species and hydrophobicity. For these reasons, the total retention rate of IBP was decreased by decreasing hydrophobic adsorption from pH 3.5 to 10.5. These results suggest that although

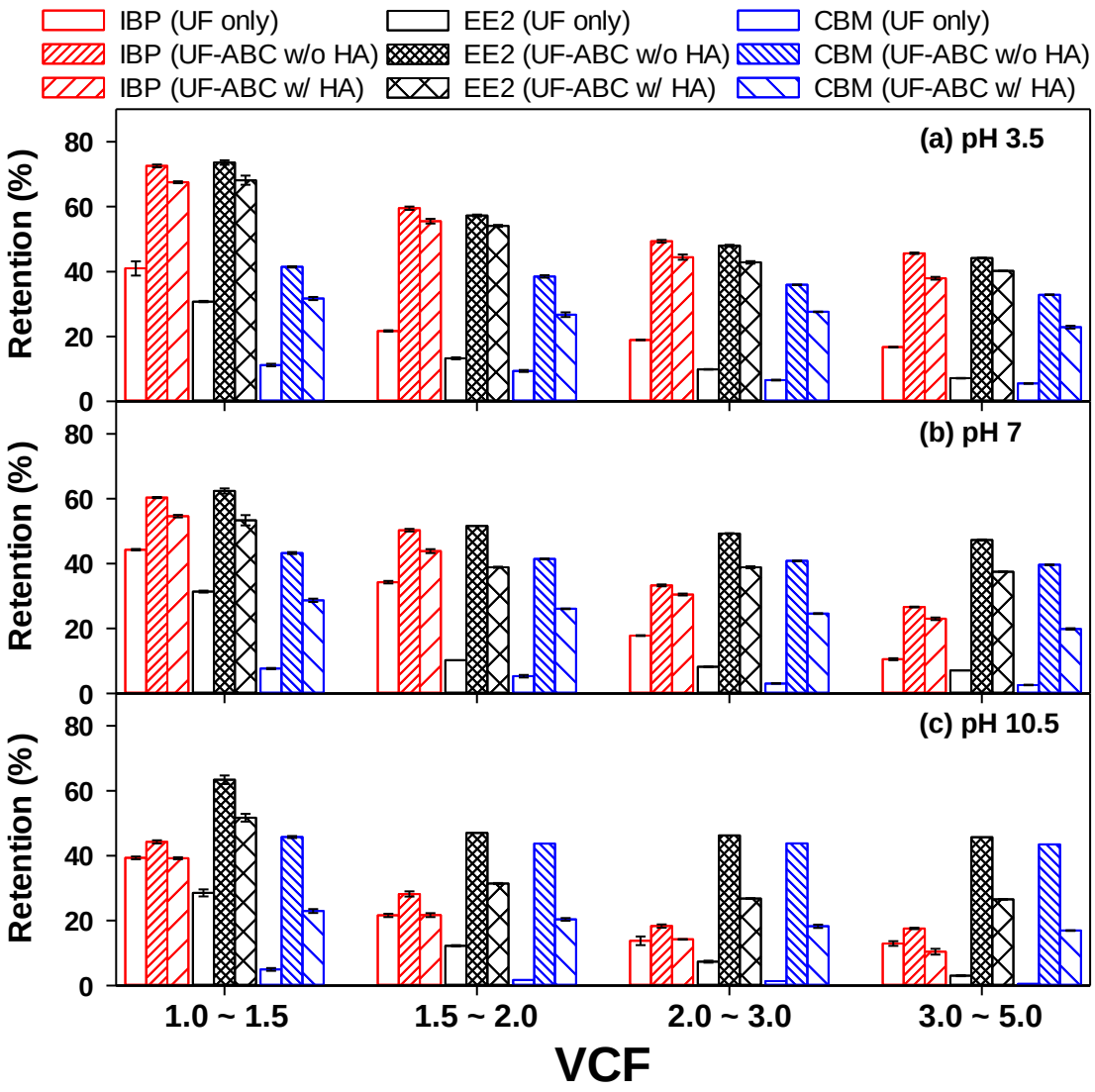

Figure 5.1 Retention of IBP, EE2, and CBM by UF only, UF-ABC without (w/o) HA, and UF-ABC with (w/) HA at varying pH conditions. Operation conditions: ΔP = 520 kPa (75 psi); stirring speed = 300 rpm; HA = 5 mg/L as DOC; ABC= 10 mg/L; conductivity = 300 μS/cm; pre-contract time with ABC and HA = 4 h.

charge effect is an important mechanism, hydrophobic adsorption was more effective in terms of retention of IBP.

The retention rates of EE2 and CBM for the three different systems was relatively constant. The ionic form of EE2 changed from neutral to negative only at pH 10.5. The dissociated EE2 improved charge effect but was not easily adsorbed on ABC or the membrane, as described previously. This phenomenon can be explained by the log D_{OW} values of EE2 of 3.90, 3.90, and 3.57 at pH 3.5, 7, and 10.5, respectively. The altered hydrophobicity of EE2 indicates that, although electrostatic repulsion is slightly increased at pH 10.5, EE2 has a constant retention rate over a wide range of pH conditions due to still relatively high hydrophobic adsorption. The CBM was non-ionizable over the pH range of the experiment, and was mostly controlled by adsorption, resulting in less variability in retention rate. In addition, the results show that adsorption on ABC can play a critical role with respect to the retention rate.

Figures 5.4 and 5.5 present the removal rate by adsorption for seven adsorbent cases in UF-ABC with HA. As a general observation, the adsorption of each compound increased with contact time (Figure 5.4), while the adsorption rate was found to vary depending on the properties of each adsorbent (Figure 5.5). Removal by adsorption of the selected PhACs increased significantly in the presence of both ABC and membrane, because chemicals can be adsorbed on both materials. This explains why the retention rate of IBP was higher than that of EE2 and CBM in the UF only process: IBP, which is the most negatively charged among the selected PhACs, is retained more on the feed side. In the ABC-UF system, hydrophobic adsorption on the ABC is the dominant mechanism and the rate of chemical removal positively correlates with the hydrophobicity of each of the

selected PhACs. The adsorption of organic compounds could be improved with HA due to HA-PhACs partitioning (Heo et al. 2012). However, competition for adsorption sites between HA and the chemicals was greater relative to the adsorption of chemicals on the HA.

5.4 Flux decline in the ABC-UF

Based on the retention rate and mechanism for selected PhACs, the ABC-UF is a potential replacement for the UF only system. Therefore, permeate flux was analyzed for the single UF and ABC-UF in the presence/absence of HA, to evaluate the hybrid system. Normalized flux declining trends are shown in Figure 5.6, at three pH conditions as a function of the VCF. The normalized flux was defined as the current permeate flux divided by the flux of the virgin membrane under comparable conditions. Because flux is similar for the three compounds, the average flux at each condition is represented by a single point with a standard deviation. The normalized flux of single UF and ABC-UF without HA gradually decreased with increasing VCF. These systems show similar flux behavior regardless of pH conditions, achieving a flux of approximately 0.85. This result indicates that, although ABC is expected to cause serious fouling compared with single UF, ABC does not strongly affect the permeate flux decline in the absence of HA when compared with the UF only system. As shown in Figure 5.5, the membrane can adsorb selected PhACs. This deposition of certain compounds on membrane surface or pore may cause a flux decline by reducing the membrane pore size (Stoquart et al. 2012). The ABC can deposit on the membrane surface and can simultaneously alleviate membrane fouling by adsorbing compounds (Sima et al. 2017). Therefore, the flux change of the UF only and ABC-UF without HA is almost the same. On the other hand, severe flux decline was

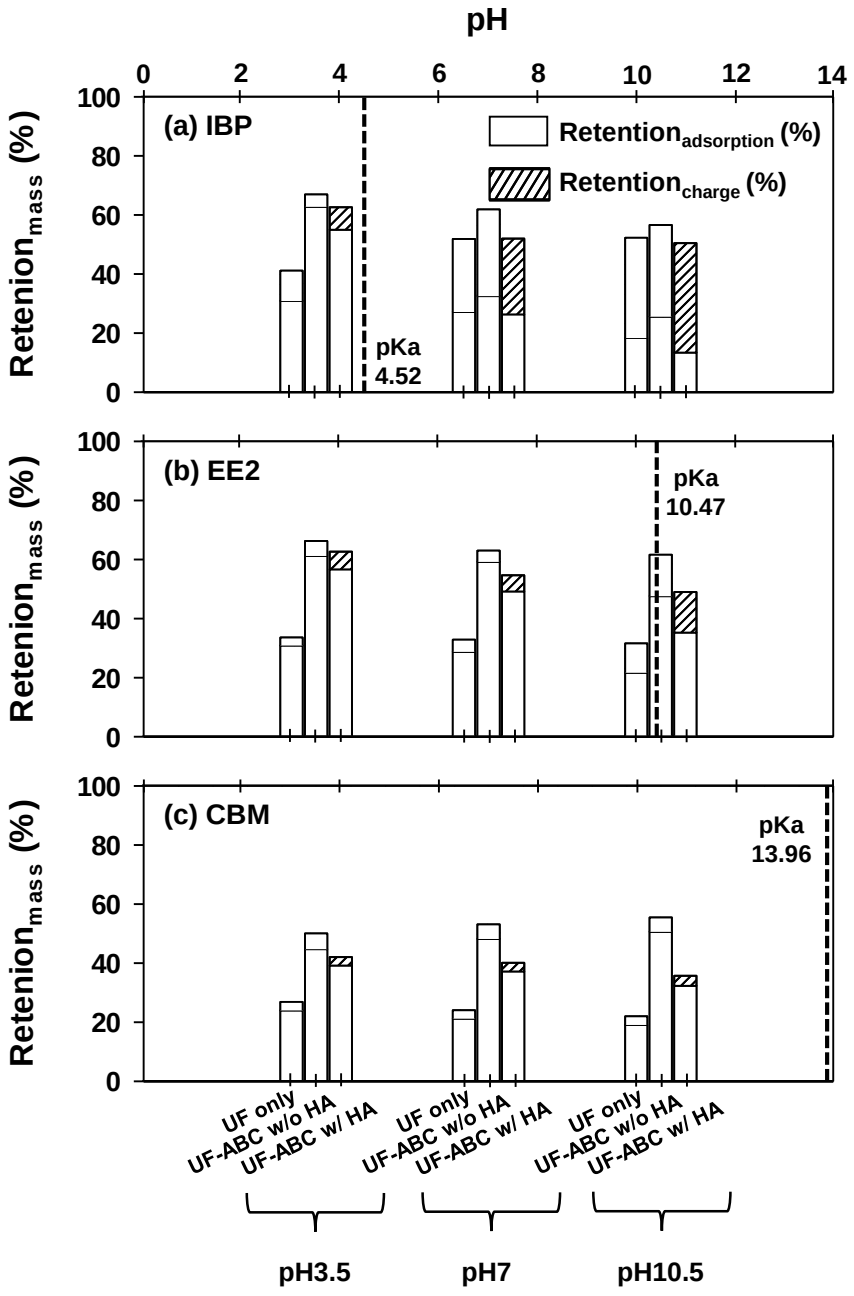

Figure 5.2 Comparison of retention based on mass for UF only, UF-ABC without HA, and UF-ABC with HA. Operation conditions: ΔP = 520 kPa (75 psi); stirring speed = 300 rpm; VCF = 5; HA = 5 mg/L as DOC; ABC = 10 mg/L; conductivity = 300 µS/cm; pre-contract time with ABC and HA = 4 h. Vertical dashed lines indicate p*K*a values of each target adsorbate.

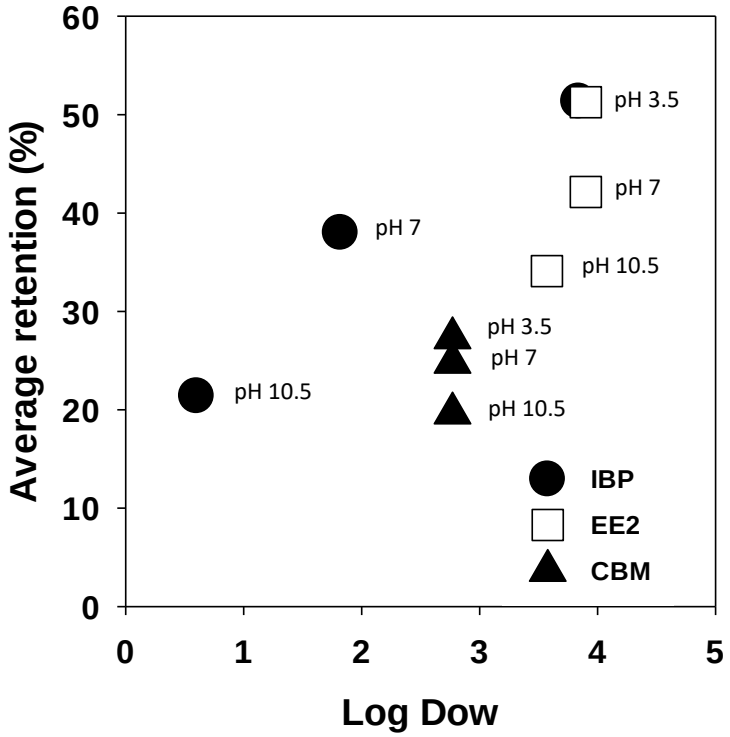

Figure 5.3 Average retention of IBP, EE2, and CBM by UF-ABC at varying log D_{OW} values. Operation conditions: HA = 5 mg/L as DOC; VCF = 1.0-5.0; ABC = 10 mg/L; conductivity = 300 µS/cm.

observed in the case of ABC-UF with HA. The flux decreased rapidly as the pH decreased, decreasing to 0.75, 0.77, and 0.79 for pH values of 3.5, 7, and 10.5, respectively. This serious flux decline is due to pore plugging on the membrane surface or pore (pore size = 1.03 nm), in turn due to the HA, which has average molecular weight in the range of 170 to 22,600 Da. A previous study reported that adhesion between a membrane and HA increased with decreasing pH, due to decreasing zeta potential and increasing particle size (Meng et al. 2015). Also, Table 5.2 shows that the average retention rate of HA is 76.7, 80.3, and 83.1% at pH 3.5, 7, and 10.5, respectively. It can be inferred that more HA is present as a foulant on the membrane surface and interior membrane pores at lower pH values. Therefore, severe flux decline occurs in the UF-ABC system with HA due to hydrophobic interactions between membrane and HA under acidic conditions where membrane becomes relatively less negatively charged and HA is relatively undissociated (Yoon, Westerhoff et al. 2006).

5.5 Comparison of the ABC-UF and PAC-UF systems: retention and flux decline

Recently, combined PAC membrane systems (PAC-UF) have mostly been applied to improve the capability of membrane systems to effectively remove micropollutants (Huck et al. 2009, Jia et al. 2009, Shao et al. 2017). Thus, to evaluate the capability of ABC-UF, ABC-UF was compared with PAC-UF in terms of retention rate and flux behavior at pH 7. Figure 5.7 presents the retention rate for each of the selected PhACs in both the ABC-UF and PAC-UF. The results indicated that PAC-UF marginally improved retention by 4.2 - 7% in the absence of HA, and by 5.5 - 9% in the presence of HA, compared to ABC-UF. This can be explained by the elemental composition, structural characteristics, and surface properties of ABC and PAC (Table 5.1). First, although the

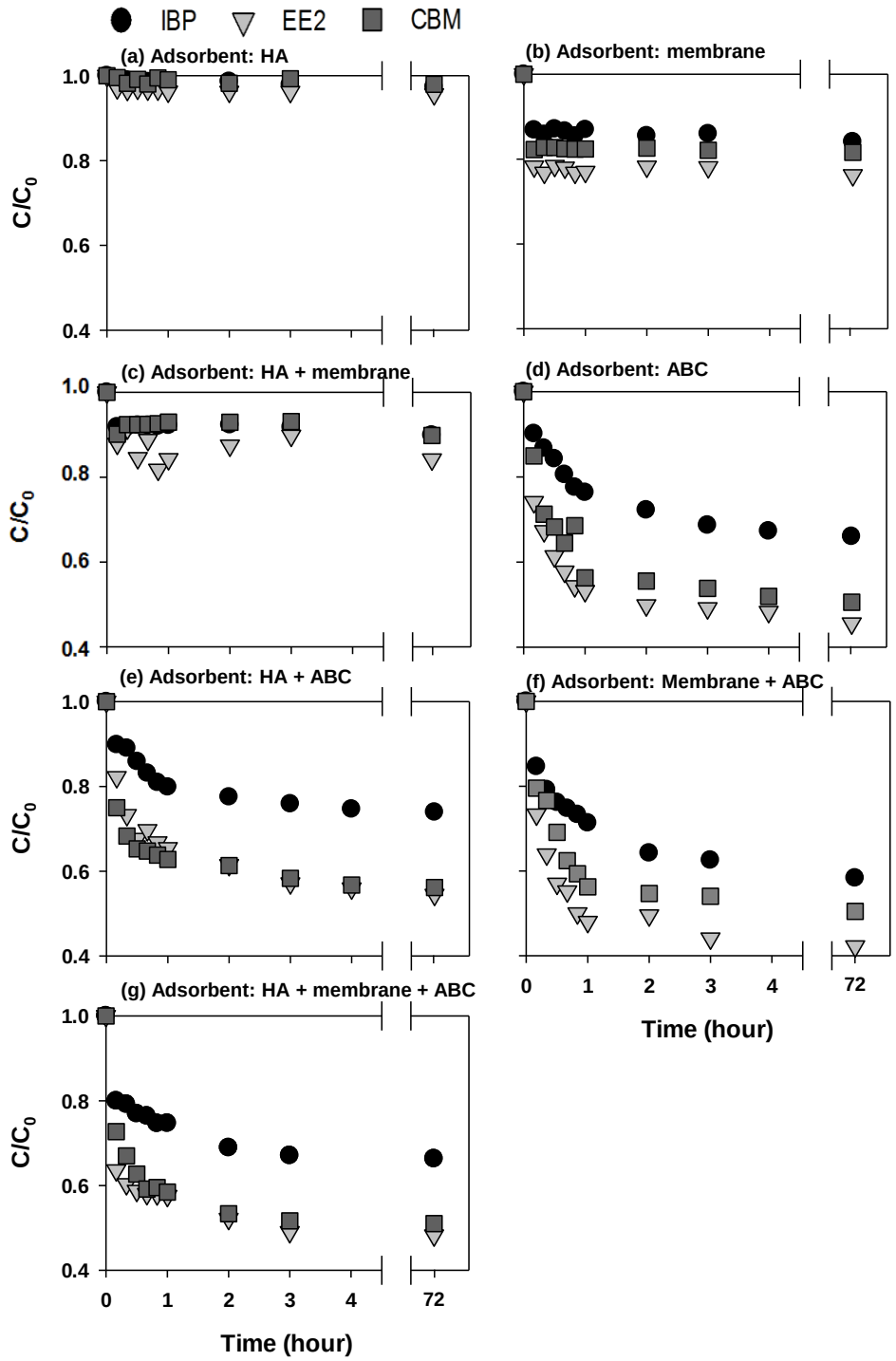

Figure 5.4 Adsorption of selected pharmaceuticals under different adsorbent scenarios as a function of time. Operation conditions: C_0 = 10 μM; HA = 5 mg/L as DOC; membrane = 14.6 cm^2; ABC = 10 mg/L; pH = 7 at 20°C; conductivity = 300 μS/cm; stirring speed = 300 rpm.

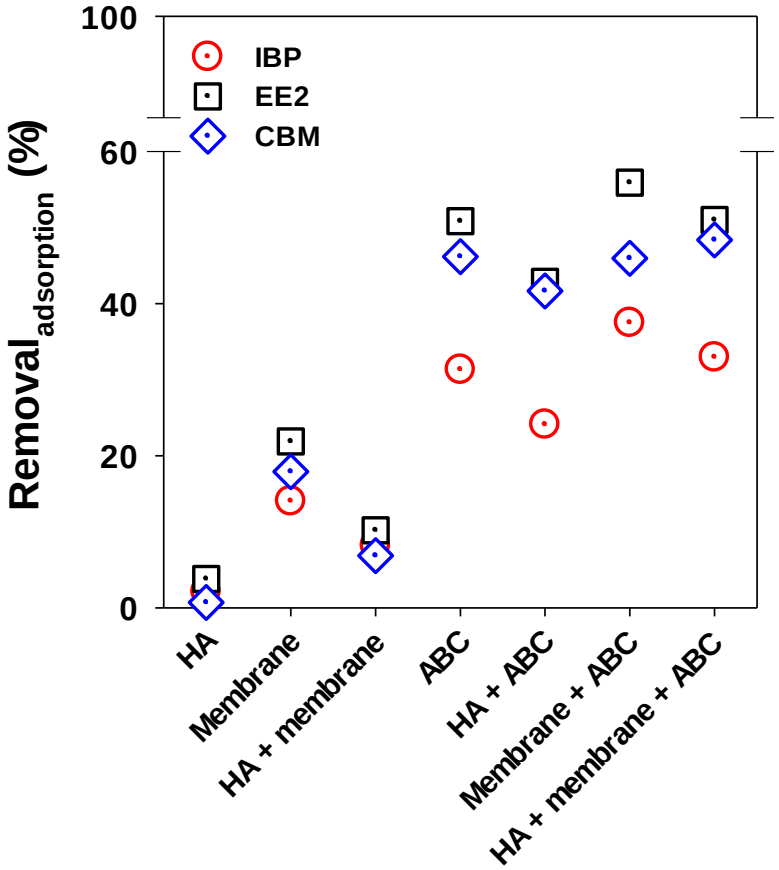

Figure 5.5 Adsorption of IBP, EE2, and CBM on each adsorbent with a contact time of 3 h. Operation conditions: C_0 = 10 µM; HA = 5 mg/L as DOC; membrane = 14.6 cm^2; ABC = 10 mg/L; pH = 7 at 20°C; conductivity = 300 µS/cm; stirring speed = 300 rpm.

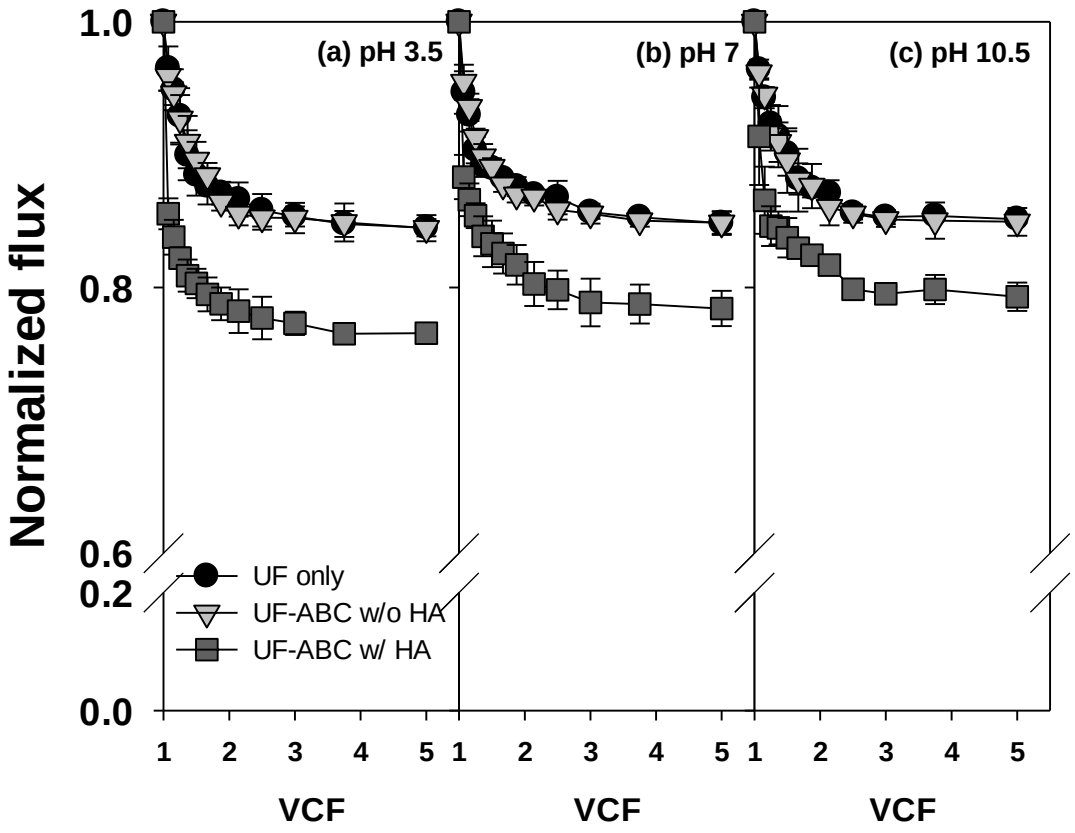

Figure 5.6 Normalized flux decline for UF only, UF-ABC without HA, and UF-ABC with HA at varying pH conditions. Operation conditions: ΔP = 520 kPa (75 psi); stirring speed = 300 rpm; HA = 5 mg/L as DOC; ABC = 10 mg/L; conductivity = 300 µS/cm; pre-contract time with ABC and HA = 4 h.

Table 5.2 Comparison of HA removal rate (%) as a function of VCF for various pH conditions and UF-adsorbent systems.

		VCF											
		1.1	1.2	1.3	1.4	1.5	1.7	1.9	2.1	2.5	3.0	3.8	5.0
ABC-UF pH 3.5	IBP	69.6	68.6	75.2	69.8	69.4	68.1	72.0	71.1	72.6	73.3	70.6	71.4
	EE2	78.3	75.3	80.6	82.9	82.7	84.0	85.1	84.8	83.7	86.0	85.2	85.0
	CBM	72.3	69.3	72.5	73.7	74.5	74.1	75.5	82.0	81.7	81.6	78.5	79.7
ABC-UF pH 7	IBP	75.6	75.1	75.9	77.4	77.1	78.6	76.2	76.6	76.4	76.9	76.8	79.0
	EE2	83.4	84.5	86.7	83.6	86.3	87.2	86.5	86.9	86.8	85.3	87.3	87.0
	CBM	69.8	71.7	77.3	77.5	80.6	76.2	80.4	80.5	79.8	80.9	80.8	80.9
ABC-UF pH 10.5	IBP	76.5	79.0	77.5	80.0	80.9	81.3	80.6	80.7	81.2	82.6	82.0	83.0
	EE2	88.5	89.4	89.5	89.3	89.2	90.2	87.3	88.2	88.9	89.1	90.1	90.2
	CBM	78.5	78.0	78.9	80.3	79.1	79.4	80.2	79.4	77.7	81.3	81.2	81.6
PAC-UF pH 7	IBP	78.3	79.3	80.5	81.1	81.8	83.2	83.7	84.0	82.5	84.2	85.3	85.4
	EE2	81.5	87.1	87.5	87.9	88.1	89.9	89.1	88.7	88.8	88.6	89.2	89.1
	CBM	75.8	79.2	80.3	81.7	81.2	84.0	82.0	81.7	82.6	81.8	84.8	84.1

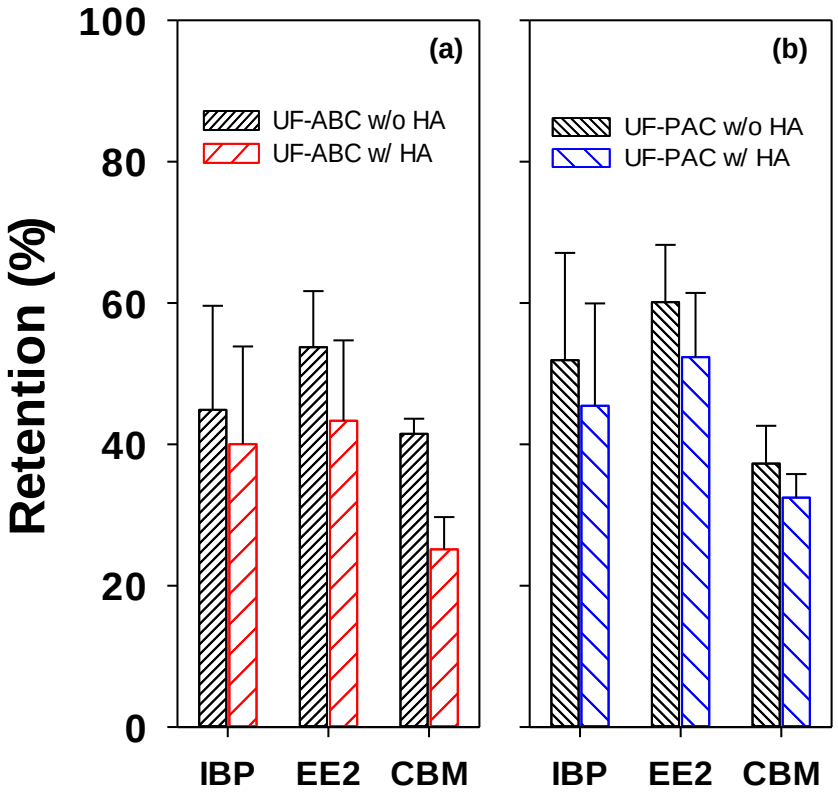

Figure 5.7 IBP, EE2, and CBM retention by (a) UF-ABC and (b) UF-PAC. Operation conditions: ΔP = 520 kPa (75 psi); stirring speed = 300 rpm; pH = 7; conductivity = 300 µS/cm; HA = 5 mg/L as DOC; ABC = 10 mg/L; PAC = 10 mg/L; pre-contact time with A and PAC = 4 h.

stronger aromaticity of ABC improved adsorption (Nguyen et al. 2007, Jung, Park et al. 2013), the lower surface area and pore volume of ABC restricted the adsorption capacity (Nguyen, Cho et al. 2007, Ji et al. 2010). Furthermore, previous studies have suggested that the polarity index (O/N + O/C) positively correlates with adsorption capacity (Jung, Park et al. 2013) and hydrophobicity (Chun, Sheng et al. 2004, Martín-González, González-Díaz et al. 2014), implying that a lower PAC polarity index encourages higher adsorption affinity.

The normalized permeate flux of the ABC-UF was different to that of the PAC-UF, as shown in Figure 5.8. The results showed that the normalized flux of PAC-UF without HA was 0.76 and that of the PAC-UF with HA decreased rapidly at the beginning of the experiment, to reach about 0.70. This phenomenon is a result of fouling generated by the PhACs, PAC, and/or HA, which block the membrane surface and pores, resulting in decreased flux, as previously described in Section 3.3. Although PAC can remove PhACs by adsorbing (Figure 5.7), it can be more readily deposited by interacting with the membrane due to the relatively high adsorption capacity of PAC. This resulted in a significant decline in flux in the PAC-UF. Furthermore, Figure 5.9. shows that the zeta potential values of PAC and ABC were -7.3 and -10.3 mV at pH 7, respectively. As a result, repulsion between PAC and the membrane is slightly weaker compared with ABC (Meng, Tang et al. 2015). Although, the retention rate of UF-PAC is slightly better than that of UF-ABC due to strong hydrophobicity, surface area, and pore volume, UF-ABC was superior to UF-PAC in terms of flux decline.

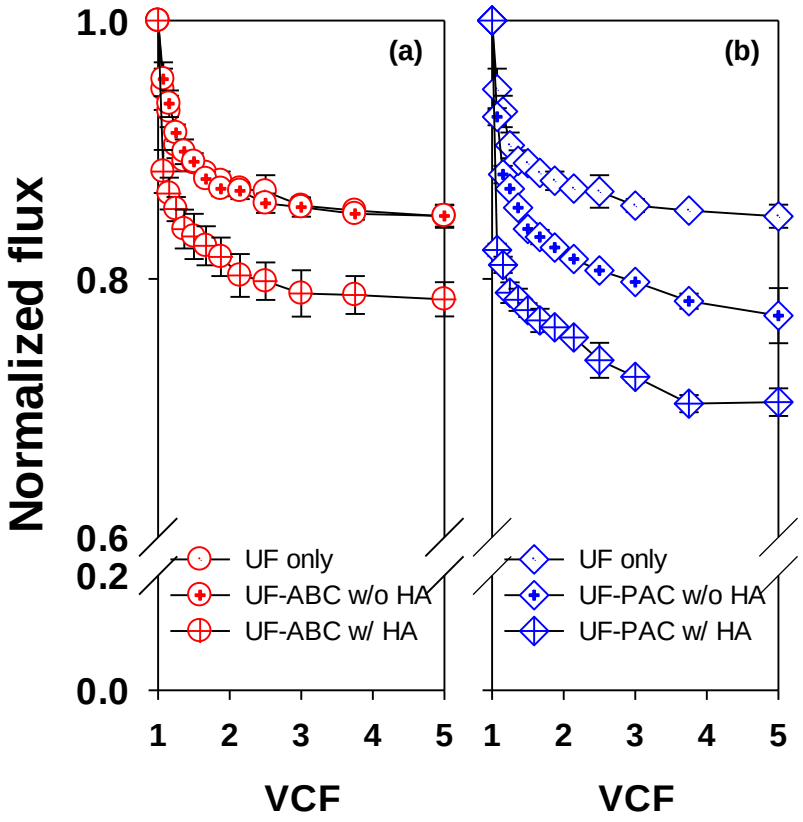

Figure 5.8 Comparison of normalized flux decline: (a) UF only, UF-ABC without HA, and UF-ABC with HA, and (b) UF only, UF-PAC without HA, and UF-PAC with HA. Operation conditions: ΔP = 520 kPa (75 psi); stirring speed = 300 rpm; pH = 7; conductivity = 300 µS/cm; HA = 5 mg/L as DOC; ABC = 10 mg/L; PAC = 10 mg/L; pre-contact time with A and PAC = 4 h.

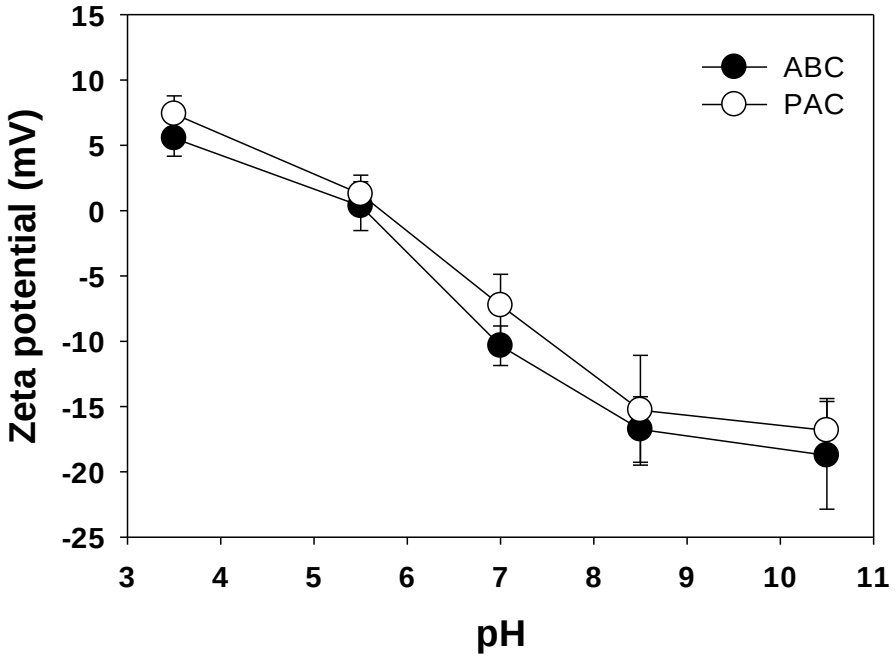

Figure 5.9 Zeta potentials of ABC and PAC as a function of pH. Operation conditions: HA = 5 mg/L as DOC; ABC and PAC = 10 mg/L; pH = 7 at 20°C; conductivity = 300 µS/cm.

5.6 Summary

In this study, selected target pharmaceuticals (PhACs) including ibuprofen (IBP), 17 α-ethinyl estradiol (EE2), and carbamazepine (CBM) were removed by an ultrafiltration-activated biochar hybrid system (ABC-UF). Based on characteristic analysis, ABC, a by-product of combustion of waste, is a promising alternative to commercially available powdered activated carbon (PAC) due to its enhanced aromatization and porous properties. Three different systems, including UF only and ABC-UF with/without humic acid (HA) were evaluated. The average retention rate of target PhACs within the ABC-UF system (without HA: 45.2%, and with HA: 34.4%) was much higher than that of the UF only (15.4%), suggesting that hydrophobic adsorption by ABC was the dominant mechanism. In addition, although fouling is expected in ABC-UF due to the presence of ABC, the flux decline of ABC-UF showed similar flux behavior to that of the UF only system. The ABC-UF was compared to UF-PAC with respect to retention rate and permeate flux. The average retention for the target PhACs was slightly higher in PAC-UF than in ABC-UF (41.4%) for the target PhACs. However, UF-ABC was considered to be a good alternative system because the normalized flux of ABC-UF (0.85 and 0.77) was superior to PAC-UF (0.76 and 0.70) in the absence/presence of HA, respectively. Consequently, ABC-UF was shown to be a suitable alternative to PAC-UF with respect to both retention and fouling reduction.

CHAPTER 6

METAL ORGANIC FRAMEWORK-ULTRFILTRATION HYBRID SYSTEM FOR REMOVING SELECTED PHARMACEUTICALS AND NAUTRAL ORGANIC MATTER[3]

6.1 Characterization of MOFs

The synthesized MOFs were characterized by XRD, FT-IR, XPS, and TEM-EDS. The XRD patterns indicate that, by matching well with the simulated patterns, MIL-100(Fe) and MIL-101(Cr) were successfully synthesized under the applied conditions (Figure 6.1a). Furthermore, the FT-IR spectrum of MIL-100(Fe) clearly exhibited peaks at 1,635, 1,383, 762, 711, and 485 1/cm (Figure 6.1b), in excellent agreement with the corresponding functional groups of the known structure (Horcajada, Surblé et al. 2007, Wang et al. 2014). The peaks at 1,635 and 1,383 1/cm can be assigned to the carboxyl groups of organic ligands within MIL-100(Fe). The peaks of C-H bending are at 762 and 711 1/cm. Fe-O is indicated by the peak at 485 1/cm. The FT-IR spectrum of MIL-101(Cr) is similar to that obtained in previous studies (Figure 6.1b) (Férey, Mellot-Draznieks et al. 2005, Hu et al. 2013). The vibrational stretching frequencies of O-C-O are at 1,620 and 1,400 1/cm, indicating the presence of dicarboxylate linkers within the MIL-101(Cr)

[3] Reprinted here with permission of publisher: Sewoon Kim *et al*., A metal organic framework-ultrafiltration hybrid system for removing selected pharmaceuticals and natural organic matter. Chemical Engineering Journal 382 (2020) 122920.

structure. The peaks between 500 and 1,600 1/cm can be assigned to the vibrations of benzene rings, including C=C at 1,510 1/cm, C-H at 746 1/cm, -COO at 587 1/cm. The XPS spectrum shows the surface chemical states of MIL-100(Fe) (Figure 6.1c) and MIL-101(Cr) (Figure 6.1d). For both MIL-100(Fe) and MIL-101(Cr), the XPS spectrum of C 1s contains two peaks at 284.8 and 288 eV, which correspond to phenyl and carboxyl signals, respectively (Zhu, Yu et al. 2012, Jeong et al. 2016). The O 1s peaks at 531.7 and 532 eV correspond to the Fe-O-C and Cr-O-C species in the XPS spectra of MIL-100(Fe) and MIL-101(Cr), respectively (Vu et al. 2014, Liang et al. 2015). The Fe 2p spectrum for MIL-100(Fe) can be deconvoluted into two peaks centered at 712.3 and 724.8 eV, corresponding to the peaks of Fe 2p3/2 and Fe 2p1/2, respectively (Zhang et al. 2015). The spectrum of Cr 2p for MIL-101(Cr) was assigned to two peaks at 577 and 587 eV, corresponding to the Cr 2p3/2 and Cr 2p1/2 signals, respectively (Jeong, Kim et al. 2016). We evaluated the distributions of elements in MIL-100(Fe) and MIL-101(Cr) by carrying out EDS mapping analysis, and the results are shown in Figure 6.1c and 6.1d (inset). The textural properties of both MOFs were estimated from N_2 adsorption-desorption isotherms gathered at 196°C (77K) (Table 6.1). Both MOFs exhibit large surface areas and pore volumes, as expected from highly microporous frameworks. Furthermore, a stack of PSD profiles for both MOFs materials shows the presence of pores with windows in the 9–12 Å region, as well as spherical cavities with sizes in the region 21–36 Å (Figure 6.2). These values agree with data previously reported elsewhere (Férey, Mellot-Draznieks et al. 2005, Huo and Yan 2012). Therefore, the XRD, FT-IR, XPS, TEM-EDS results and N_2 isotherms lead to the conclusion that lab-made MIL-100(Fe) and MIL-101(Cr) was successfully synthesized and has strong potential for applications to adsorption-UF hybrid systems.

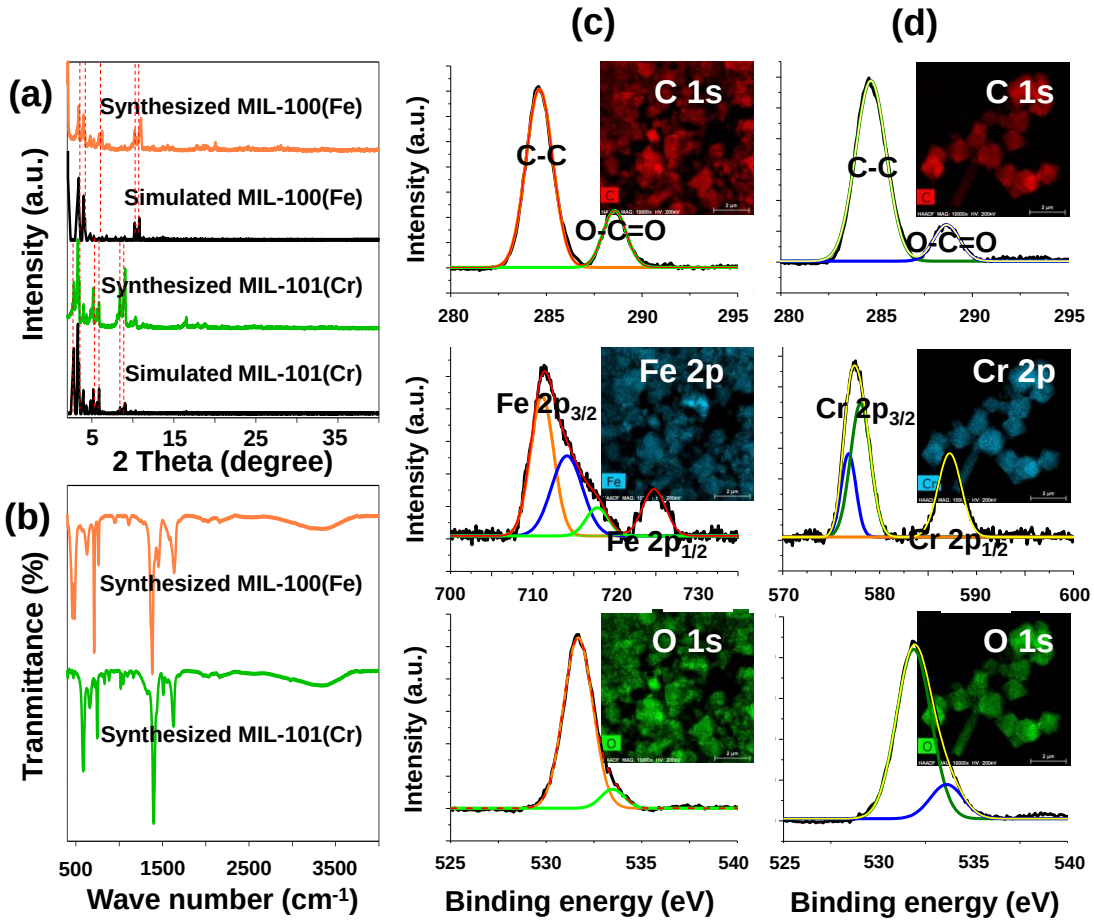

Figure 6.1 Characteristics of the MIL-100(Fe) and MIL-101(Cr) using (a) XRD, (b) FT-IR, (C) XPS and TEM-EDX elemental mapping (inset) of MIL-100(Fe), and (d) XPS and TEM-EDX elemental mapping (inset) of MIL-101(Cr).

Table 6.1 Textural properties of MIL-100(Fe) and MIL-101(Cr).

Adsorbent	**MIL-100(Fe)**	**MIL-101(Cr)**
BET surface area (m^2/g)[a]	1,586	2,505
Langmuir surface area (m^2/g)[a]	2,637	3,966
Total pore volume (cm^3/g)[b]	0.89	1.39
Pore diameter (Å)[b]	window:9, cage:23, 28	window:12, cage:26, 36

[a] From N_2 equilibrium adsorption gathered at 77 K.
[b] From Horvath-Kawasoe method.

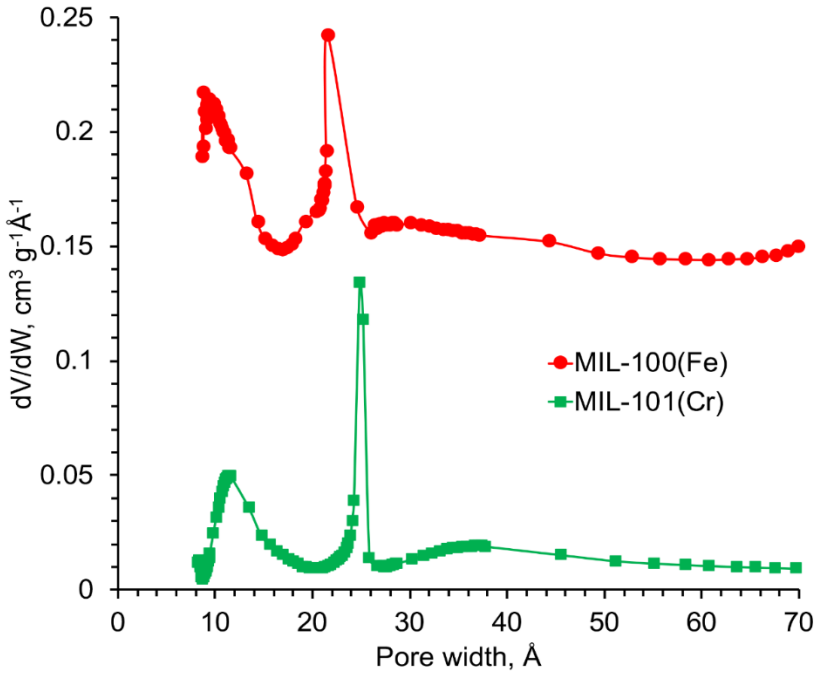

Figure 6.2 Pore size distribution profiles based on Horvath – Kawazoe's (H-K) and Barrett-Joyner-Halenda (BJH) analyses of the N_2 equilibrium adsorption data gathered at -196˚C.

6.2 Performance of MOF-UF for PhACs

Figure 6.3 shows the retention rate of selected PhACs by the UF only, MIL-100(Fe)-UF, and MIL-101(Cr)-UF as a function of VCF. The retention rates of IBP and EE2 for the UF only were 26.8–17.2% and 34.5–19.4% for pH 3, 49.4–40.5% and 34.3–25.1% for pH 7, and 44.1–38.6% and 65.3–46.3% for pH 11, respectively. In the case of the MOF-UF, the retention rates of IBP and EE2 were enhanced in comparison to the UF only. The retention rates of IBP/EE2 for the MIL-100(Fe)-UF were 40.8–23.8%/ 50.5–35.1%, 69.7–30.9%/47.1–39.1%, and 46.1–40.1%/ 61.6–52.9% for pH 3, 7, and 11, respectively. Furthermore, the retention rates of IBP/EE2 for the MIL-101(Cr)-UF were 54.9–24.0%/61.1–48.1%, 71.7–42.1%/60.5–45.1%, and 57.9–51.6%/72.2–66.1% for pH values of 3, 7 and 11, respectively. The retention rate of three different systems is attributable to interaction associated with the physicochemical properties of membrane, MOFs, and selected PhACs. In this study, three different mechanisms govern the removal of those selected PhACs; which include size effect, electrostatic interactions, and hydrophobic interactions. Although the size exclusion effect is less apparent because the pore size of the membrane (26–30 Å as shown in Table 4.2) is bigger than the size of the PhACs (10.1 Å for IBP and 12.3 Å for EE2, as shown in Table 4.1), parts of the compound were removed according to the membrane size exclusion effect (Kim et al. 1994, Howe and Clark 2002). Furthermore, the contribution of MIL-101(Cr) to the retention rate was higher under all experimental conditions compared to the MIL-100(Fe). This is presumably because MIL-101(Cr) has a larger surface area and total pore volume as shown in Table 6.1, resulting in more adsorption. Furthermore, because the sizes of IBP (10.1 Å) and EE2 (12.3 Å) molecules are slightly larger than the pores of MIL-100(Fe), which act as windows

(9 Å), IBP and EE2 molecules do not easily enter the pores of MIL-100(Fe) (Horcajada et al. 2006, Huo and Yan 2012).

It is important to consider retention rate as a function of VCF so that appropriate technologies can be designed. Although the number of available vacant sites of the membrane and MOF for adsorption decreases as the VCF increases (Hasan, Jeon et al. 2012), the PhACs retention rate did not decrease significantly with increasing VCF in any of the three systems tested. Also, Figure 6.4 shows that the normalized flux of the PhACs did not decrease significantly with increasing VCF. The membrane zeta potential, which enables us to assess the membrane surface charge density (Figure 6.5), suggests that the PhACs and MOF might not be significantly deposited or adsorbed on the membrane due to electrostatic repulsion (Childress and Elimelech 2000). Thus, we concluded that the retention rate and flux decline associated with PhACs removal during filtration are somewhat slightly affected by the higher VCF of the MOF-UF.

To comprehensively investigate the retention mechanism, we plotted the retention performance by the proportions and log D_{OW} values (representing hydrophobicity) of the PhACs (Figure 6.6). The retention rates of both PhACs were in the order: UF only < MIL-100(Fe)-UF < MIL-101(Cr)-UF. In particular, the retention of IBP (Figure 6.6a) and EE2 (Figure 6.6b) varied significantly as the pH increased above their p*Ka*, exhibiting similar trends to their speciation curves. This can be explained in terms of charge exclusion, where dissociated PhACs are better retained (Chu et al. 2017). Furthermore, EE2 exhibited slightly higher retention than IBP when they were present in similar proportions, due to its higher hydrophobicity (log D_{OW} = 3.9 at pH 3 and 7, and 3.2 at pH 11, for EE2; and 3.8 at pH 3, 1.7 at pH 7, and 0.3 at pH 11 for IBP) (Jung, Park et al. 2013). It is noteworthy that

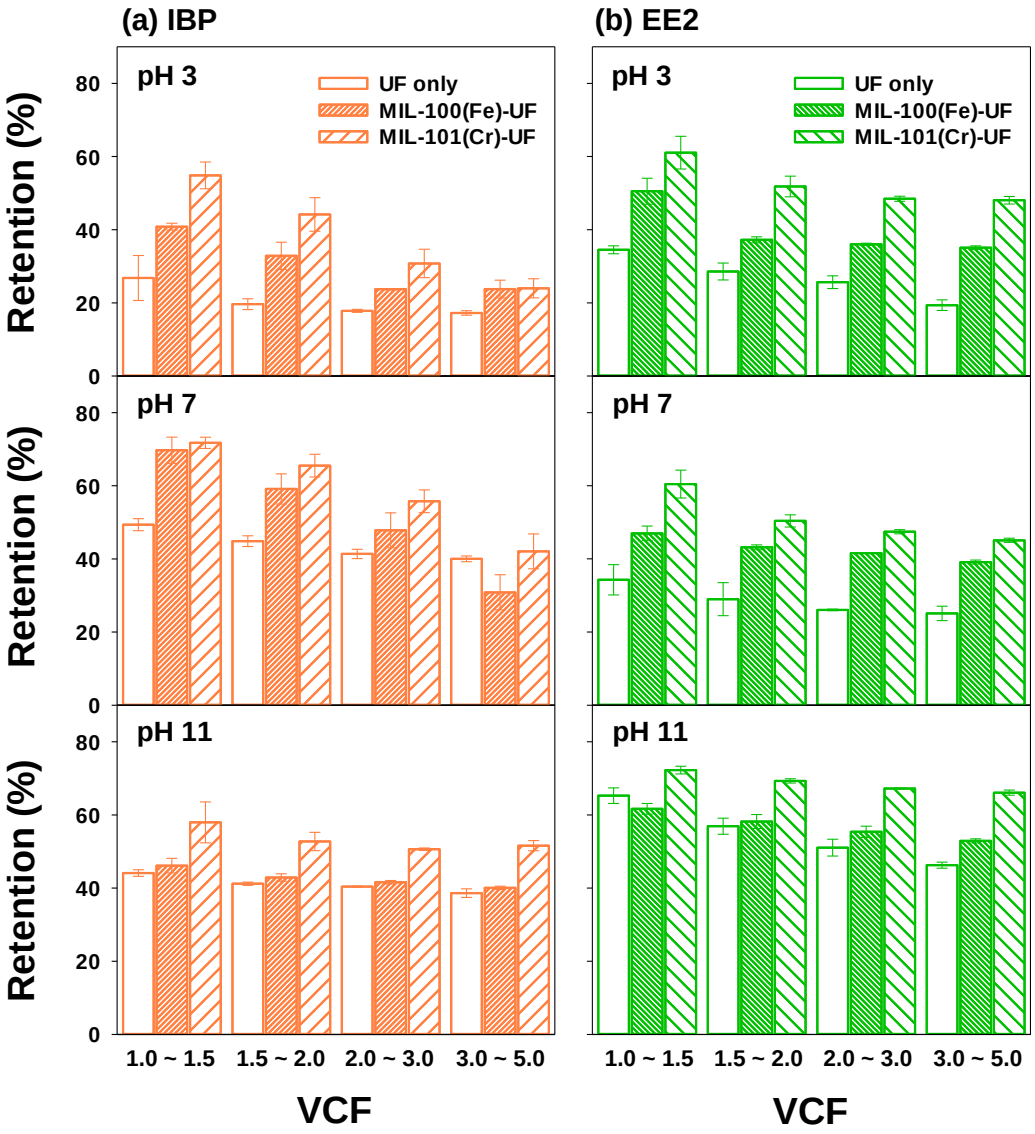

Figure 6.3 Retention of (a) IBP and (b) EE2 as a function of VCF by UF only, MIL-100(Fe)-UF, and MIL-101(Cr)-UF. Operation conditions: ΔP = 520 kPa (75 psi); stirring speed = 200 rpm; MOF = 20 mg/L; initial selected PhACs concentration = 10 μM; conductivity = 300 μS/cm; pre-contact time with MOF = 2 h.

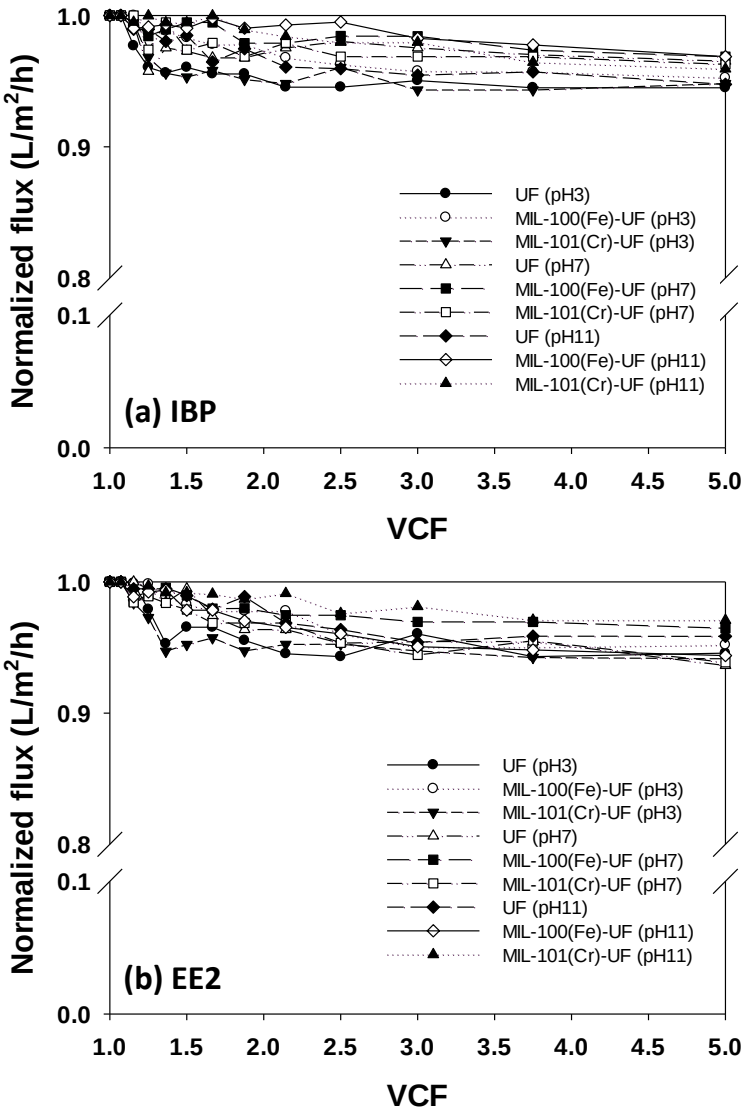

Figure 6.4 Normalized flux decline of (a) IBP and (b) EE2 as a function of VCF by UF only, MIL-100(Fe)-UF, and MIL-101(Cr)-UF at varying pH conditions. Operation conditions: ΔP = 520 kPa; stirring speed = 200 rpm; MOF = 20 mg/L; initial selected PhAC concentration = 10 μM; conductivity = 300 μS/cm; pre-contact time with MOF = 2 h.

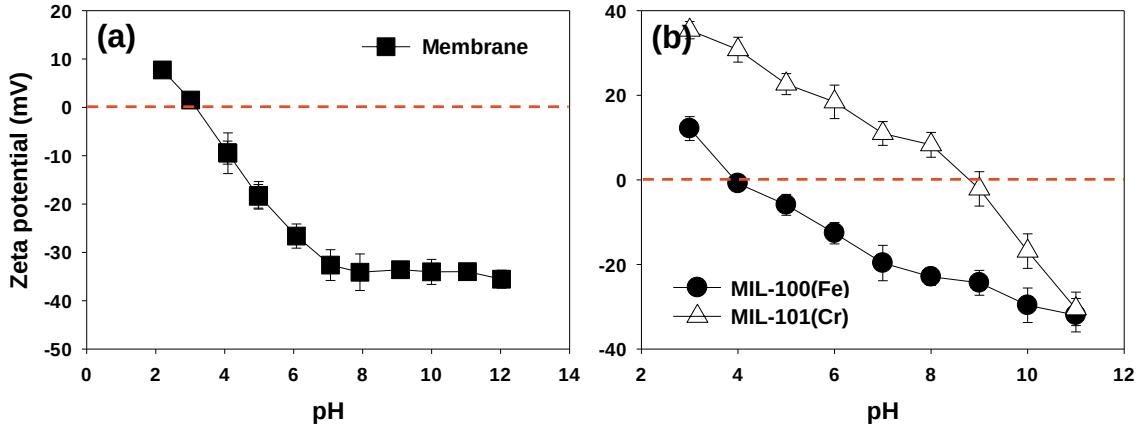

Figure 6.5 Zeta potential of (a) the UF membrane used in this study and (b) the MOFs as a function of pH.

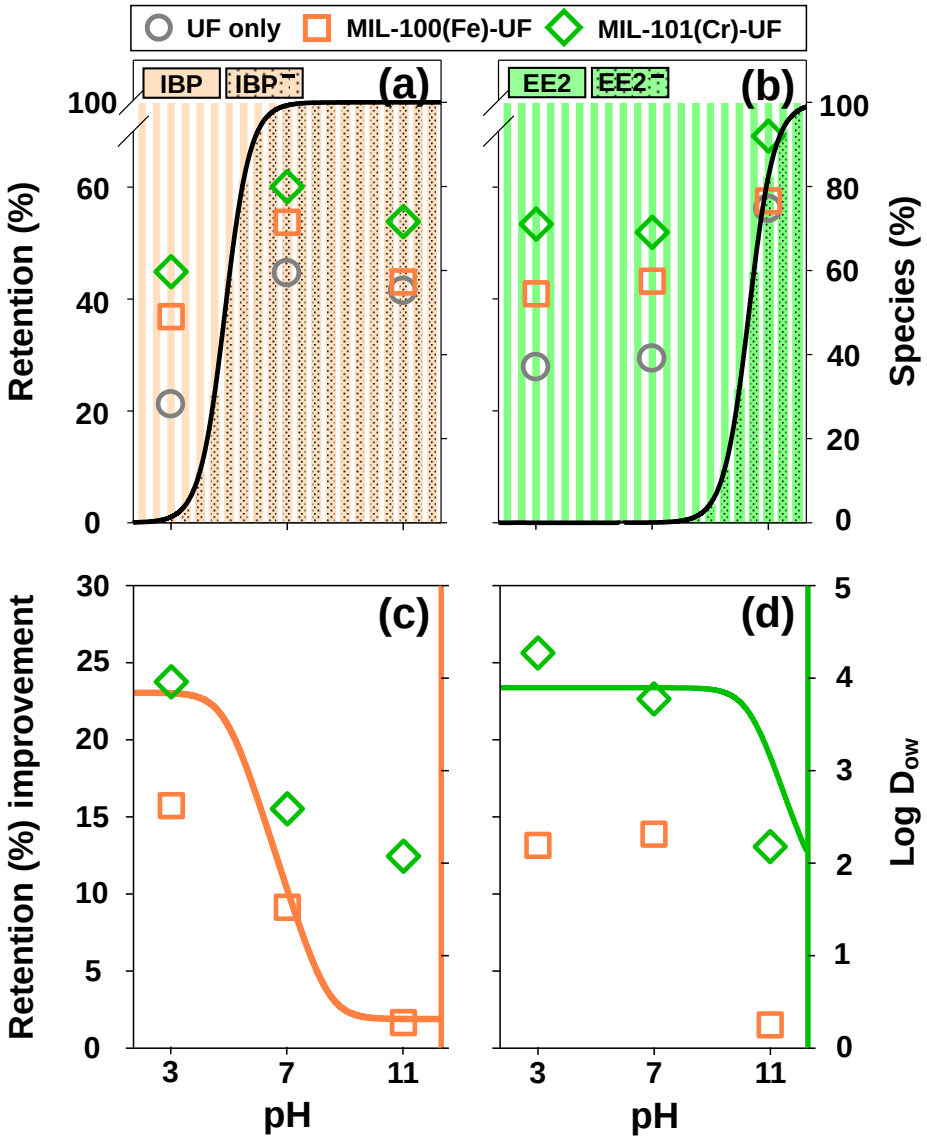

Figure 6.6 Retention rate of (a) IBP, and (b) EE2 by UF only, MIL-100(Fe)-UF, and MIL-101(Cr)-UF at varying pH conditions with the fraction of species of IBP and EE2. Retention rate improvement of (c) IBP, and (d) EE2 by the hybrid system in comparison with the UF only system. Operation conditions: ΔP = 520 kPa; stirring speed = 200 rpm; MOF = 20 mg/L; initial selected PhAC concentration = 10 μM; conductivity = 300 μS/cm; pre-contact time with MOF = 2 h.

the relative proportions and hydrophobicity of PhACs play an important role in the retention performance of MOF-UF. Figure 6.6c and d shows the improvement in retention rate for the MOF-UF with variation in log D_{OW} relative to UF only. Due to their relatively higher hydrophobicity at lower pH values, the PhACs exhibited greater retention rate improvements due to hydrophobic attraction to the MOFs in the MOF-UF. In contrast, at higher pH values, PhACs with relatively lower hydrophobicity are less amenable to adsorption by the negatively charged MOF (estimated based on zeta potential; see Figure 6.5b) and membrane. It is also interesting to note that the retention rates with the MIL-100(Fe)-UF and UF only were similar at pH 11; the retention (%) improvement is 1.6 for IBP and 1.5 for EE2. This could be explained by the fact that MIL-100(Fe) is decomposed at pH 11, changing to a reddish-brown color (Xu et al. 2013, Bezverkhyy et al. 2016). Taken together, these observations indicate that the solution pH contributes considerably to the overall retention performance of the MOF-UF, in accordance with the physicochemical properties of the PhACs and stability of the MOF.

6.3 Performance of MOF-UF for NOM

NOM, which is composed of a heterogeneous structural mixture of aromatic and aliphatic compounds with varying molecular sizes, exists in virtually all environmental systems (Lee, Seo et al. 2015). The presence of NOM not only results in offensive odors and taste, but also acts as a potential precursor due to complexation with organic chemicals such as PhACs (Jung, Phal et al. 2015, Petrie et al. 2015). The retention rates of HA and TA under homogeneous and heterogeneous NOM conditions (HA:TA = 10:0 for NOM 1, 5:5 for NOM 2, and 0:10 for NOM 3) are presented in Figure 6.7. NOM was removed at

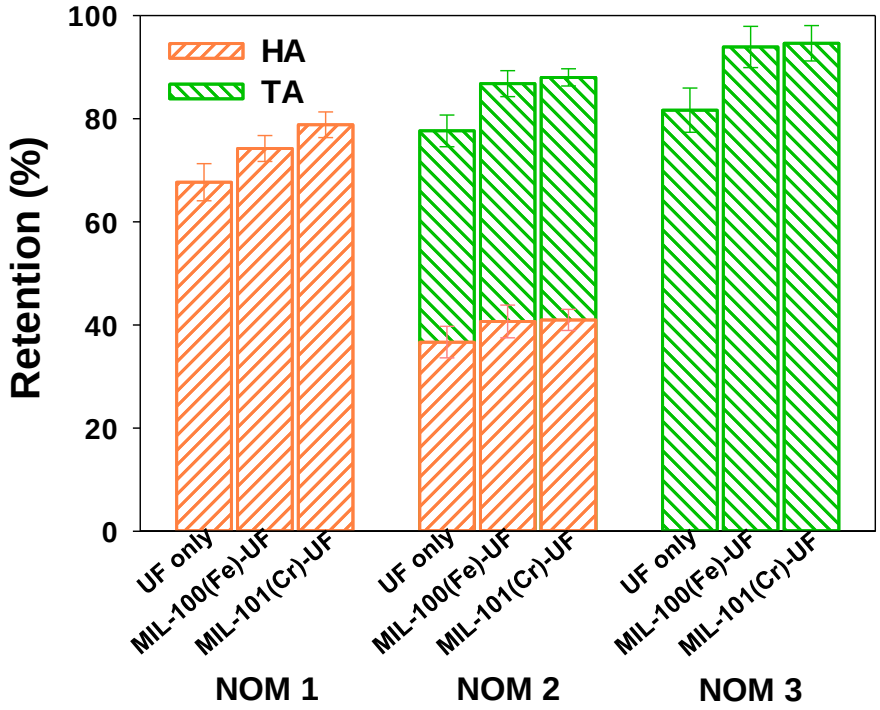

Figure 6.7 Retention rate of the mixed HA and TA solutes by UF only, MIL-100(Fe)-UF, and MIL-101(Cr) for different NOM combinations. Operation conditions: ΔP = 520 kPa; stirring speed = 200 rpm; MOF = 20 mg/L; initial NOM = 10 mg/L as DOC; pH = 7.0; conductivity = 300 µS/cm; pre-contact time with MOF = 2 h.

high rates by the MIL-100(Fe)-UF and MIL-101(Cr)-UF (74.2 and 78.8% for NOM 1, 86.8 and 88.0% for NOM 2, and 93.9 and 94.7% for NOM 3, respectively), while the UF only also showed reasonable retention rates (67.7% for NOM 1, 77.7% for NOM 2, and 81.7% for NOM 3). These data confirm the beneficial effects of MOF adsorption as an upstream treatment process. In particular, the highest retention rates for all NOM solutions were achieved with the MIL-101(Cr)-UF. As stated previously, these results accord with the textural properties of MOF. Also, the reason presumably is that greater π-π interactions between NOM and MIL-101(Cr) provide slightly higher retention rates where, according to its chemical formula, MIL-101(Cr) has more aromatic rings than MIL-100(Fe) (Hyung and Kim 2008). Moreover, because NOM, which contains negatively charged carboxy and phenolic hydroxyl groups, was in a dissociated state at pH 7 (Sun et al. 2017), the relatively positively charged MIL-101(Cr), as supported by the zeta potential analysis (Figure 6.5b), resulted in electrostatic attraction to the NOM.

The results also indicated that the retention rate increased with the TA concentration. The TA stabilizes the particles in the solution more so than does HA due to its total potential energy, which incorporates both Brownian motion and van der Waals attraction (Phenrat et al. 2010, Jung, Phal et al. 2015). Thus, TA can disrupt the aggregation of MOFs via electrostatic interaction and steric repulsion, because more adsorption sites can be provided in the presence of TA solution. Furthermore, the molecular size distribution of TA (< 17,000 Da) is somewhat smaller than that of HA (170–22,600 Da) (Lin et al. 1999, Lin and Xing 2008). Although HA is relatively hydrophobic compared to TA, HA can barely pass the MOF membrane pore due to its molecular size (Beckett et al. 1987, Chin et al. 1994). Furthermore, TA exhibited relatively larger declines in flux

compared to HA (in the order NOM 1 < NOM 2 < NOM 3) (Figure 6.8). Likewise, the relatively small TA molecules can be deposited on/in the membrane surface/pore more easily than HA, thus reducing the pore size and causing membrane fouling. These findings demonstrate that the MOF-UF performed better than the UF only, in terms of both the retention rate and flux decline of NOM. Also, TA can exacerbate permeate flux relative to HA due to the size of the TA molecules.

6.4 Comparison between the MOF-UF and PAC-UF system: retention and flux decline

The results of the previous experiment showed that the MIL-101(Cr)-UF is most effective in terms of retention and permeate flux, for both PhACs and NOM. We carried out a performance comparison between the MOF-UF and PAC-UF (Figure 6.9). The retention rates for the selected PhACs and NOM were slightly superior for the MIL-101(Cr)-UF compared to the PAC-UF at pH 7, by 7.3% for IBP, 1.9% for EE2, 7.9% for NOM 1, 7.3% for NOM 2, and 5.4% for NOM 3. This increased retention rate can be explained by the differences in textural characteristics between MIL-101(Cr) and PAC. Despite the similar pore diameters of the two absorbents (26 Å for MIL-101(Cr), 21.9 Å for PAC), the greater total pore volume of MIL-101(Cr) (1.39 cm^3/g) provides higher adsorption capability than PAC (0.24 cm^3/g).

The normalized fluxes of IBP, EE2, NOM 1, NOM 2, and NOM 3, for the MIL-101(Cr)-UF at VCF 5, were 0.97, 0.96, 0.88, 0.85, and 0.80, respectively, compared to 0.83, 0.81, 0.81, 0.80, 0.74, respectively for the PAC-UF. As previously demonstrated (see Figure 5.4), the MOF did not generate severe fouling with respect to PhACs. In contrast, use of PAC, which is more hydrophobic than MIL-101(Cr) (Bhadra et al. 2015, Zhang et

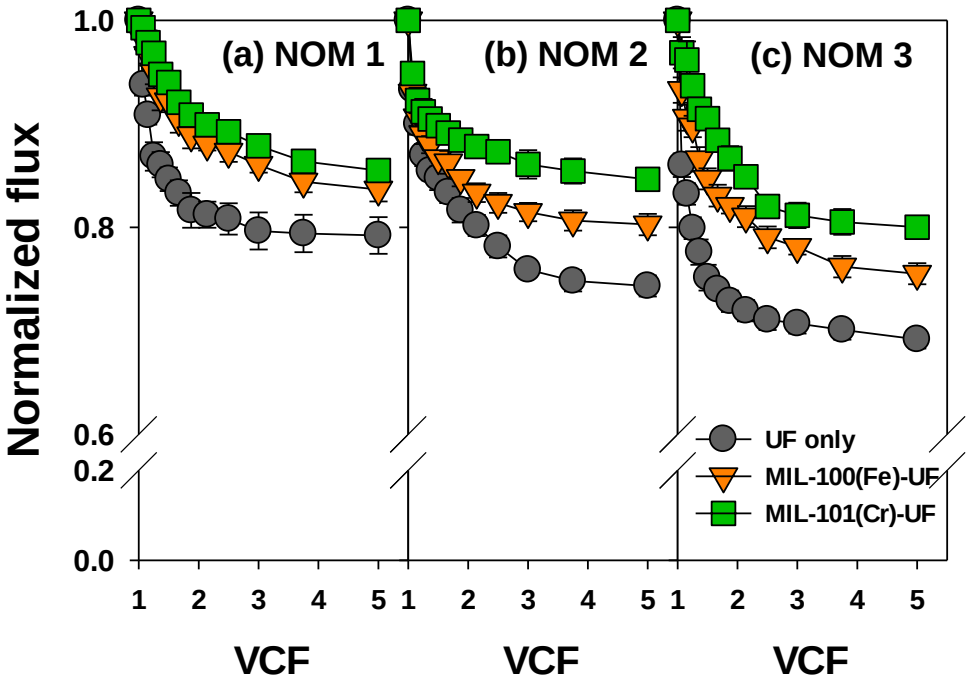

Figure 6.8 Normalized Flux decline of (a) NOM 1, (b) NOM 2, and (c) NOM 3 for UF only, MIL-100(Fe)-UF, and MIL-101(Cr)-UF as a function of VCF. Operation conditions: ΔP = 520 kPa; stirring speed = 200 rpm; MOF = 20 mg/L; initial NOM = 10 mg/L as DOC; pH = 7.0; conductivity = 300 µS/cm; pre-contact time with MOF = 2 h.

al. 2017), can result in marked fouling due to hydrophobic deposits on the polyamide membrane (Perreault et al. 2013). Thus, PAC-UF can cause a more serious decline in flux than the MIL-101(Cr)-UF for PhACs. In the case of NOM, despite the normalized flux performance of the MIL-101(Cr)-UF being slightly better than that of the PAC-UF, both systems exhibited serious flux. As shown previously (see Figure 6.5), this observation could be explained by the fact that NOM plays an important role in flux decline. Therefore, The MIL-101(Cr)-UF was superior to the PAC-UF with regard to retention and flux performance for both PhACs and NOM. However, the reasons for NOM fouling in the MOF-UF remain unclear, as do the reasons for the severe flux decline seen for the MOF-UF with respect to NOM.

6.5 Fouling resistance in the MOF-UF

To evaluate the fouling characteristics and classify reversible/irreversible fouling in the hybrid systems, we assessed the UF only, MIL-101(Cr)-UF, and PAC-UF via a resistance-in-series model for three different NOM combinations that are all known to cause severe flux decline (Table 6.2). Both hybrid systems reduced total membrane fouling (R_t), under all NOM combinations, relative to the UF only. Also, the R_t of the MIL-101(Cr)-UF was lower than that of PAC-UF. This is because the higher adsorption of NOM onto MIL-101(Cr) reduces the amount of fouling compared to PAC, leading to better R_t values. Furthermore, due to the relatively higher hydrophilicity of MIL-101(Cr), water can penetrate the membrane more easily relative to PAC (Bhadra, Cho et al. 2015, Zhang, Sang et al. 2017). The R_t value increased with increasing proportion of TA in the solution, consistent with the retention rate pattern shown in Figure 6.9. With higher TA concentrations (although still smaller than the HA concentration), further blockage of the

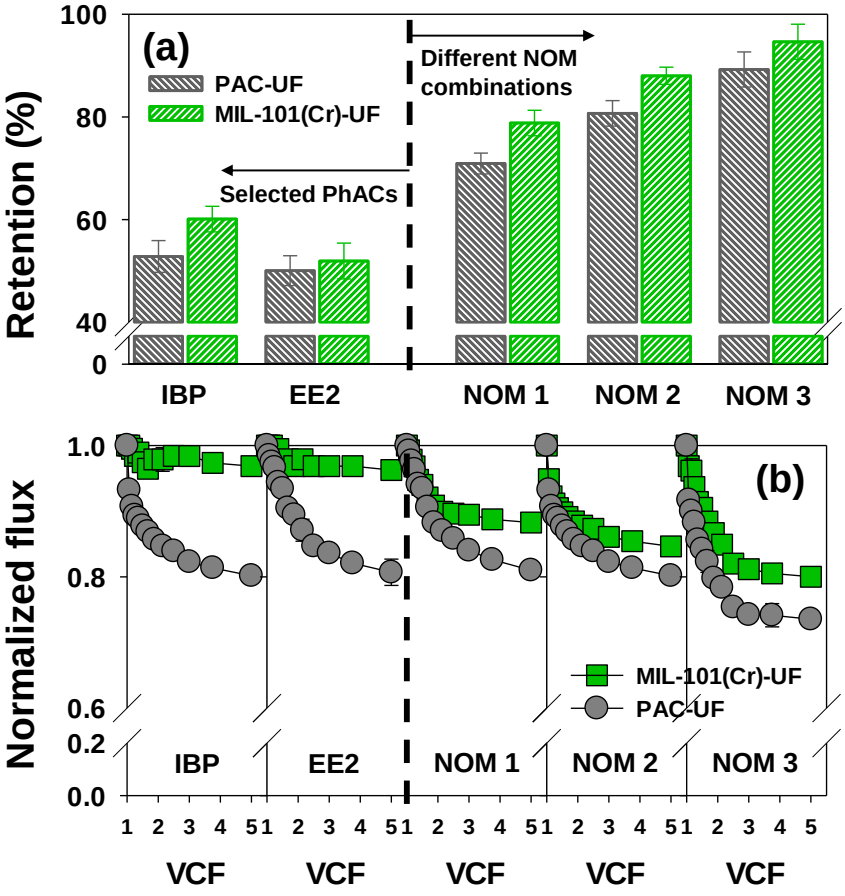

Figure 6.9 (a) Retention rate and (b) normalized flux decline of selected PhACs and different NOM combinations by MIL-101(Cr)-UF and PAC-UF. Operation conditions: ΔP = 520 kPa; stirring speed = 200 rpm; MOF = 20 mg/L; initial selected PhAC concentration = 10 μM; initial NOM = 10 mg/L as DOC; pH = 7.0; conductivity = 300 μS/cm; pre-contact time with MOF = 2 h.

membrane surface and/or pores may occur (Huang et al. 2011, Chu, Shankar et al. 2017). The cake formation resistance ratio (R_c/R_t) was in the order: NOM 3 < NOM 2 < NOM 1, while the adsorptive fouling resistance ratio (R_{ad}/R_t) was in the order: NOM 1 < NOM 2 < NOM 3. This indicates that, while HA formed a cake layer on the membrane surface more readily than TA, TA was more easily adsorbed and/or blocked by the membrane pore, due to size exclusion effects. Moreover, a previous study reported that fouling by cake layers is considerable with large-sized solutes and fouling by adsorptive membranes is mainly affected by small-sized solutes during filtration (Zularisam et al. 2006, Chu et al. 2016).

Reversible and irreversible fouling is evaluated based on the δ value, which is the total resistance per mass of retained NOM (Susanto and Ulbricht 2008, Chu, Huang et al. 2016). For the three different systems tested in this study, the δ value increased with the TA concentration. Higher δ values correspond to high potential for additional blockage and/or deposits on the membrane. Furthermore, the δ values ($\times 10^{12}$ m/g) of NOM 1 (88.7 for the MIL-101(Cr)-UF and 90.0 for the PAC-UF) and NOM 2 (99.1 for the MIL-101(Cr)-UF and 99.8 for the PAC-UF) were lower compared to the UF only (NOM 1, 95.8; NOM 2, 101). However, an increased value of δ with the hybrid systems relative to the UF only was seen for NOM 3 (UF only, 95.8; MIL-101(Cr)-UF and PAC-UF, both 112). These results agree with the fact that the R_{ad} values of NOM 1 and NOM 2 were significantly decreased by changing from the UF only to the hybrid systems, although the R_{ad} value of NOM 3 decreased less markedly. Thus, the relatively small-sized NOM (TA in this study) could exacerbate irreversible fouling by being adsorbed on the membrane pore. Consequently, resistance to both the cake layer and adsorptive membrane fouling were enhanced with use of the MIL-101(Cr). Also, the size exclusion effect, which causes

Table 6.2 Fouling resistances and cake layer characteristics as a function of unit retained DOC mass for different NOM combination by the different system according to resistance-in-series model.

	UF only			MIL-101(Cr)-UF			PAC-UF		
	NOM 1	NOM 2	NOM 3	NOM 1	NOM 2	NOM 3	NOM 1	NOM 2	NOM 3
R_t ($\times 10^{12}$ m^{-1})	94.5	98.4	106	83.0	87.3	94.9	84.8	91.3	99.6
R_m ($\times 10^{12}$ m^{-1})	73.4	73.1	73.3	73.3	73.2	73.3	73.5	73.2	73.2
R_c ($\times 10^{12}$ m^{-1})	15.9	12.4	11.1	10.2	6.63	6.00	13.4	7.92	7.50
R_{ad} ($\times 10^{12}$ m^{-1})	8.72	9.37	21.6	3.09	3.85	15.6	3.35	4.74	18.8
R_c/R_t	0.16	0.13	0.10	0.12	0.08	0.06	0.15	0.09	0.08
R_{ad}/R_t	0.09	0.10	0.20	0.04	0.04	0.16	0.04	0.05	0.19
δ ($\times 10^{12}$ m/g)	95.8	101	110	88.7	99.1	112	90.0	99.8	112

irreversible fouling (Chu, Huang et al. 2016), was presumed to be the dominant reason for the decline in flux seen during NOM retention.

6.6 Summary

In this study, we combined metal organic frameworks (MOFs) with ultrafiltration (UF) hybrid systems (MOF-UF) to treat selected pharmaceutically active compounds (PhACs), including ibuprofen and 17α-ethinyl estradiol, and natural organic matter (NOM) (humic acid and tannic acid; ratios of 10:0, 5:5, and 0:10). Due to the high tunable porosity of MOFs, these materials have strong potential for removing contaminants and reducing fouling in adsorbent-UF hybrid systems. The average retention rate of PhACs in MOF-UF (53.2%) was enhanced relative to the UF only (36.7%). The average retention rate of NOM in the MOF-UF (86.1%) was higher than that with UF only (75.7%). Also, the average normalized flux of NOM in the MOF-UF (0.79) was better than that with UF only (0.74). This is because the PhACs were effectively adsorbed on the MOF due to their strong porous characteristics. We compared MOF-UF and powdered activated carbon-UF (PAC-UF) system in terms of rates and flux decline. The average retention rates for the MOF-UF were higher relative to PAC-UF, by4.6% for PhACs and 6.9% for NOM. However, although the normalized flux in the MOF-UF was better than that in the PAC-UF, for both PhACs and NOM, severe flux decline for NOMs was seen for with the MOF-UF and PAC-UF. We evaluated the effects of NOM with respect to fouling by applying a resistance-in-series model and found that fouling was dominantly affected by the molecular sizes of the solutes in the solution.

CHAPTER 7

FOULING AND RETENTION MECHANISMS OF SELECTED CATIONIC AND ANIONIC DYES IN A $TI_3C_2T_X$ MXENE-ULTRAFILTRATION HYBRID SYSTEM[4]

7.1 Characterization of the MXene

The morphology of MXene, which is a multilayered two-dimensional material, can be seen in the SEM image in Figure 7.1a. The TEM micrograph (Figure 7.1b and c) clearly also indicated that the MXene was multi-layered, with a gap thickness from 0.92–0.95 nm, similar to the results obtained in a previous study (Naguib et al. 2014). Furthermore, the XRD pattern for the MXene, shown in Figure 7.1d, is consistent with previously reported studies, indicating successful synthesis of the MXene (Tariq et al. 2018, Wei et al. 2018). The material surface charge density can be estimated from the zeta potential value. The point of zero charge (PZC) of the MXene was measured at pH 3 based on the zeta potential value, as shown in Figure 7.1e. This is presumably because the T_x, which represent surface termination units in $Ti_3C_2T_x$ Mxene, are -OH, -O, and/or -F (Lukatskaya, Mashtalir et al. 2013). Also, PZC of the membrane was shown at pH 3 in Figure 7.2. These PZC values indicate that both MXene and membrane negatively charged under neutral pH can actively

[4] Reprinted here with permission of publisher: Sewoon Kim *et al*., Fouling and retention mechanisms of selected cationic and anionic dyes in a $Ti_3C_2T_x$ MXene-ultrafiltration hybrid system. ACS Applied Materials & Interfaces 12(14) (2020) 16557-16565

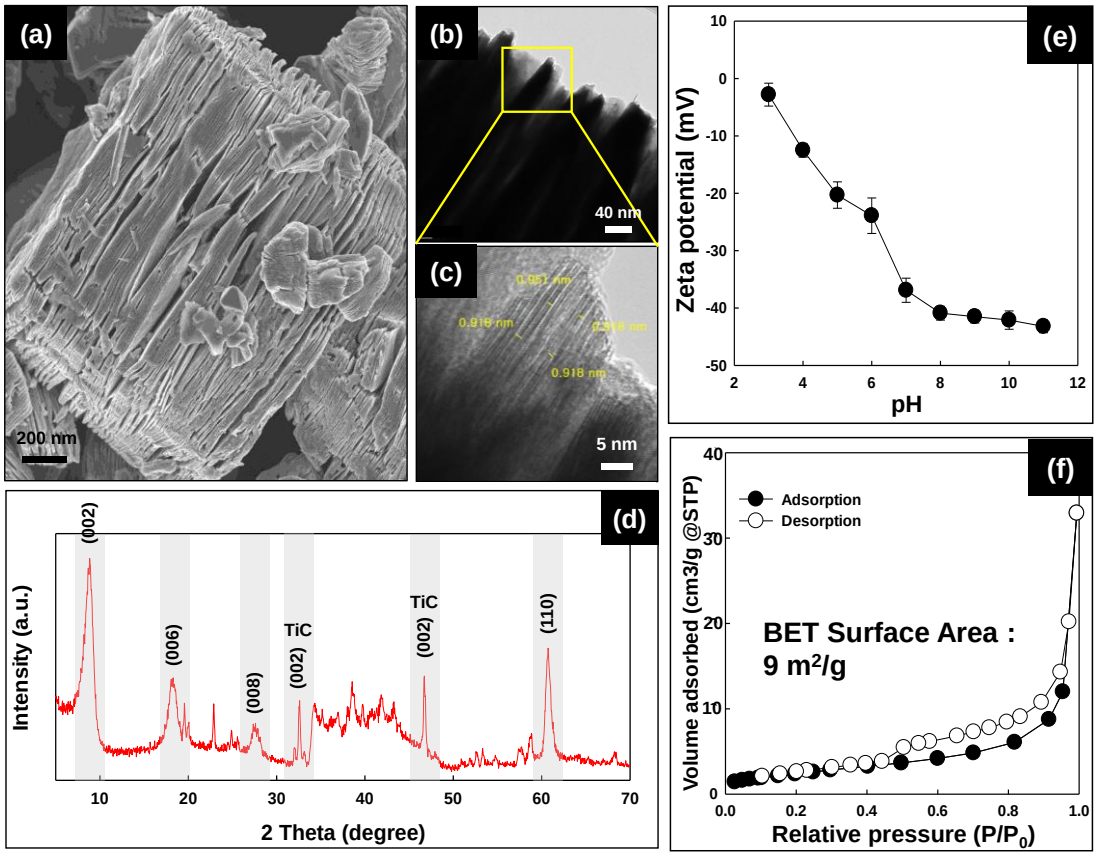

Figure 7.1 Characteristics of MXene using (a) SEM, (b) and (c) TEM, (d) XRD, (e) Zeta-potential analyzer, and (f) porosimeter.

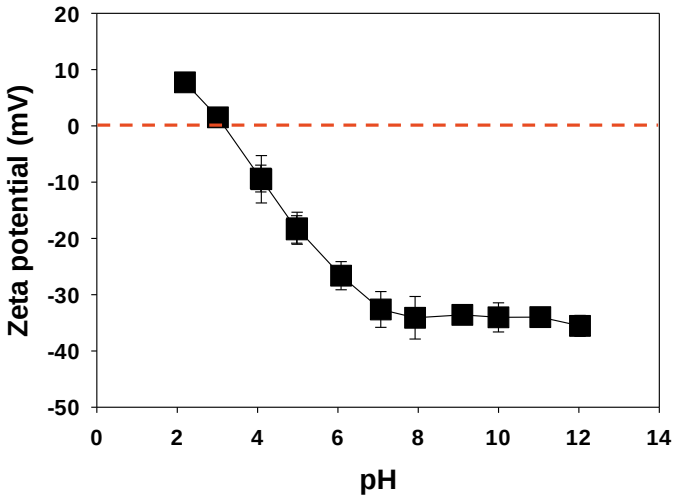

Figure 7.2 Zeta potential value of membrane used in this study with pH variations.

adsorb positively charged compounds through electrostatic attraction, while those may have small adsorption with negatively charged compounds due to electrostatic repulsion. Finally, the BET surface area of the MXene was estimated from the equilibrium data of adsorption and desorption of nitrogen at -196℃. Figure 7.1f shows the 9 m^2/g MXene surface area; this value is similar to that reported earlier (Fard et al. 2017). Therefore, the SEM, TEM, XRD, zeta potential analysis, and surface area results indicate that MXene has potential for use in adsorbent-UF for removal of the selected dyes.

To confirm the feasibility of MXene-UF to remove dyes compound, Figure 7.3 presents that retention rate and normalized flux in single UF, MXene-UF, and PAC-UF with synthetic dye wastewater as a feed solution. Also, the composition of synthetic dyes wastewater was described in Table 7.1. While 65.4% of dyes retention rate in single UF was achieved, significantly higher retention rates in the presence of 20, 50, and 100 mg/L each adsorbent were observed; 80.2%, 90.7%, and 99.1% for MXene-UF, and 85.5%, 91.7%, and 99.5% for PAC-UF, respectively. Also, although similar normalized flux was shown with increasing MXene dose (0.90 for 20 mg/L, 0.89 for 50 mg/L, and 0.89 for 100 mg/L) compared to single UF (0.90), significant flux decline was observed in PAC-UF with increasing PAC dose (0.79 for 20 mg/L, 0.72 for 50 mg/L, and 0.60 for 100 mg/L). These results indicate that MXene-UF can be applied to treat dye containing wastewater with high retention rate and less flux decline. Meanwhile, mechanism evaluation for retention and fouling is very important to understand performance. Thus, the effect of each composition for detailed performance was confirmed by following studies.

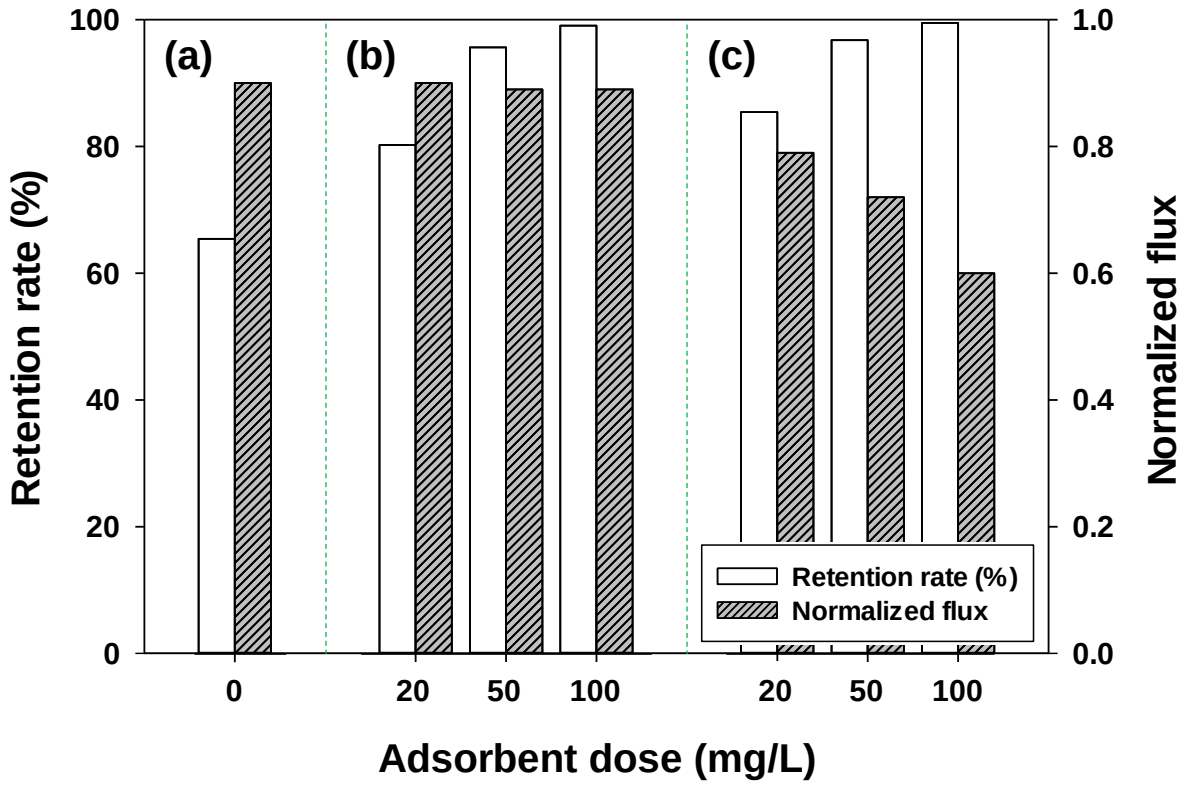

Figure 7.3 Retention and normalized flux variation for synthetic dye wastewater in (a) single UF, (b) MXene-UF, and (c) PAC-UF. Operating conditions: VCF = 1.25 (recovery = 20%), ΔP = 75 psi (520 kPa), pre-contact time = 2 h, and stirring speed = 200 rpm.

Table 7.1 Composition of the synthetic dyes wastewater used in this study.

Composition	Concentration
Dyes (MB)	2 mg/L
Humic acid	5 mg/L
NaCl	300 μS/cm
Na_2SO_4	300 μS/cm
$CaCl_2$	300 μS/cm
pH	7

7.2 Flux decline in hybrid system

The declining flux behaviors of the selected dyes in the single UF, MXene-UF, and PAC-UF treatments are shown as a function of VCF in Figure 7.4. The normalized fluxes of MB and MO in single UF at VCF = 5 decreased gradually, to 0.86 and 0.90, respectively. A slightly higher normalized flux was observed MXene-UF (0.90 for MB and 0.92 for MO at VCF = 5) than in single UF. In contrast, a rapid flux decline was observed for MB and MO in PAC-UF, with values of 0.72 and 0.75, respectively, at VCF = 5. These results show that MB more impacted on the flux decline than MO. Both compounds have a similar molecular weight (319.85 g/mol for MB and 327.33 g/mol for MO); however, positively charged MB can be more readily deposited on the negatively charged membrane at pH 7 compared to negatively charged MO, resulting in a decreasing membrane surface and pore size (An et al. 2016, Ma et al. 2017). In addition, enhanced membrane flux was observed in MXene-UF compared to single UF, while deterioration of the permeate flux was observed in PAC-UF. This is presumably because, while some MXenes with OH and/or O terminations can interact with COOH, NHCO and NH_2 in a polyamide membrane by forming hydrogen bonds (Xu et al. 2013, Zhang et al. 2018), most MXenes with negative charge (estimated based on zeta potential value; Figure 7.1e) cannot easily attach onto the membrane due to electrostatic repulsion. In contrast, PAC has more functional groups, higher hydrophobicity, and less negatively characteristics compared to MXenes, so flux decline can arise through PAC deposition on the membrane (Löwenberg, Zenker et al. 2014, Kim, Muñoz-Senmache et al. 2020).

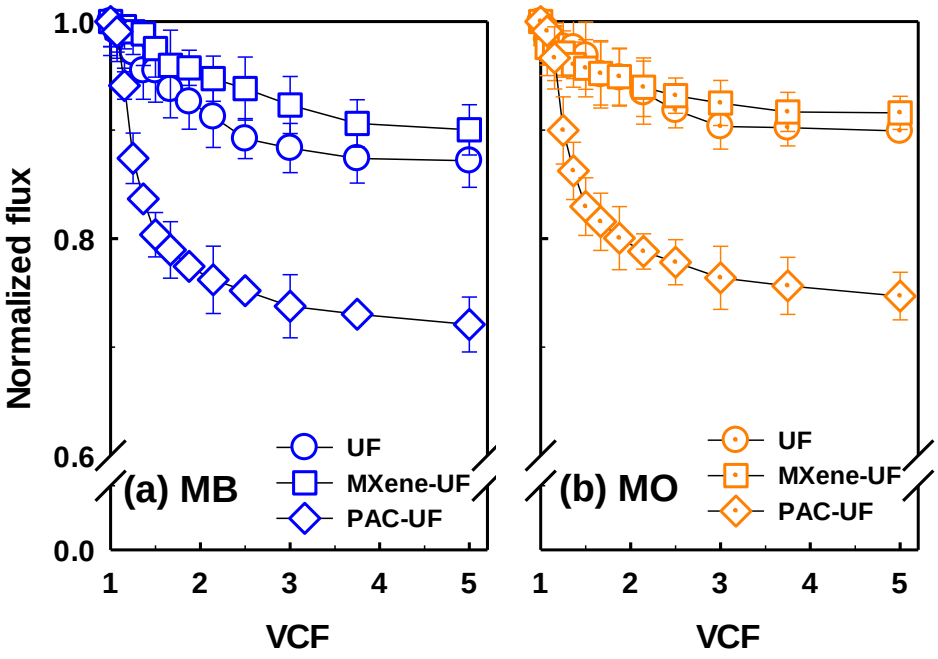

Figure 7.4 Normalized flux variation as a function of VCF for (a) MB and (b) MO. Operating conditions: ΔP = 75 psi (520 kPa), adsorbent = 20 mg/L, dye = 2 mg/L, pH = 7, conductivity = 100 μS/cm, pre-contact time = 2 h, and stirring speed = 200 rpm.

Table 7.2 Fouling resistances, specific cake resistances (ε), and specific adsorption resistances (δ) for selected dyes in the single UF, MXene-UF, and PAC-UF system.

	MB			MO		
	UF	MXene-UF	PAC-UF	UF	MXene-UF	PAC-UF
R_t ($\times 10^{12}$ m^{-1})	88.8	85.0	106	85.4	83.9	102
R_m ($\times 10^{12}$ m^{-1})	76.5	76.5	76.5	76.8	769	76.2
R_c ($\times 10^{12}$ m^{-1})	7.99	4.76	25.3	5.91	5.43	22.4
R_{ad} ($\times 10^{12}$ m^{-1})	4.28	3.72	4.31	2.70	1.63	3.44
R_c/R_t	0.09	0.06	0.24	0.07	0.06	0.22
R_{ad}/R_t	0.05	0.04	0.04	0.03	0.02	0.03
ε ($\times 10^{12}$ m/g)	22.7	13.8	76.5	14.7	13.8	59.9
δ ($\times 10^{12}$ m/g)	12.1	10.8	13.0	6.72	4.13	9.21

Comprehensive understanding of fouling resistance is essential for improving the performance of this hybrid system. Therefore, evaluation of fouling phenomena was conducted using a resistance-in-series model, as shown in Table 7.2. The overall filtration resistance (Rt) with MB (88.8 for single UF, 85.0 for MXene-UF, and 106 for PAC-UF) was higher than for MO (85.4 for single UF, 83.9 for MXene-UF, and 102 for PAC-UF), indicating that a relatively larger flux decline was generated with MB. A higher value for both cake formation resistance (R_c) (7.99 for single UF, 4.76 for MXene-UF, and 25.3 for PAC-UF) and adsorptive fouling resistance (R_{ad}) (4.28 for single UF, 3.72 for MXene-UF, and 4.31 for PAC-UF) was obtained with MB compared to MO, for all three systems (R_c: 5.91 for single UF, 5.43 for MXene-UF, and 22.4 for PAC-UF, R_{ad}: 2.70 for single UF, 1.63 for MXene-UF, and 3.44 for PAC-UF). These results support the conclusion that MB can be more easily deposited on both the surface of, and inside, the membrane by electrostatic attraction. In addition, the value of R_c/R_t for MB and MO in MXene-UF was the same, at 0.06, while R_{ad}/R_t for MB (0.04) was higher than that for MO (0.02). This also indicates that MO can generate relatively lower adsorptive fouling due to electrostatic repulsion. Furthermore, MXene was a positive influence on both the R_c and R_{ad} values in filtration compared to single UF, which indicates that electrostatic repulsion rather than hydrogen bonding occurs between MXene and the membrane. However, the highest R_t, R_c, and R_{ad} values were observed for PAC-UF compared to single UF and MXene-UF, demonstrating that PAC acts as a foulant by adsorbing and depositing on the membrane.

To quantify the reversible and irreversible fouling potential of the three different systems, the total cake formation resistance per mass of the retained selected dyes and/or adsorbent (specific cake resistance, ε) and the total adsorptive resistance per mass of the

retained selected dyes and/or adsorbent (specific adsorptive resistance, δ) were evaluated (Susanto and Ulbricht 2008). A number of previous studies have suggested that cake formation resistance caused by the deposition of foulants is generally reversible (Aoustin et al. 2001). In contrast, the internal pore fouling resistance of the membrane due to the adsorption of foulants is often irreversible (Jucker and Clark 1994). Both the ε and δ values of single UF (ε: 22.7, δ: 12.1 for MB, ε: 14.7, δ: 6.72 for MO) were higher than for MXene-UF (ε: 13.8, δ: 10.8 for MB, ε: 13.8, δ: 4.13 for MO) and lower than for PAC-UF (ε: 53.1, δ: 36.4 for MB, ε: 37.5, δ: 31.6 for MO). These observations indicate that the amount of dye and/or adsorbent, as a potential cause of both cake formation and adsorptive resistance in single UF, was higher than in MXene-UF and lower than in PAC-UF. In other words, MXene can enhance the ε and δ values by adsorbing dyes and not depositing excessively on the membrane. However, although PAC can adsorb the selected dyes, additional deposition occurs with PAC acting as a foulant. The ε value was higher than the δ value under all experiment conditions, indicating that reversible fouling dominates over irreversible fouling. Therefore, MXene-UF is superior to single UF and PAC-UF in terms of flux decline, due to dye adsorption by MXene and low deposition of MXene on the membrane because of electrostatic repulsion.

7.3 Fouling mechanisms in hybrid system

To analyze the flux decline of MB and MO in detail, permeate flux modeling was performed for single UF, MXene-UF, and PAC-UF, as shown in Figure 7.5. Permeate flux modeling (J^2 vs. *time*) based on experimental flux data is widely used to evaluate model constants (α and β) and MFI values in linear form (Chu, Huang et al. 2016). In particular, the MFI value, which is based on the cake filtration fouling mechanism, is needed to obtain

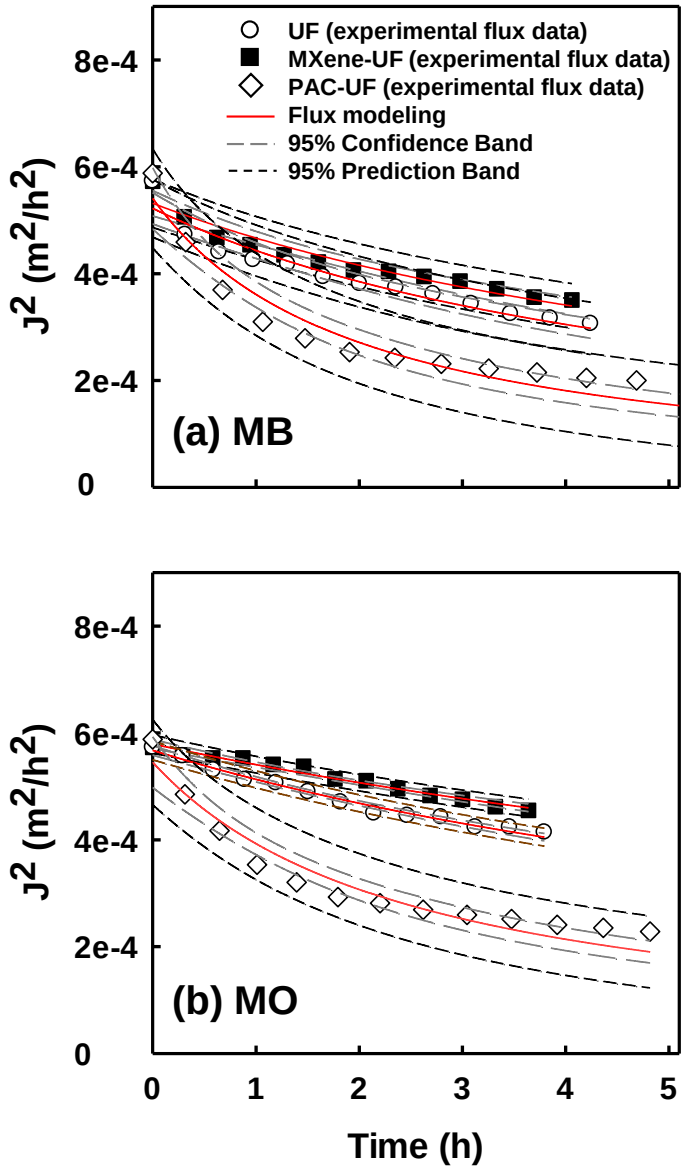

Figure 7.5 Flux decline analysis for (a) MB and (b) MO via permeate flux modeling in the single UF, MXene-UF, and PAC-UF system.

Table 7.3 Analyses of permeate flux modeling for MB and MO in the single UF, MXene-UF, and PAC-UF system.

		α (min^2/m^2)	β (min/m^2)	r^2	MFI (min/m^2)
MB	UF	1,915	341	0.9275	85.2
	MXene-UF	1,880	262	0.9270	65.5
	PAC-UF	1,849	919	0.9293	230
MO	UF	1,762	186	0.9227	46.6
	MXene-UF	1,726	123	0.9209	30.8
	PAC-UF	1,834	711	0.9296	178

the fouling potential and mitigate flux decline (Boerlage et al. 2002, Ju et al. 2015). The model constants and MFI values are presented in Table 7.3. Less cake formation is observed for MXene-UF compared to single UF, as stated previously, leading to a lower MFI value. This result supports the conclusion that the MXene has a positive effect on flux decline due to electrostatic repulsion with the membrane. In contrast, it was found in the previous section that PAC, as a foulant, had a negative effect on the permeate flux through deposition on the membrane. This can also be seen in the higher MFI value for PAC-UF, because the MFI value is proportional to the extent of cake formation. This finding indicates that PAC can more easily form a cake layer than the MXene, consistent with the result of the resistance-in-series model.

Four conceptual blocking models, which have been widely used to evaluate membrane fouling at constant transmembrane pressure, were generated to describe the fouling mechanism (Figure 7.6) (Chu, Huang et al. 2016, Kirschner et al. 2019). The r^2 values obtained by linear regression on each fouling mechanism are summarized in Table 7.4. It appears that, although the value for cake filtration (r^2: 0.9959 for MB and 0.9584 for MO) was slightly higher than that for standard blocking (r^2: 0.9951 for MB and 0.9519 for MO) for both dyes in single UF, both fouling mechanisms had relatively higher values than complete (r^2: 0.9009 for MB and 0. 9040 for MO) and intermediate blocking (r^2: 0.9006 for MB and 0.9019 for MO). This is presumably because cake filtration is caused by the accumulation of dyes in the cake layer. In addition, because both MB and MO have a size of about ~20 Å, which is smaller than the membrane pore (26~30 Å), some part of each dye can be adsorbed by hydrogen bonding into the membrane pore walls (Ma et al. 2012). Cake filtration (r^2: 0.9690) for MB in MXene-UF showed better fitting results compared

to complete (r^2: 0.9089), standard (r^2: 0.9434), and intermediate blocking (r^2: 0.9053), whereas cake filtration (r^2: 0.9876) and standard blocking (r^2: 0.9854) showed slightly higher values than complete (r^2: 0.9809) and intermediate blocking (r^2: 0.9794) for MO in MXene-UF. This indicates that MB can be adsorbed on MXene by electrostatic attraction, resulting in reduced internal membrane fouling (Mashtalir et al. 2014, Wei, Peigen et al. 2018). Cake filtration showed the best fitting results for both dyes in PAC-UF, due to deposition of PAC on the membrane surface. Also, n value was used for determining the fouling mechanism from d^2t/dV^2 versus dt/dV as shown in Figure 7.7. The n values under all conducted system were shown about 0, which confirms that cake filtration is dominant and corresponds with results of four conceptual blocking models. Therefore, flux decline caused by reversible fouling, i.e., a cake layer, is the dominant fouling mechanism for removal of the selected dyes in all three systems. In addition, both hybrid systems exhibited reduced irreversible fouling compared to single UF, due to the addition of the adsorbent during filtration.

7.4 Retention and mechanisms in the hybrid system

Figure 7.8 shows the retention performance of MB and MO at pH 7, as a function of the VCF, in single UF, MXene-UF, and PAC-UF. The average retention rate in single UF was about 45.0% for MB and 34.7% for MO. This is because both dyes can interact with the membrane. Hydrogen bonding can occur between polyamide membranes with COOH, NHCO and NH_2, and dyes with N and O (Falca et al. 2019). Also, hydrophobic interaction can occur between the aromatic rings of the membrane, and that of MB and MO (Lin and Chang 2015, Sarker et al. 2019). Furthermore, electrostatic interaction between

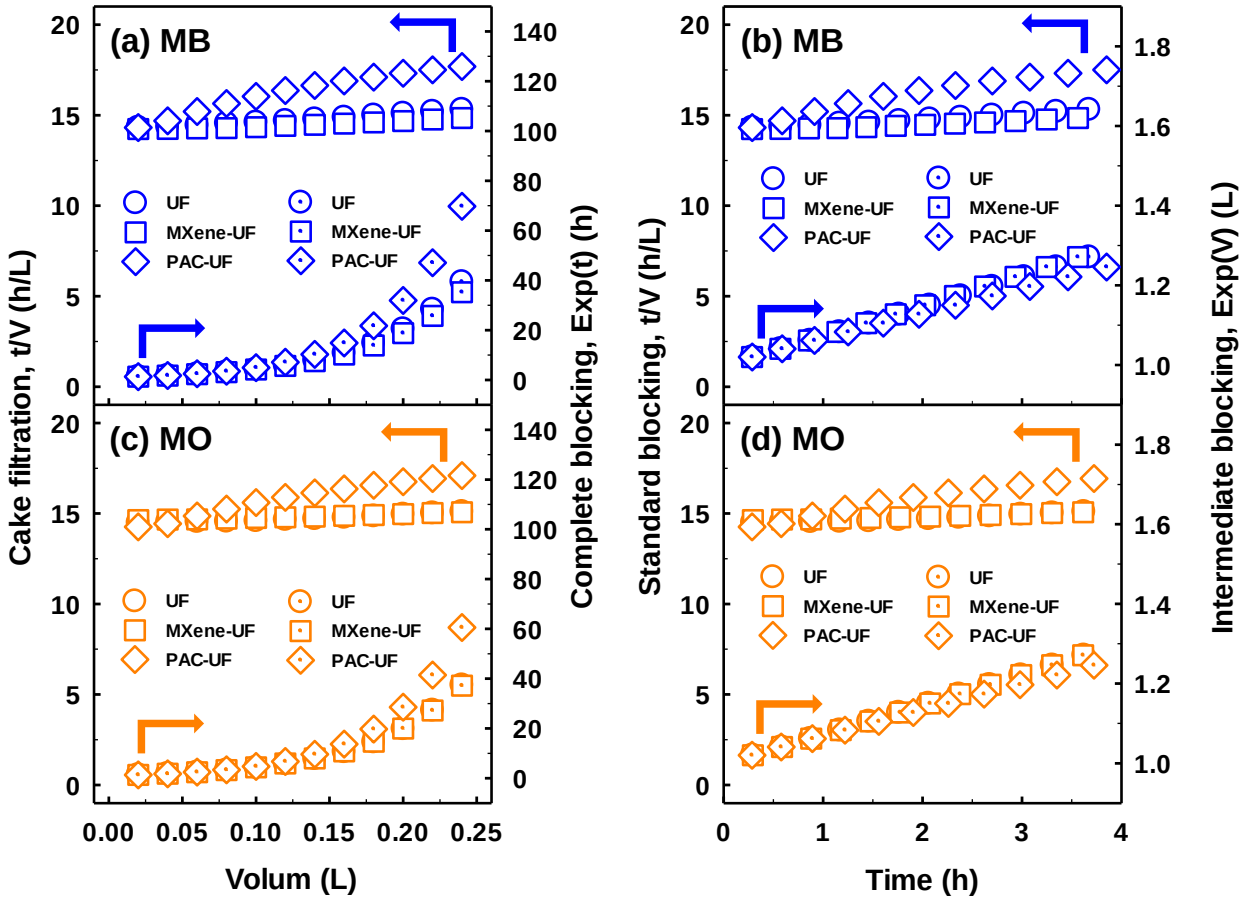

Figure 7.6 Four conceptual blocking law models at 75 psi (520 kPa) in the single UF, MXene-UF and PAC-UF system. (a) Cake filtration and complete blocking analysis for MB, (b) standard blocking and intermediate blocking analysis for MB, (c) cake filtration and complete blocking analysis for MO, and (d) standard blocking and intermediate blocking analysis for MO.

Table 7.4 Regression results using four conceptual blocking law models.

		Cake filtration			Complete blocking			Standard blocking			Intermediate blocking		
		a	b	r^2	a	b	r^2	a	b	r^2	a	b	r^2
MB	UF	4.57	14.2	0.9959	0.043	0.008	0.9009	0.297	14.2	0.9951	1.915	50.1	0.9006
	MXene-UF	2.88	14.1	0.9690	0.033	0.018	0.9089	0.194	14.1	0.9434	1.44	40.6	0.9053
	PAC-UF	0.996	14.3	0.9702	0.073	0.056	0.8792	0.838	14.4	0.9579	3.68	43.6	0.9054
MO	UF	2.81	14.4	0.9584	0.031	0.001	0.9040	0.187	14.4	0.9519	1.37	41.4	0.9019
	MXene-UF	2.00	14.6	0.9876	0.020	0.020	0.9809	0.133	14.6	0.9854	0.894	42.3	0.9794
	PAC-UF	13.3	14.1	0.9885	0.071	0.032	0.8960	0.758	14.2	0.9691	3.45	42.6	0.9176

the membrane and dyes can affect the retention rate, because MB contains positively charged nitrogen and MO has a negatively charged sulfonate group (Lin et al. 2016). A higher retention rate was observed for MB compared to MO in single-UF, because MB is hydrophobic and hence has a higher octanol-water distribution coefficient (log D_{OW}: 2.60) than MO (log D_{OW}: 1.29) at pH 7. Additionally, electrostatic attraction between MB and a negatively charged membrane can enhance the retention rate through deposition on the membrane. In contrast, some part of MO can be retained on the feed side due to electrostatic repulsion with the membrane, which prevents the dye from passing through. Nevertheless, the higher retention of MB in single UF indicates that both hydrophobic interaction and electrostatic attraction dominate. Furthermore, removal efficiencies increased with adsorbent in both hybrid systems. PAC-UF exhibited better average retention rates, of 57.7% for MB and 47.9% for MO, compared to MXene-UF (51.7% for MB and 34.9% for MO). It was previously mentioned that both hydrogen bonds and electrostatic interaction exist between the MXene and both dyes in MXene-UF (Meng, Seredych et al. 2018). However, PAC can more easily reduce the membrane surface and pore size than MXene by depositing on the membrane, resulting in a higher retention rate. Also, both dyes can be more easily adsorbed on PAC than on Mxene, because of the higher surface area and increased hydrophobic interaction, hydrogen bonding, and electrostatic interaction. Thus, PAC-UF is superior to single UF and MXene-UF in terms of retention rate.

To evaluate the adsorption capacity of the membrane and both adsorbents during filtration, an adsorption test was conducted, as shown in Figure 7.9. Both MB and MO were placed in contact with the membrane for 4 h and/or the adsorbents for 6 h. This contact time was selected to ensure the same contact time for single UF and both hybrid systems.

The adsorption removal rate was in the order PAC (35.7% and 30.9%) > MXene (26.7% and 12.4%) > membrane (16.1% and 10.5%) for MB and MO, respectively. The PAC and membrane adsorbed relatively similar amounts of both dyes, while the removal rate of MB with the MXene was higher than for MO. This is because electrostatic interaction plays an important role in the interaction between MXenes and dyes. Therefore, these results confirm that, although MXene-UF exhibited poorer retention performance than PAC-UF, as the retention rate between MB and MO is different, MXene-UF shows high selectivity due to electrostatic attraction or repulsion.

7.5 Effects of different solution conditions on dye retention in the MXene-UF

Based on the normalized permeate flux and retention rate results, the MXene-UF system has high potential to treat dyes, with higher performance seen for MB than MO. Also, in general, some of the dye constituents, such as NOM, H^+/OH^-, and inorganic ions, coexist in real ecosystems. To fully explore the performance of MXene-UF for MB, the retention rate and normalized permeate flux were confirmed under a range of solution conditions. As shown in Figure 7.10a, the retention rate of MXene-UF increased with increasing HA concentration (51.7% for no HA, 58.5% for 2.5 mg/L, and 68.3% for 10 mg/L), while the normalized flux decreased with increasing HA concentration (0.96 for no HA, 0.91 for 2.5 m/L, and 0.79 for 10 mg/L). Also, all data in Figure 7.10a was statistically not same average by one-way complete statistical analysis of variance (ANOVA) test at a confidence level of 95%. These results presumably arise because the membrane active area was diminished by HA adsorption on the membrane. Due to the range of sizes of the HA (170–22,600 Da), pore plugging of the membrane (3,000 Da) is possible (Tang et al. 2007,

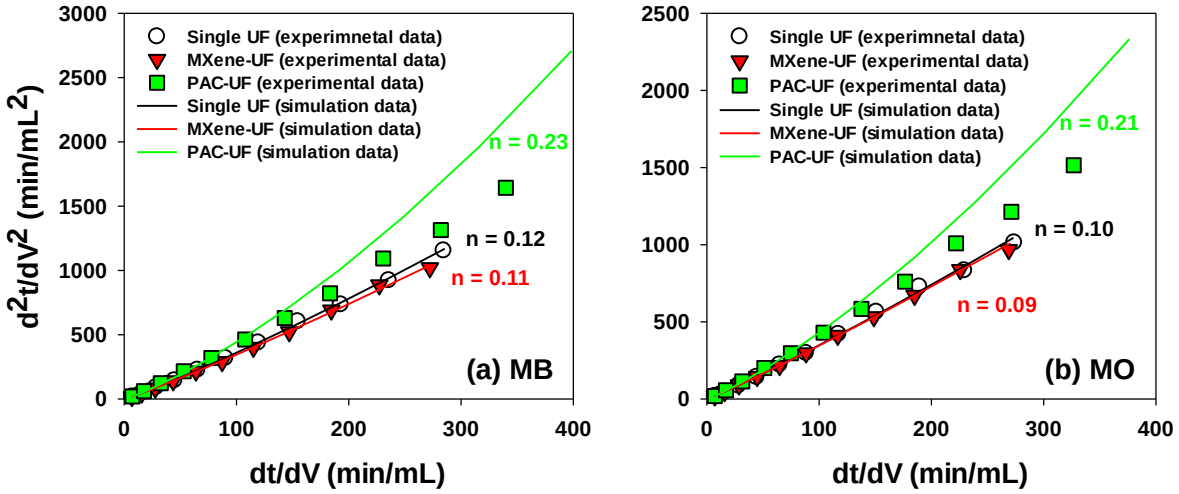

Figure 7.7 Flux decline analyses via d2t/dV2 versus dt/dV curves in single UF, MXene-UF, and PAC-UF for (a) MB and (b) MO. Operating conditions: ΔP = 75 psi (520 kPa), adsorbent = 20 mg/L, dye = 2 mg/L, pH = 7, conductivity = 100 μS/cm, pre-contact time = 2 h, and stirring speed = 200 rpm.

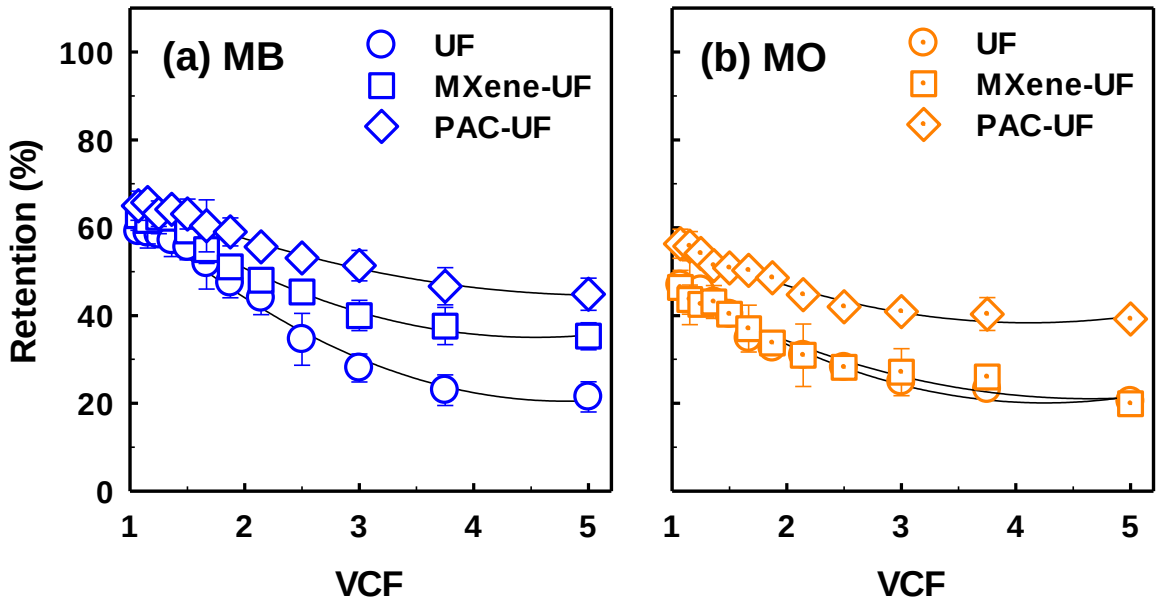

Figure 7.8 Retention variation as a function of VCF for (a) MB and (b) MO. Operating conditions: ΔP = 75 psi (520 kPa), adsorbent = 20 mg/L, dye = 2 mg/L, pH = 7, conductivity = 100 μS/cm, pre-contact time = 2 h, and stirring speed = 200 rpm.

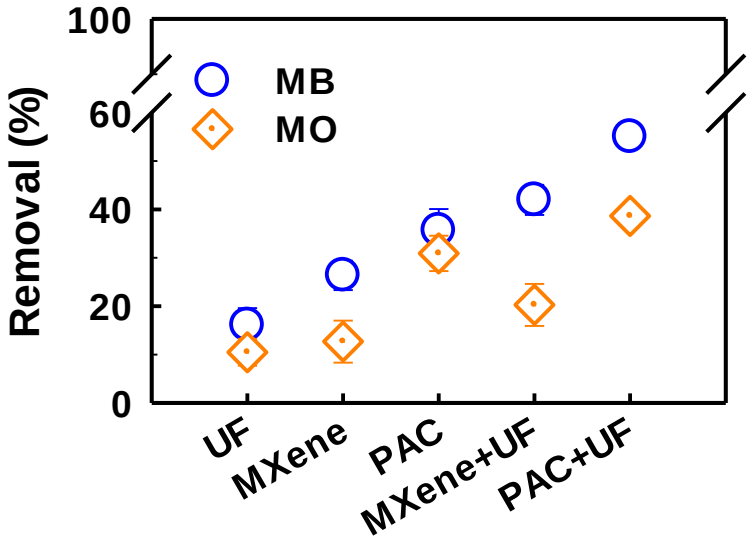

Figure 7.9 Adsorption of MB and MO on each adsorbent during filtration. Operating conditions: membrane area = 14.6 cm^2, adsorbent = 20 mg/L, dyes=2 mg/L, pH=7, conductivity=100 µS/cm, and stirring speed = 200 rpm.

Sun et al. 2017). In addition, aromatic components of HA can generate a fouling layer on the membrane surface through hydrophobic interaction (Nghiem, Vogel et al. 2008), and positively charged MB and the part of HA (which includes negatively charged carboxylic and phenolic groups at pH 7) can form complexes by electrostatic attraction as well as hydrophobic interaction, resulting in high retention and low permeate flux (Lin, Ye et al. 2016).

The retention rate of MXene-UF at pH 3.5, 7, and 10.5 was 46.7%, 51.7%, and 57.7%, respectively, as shown in Figure 7.10b. The normalized flux for MXene-UF was observed to be 0.96, 0.96, and 0.95 at pH 3.5, 7, and 10.5, respectively. Although this result shows that the retention rate was similar regardless of solution pH by ANOVA tests, a slightly higher retention rate was confirmed at pH 10.5. The MB might be adsorbed more on the MXene at higher pH due to the more abundant negative charged termination of MXene, as supported by the zeta potential result (Figure. 7.1e) (Deng et al. 2009, Ying et al. 2015, Liu et al. 2017). In overall, the results (relatively high flux decline (Figure 7.4), high retention (Figure 7.8), high adsorption removal (Figure 5), and high retention with increasing pH (Figure 7.10) for MB compared to MO) indicate that electrostatic interaction was the most critical mechanism determining the MXene-UF performance.

Finally, the retention rate and normalized flux of MXene-UF for MB was evaluated with no ions, and with NaCl, $CaCl_2$, and Na_2SO_4, as shown in Figure 7.10c. Although ANOVA tests indicate there are comparable retention results, the highest retention rate, of 51.7%, was observed with no ions (46.6% for NaCl, 43.4% for $CaCl_2$, and 47.7% for Na_2SO_4); similarly, the highest normalized flux, of 0.96, was seen with no ions (0.89 for NaCl, 0.84 for $CaCl_2$, and 0.90 for Na_2SO_4). In Section 3.4, it was shown that adsorption

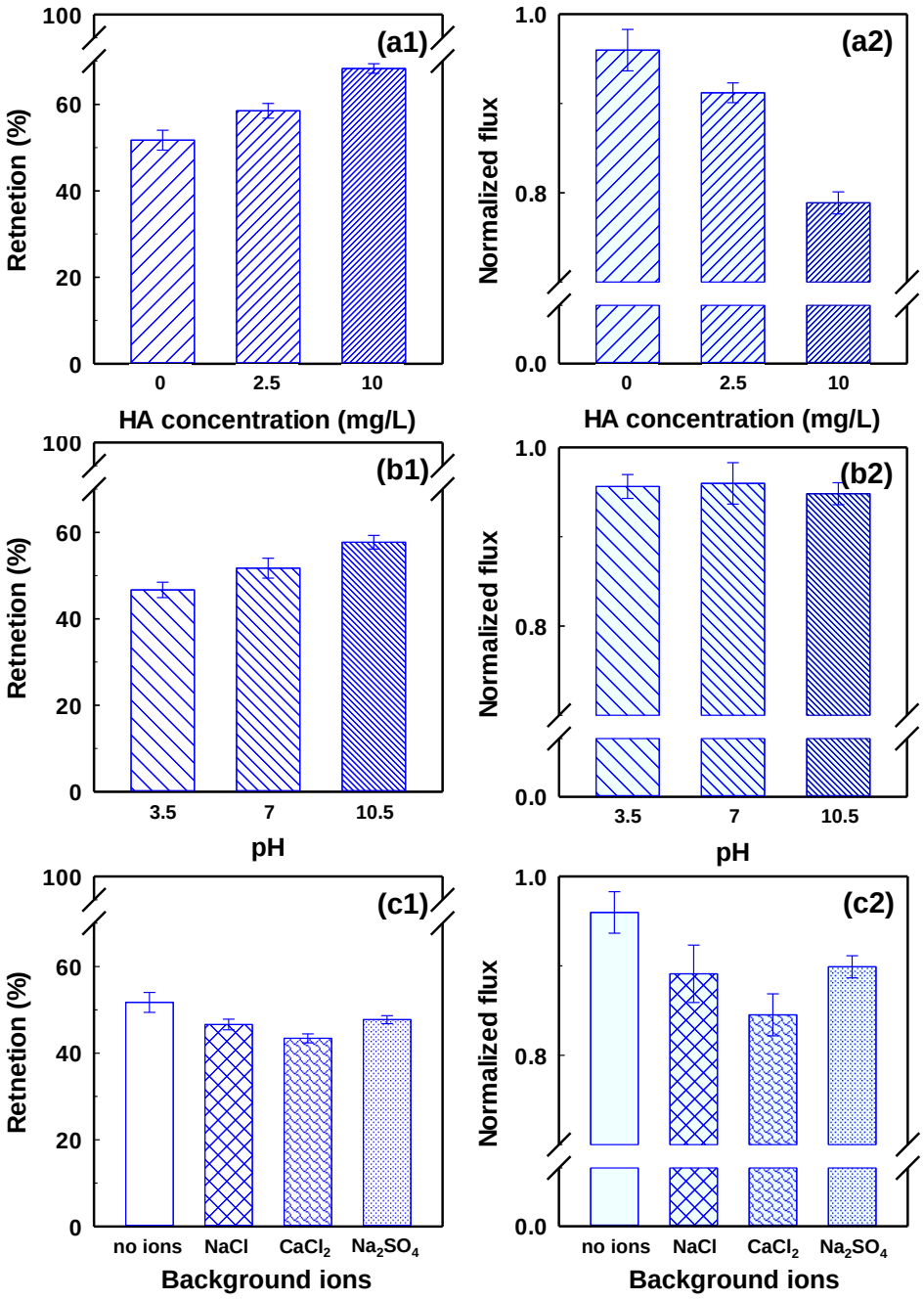

Figure 7.10 Retention and normalized flux under various (a) NOM concentrations, (b) pH conditions, and (c) background ions for MB in the MXene-UF system. Operating conditions: ΔP = 75 psi (520 kPa), adsorbent = 20 mg/L, MB = 2 mg/L, pre-contact time = 2 h, and stirring speed = 200 rpm.

by MXene is the main cause of retention for MB in MXene-UF. However, the retention rate decreased with the addition of ions because positive ions compete with MB for adsorption sites on the MXene via electrostatic attraction (Jiang et al. 2017). The normalized flux which is statistically evaluated at a confidence level of 95% by ANOVA, also decreased in the presence of ions. This is likely because the presence of ions leads to a denser fouling layer and compacted membrane pores (Visvanathan et al. 1998, Shankar, Heo et al. 2017). In addition, the formation of cross linking between Mxene and the membrane can affect the filtration system by the divalent cation bridging effect, leading to the lowest normalized flux with CaCl2 (Yin et al. 2019).

7.6 Summary

$Ti_3C_2T_x$ MXene, a very new family of nanostructured material, was applied in combination with an ultrafiltration (UF) membrane (MXene-UF) for removal of the selected dyes including methylene blue (MB) and methyl orange (MO) as the first attempt. The normalized flux of the MXene-UF (0.90 for MB and 0.92 for MO) indicated better performance than a single UF (0.86 for MB and 0.90 for MO) and a powdered activated carbon (PAC)-UF (0.72 for MB and 0.75 for MO) for both dyes. The addition of an adsorbent decreased the irreversible fouling of the hybrid system compared to single UF, due to adsorption of dyes. The observed dominant fouling mechanism was cake layer fouling, evaluated using a resistance-in-series model, permeate flux modeling, and four conceptual blocking law models. PAC in particular acted as a foulant, leading to severe flux decline. The average retention rate was found to be in the order PAC-UF (57.7% and 47.9%) > MXene-UF (51.7% and 34.9%) > single UF (45.0% and 34.7%) for MB and MO, respectively. The results showed that although PAC exhibits relatively strong adsorption

performance MXene-UF also exhibited high selectivity due to electrostatic interaction between the MXene and dyes. In addition, humic acid (HA) adsorption on the membrane led to a reduction in the effective membrane area, resulting in higher retention and lower flux for MXene-UF in the presence of HA. Furthermore, higher retention was observed for MXene-UF at pH 10.5 compared to pH 3.5 and 7, because MXene has more negative terminations at higher pH, leading to greater MB adsorption. Additionally, because of the bridging effect between the membrane and the MXene, and competition between MB and cation ions for adsorption on the MXene, lower retention and flux was observed in MXene-UF with background ions.

CHAPTER 8

OVERALL CONCLUSIONS

This study evaluated the (nano)adsorbent-UF hybrid systems to treat selected organic contaminants under various water qualities. ABC, MOF, and MXene were applied as adsorbent. Also, PhACs (IBP, EE2, and CBM), NOM, and dyes were selected as target contaminants. Furthermore Retention/fouling variation and mechanism were observed on adsorbent-UF mechanism.

In chapter 5, an ABC generated from incomplete combustion of waste biomass, combined with UF membrane system (ABC-UF), was used to treat selected PhACs, and compared to PAC-UF. Although the ABC had a lower surface area than PAC, ABC has better aromatization. The average retention rate arranged in the following order: IBP > EE2 > CBM for the UF system alone, and EE2 > IBP > CBM for the ABC-UF. These results were influenced by the properties (p*Ka* value and hydrophobicity) of each compound depending on the pH. However, the dominant mechanism of retention in the ABC-UF is hydrophobic adsorption between the compounds and ABC. The ABC-UF system without HA had no serious fouling, compared to the UF system alone. However, the ABC-UF with HA demonstrated a relatively serious flux decline because HA blocked the surface and pores of the membrane. Furthermore, although the retention rate of PAC-UF is slightly higher than ABC-UF, the ABC-UF was superior to PAC-UF in terms of flux decline. Consequently ABC-UF may serve as a suitable alternative to PAC-UF in terms of both

retention capacity and fouling reduction.

In chapter 6, we used MOF-UF hybrid systems to treat two PhACs (IBP and EE2) and NOM under three different ratios (HA:TA = 10:0, 5:5, and 0:10). Two classical MOFs were applied as upstream adsorbents: MIL-100(Fe) and MIL-101(Cr). For PhACs, the MOF-UF retention rate was better than that of the UF only under pH of 3, 7, and 11. Also, no severe fouling occurred in the case of the MOF-UF because the MOFs adsorbed the selected PhACs efficiently. In particular, MIL-101(Cr), with larger inner pores, exhibited higher solution stability than MIL-100(Fe), resulting in a higher PhAC retention rate. In the case of NOM, the retention rate and normalized flux with the MIL-101(Cr)-UF was better than that with the MIL-100(Fe)-UF and UF only. While increasing the TA concentration in the NOM solution resulted in a higher retention rate, the normalized flux in higher TA concentration solutions decreased significantly. As TA molecules are smaller than HA molecules, TA can readily adsorb onto/into the membrane surface/pore and MOF, resulting in higher retention and severe flux decline. Moreover, the MIL-101(Cr)-UF was superior to the PAC-UF in terms of both retention rate and permeate flux, for the selected PhACs and NOM. However, unlike PhACs, serious fouling was observed in NOM solutions, as previously stated. To evaluate the fouling mechanism, we applied a resistance-in-series model. The results showed that fouling is mainly in the form of cake layer fouling (reversible) for HA and adsorptive fouling (irreversible) for TA. These observations confirm that the performance of the MOF-UF hybrid system is superior to that of the UF only and PAC-UF, with respect to PhACs and NOM retention, and antifouling performance. Therefore, MOF-UF may be a suitable alternative technology to conventional system.

In chapter 7, $Ti_3C_2T_x$ MXene, as an adsorbent, was applied to a hybrid system based on adsorption combined with UF (MXene-UF) to treat selected dye compounds, including MB and MO. The normalized flux in MXene-UF (0.90 for MB and 0.92 for MO) exhibited better efficiency than a single UF system (0.86 for MB and 0.90 for MO), while another hybrid system, PAC-UF (0.72 for MB and 0.75 for MO) exhibited severe flux decline. This is because dyes can be adsorbed onto MXene, and only small quantities of MXene are deposited on the filtration membrane due to electrostatic repulsion. Both hybrid systems showed less irreversible fouling compared to single UF. A resistance-in-series model, permeate flux modeling, and four conceptual blocking law models were used to investigate the behavior of the adsorbents, and it was observed that PAC acted as a strong foulant, resulting in severe fouling in PAC-UF. The average retention rate of PAC-UF (57.7% and 47.9%) was better than that for single UF (45.0% and 34.7%) and MXene-UF (51.7% and 34.9%) for MB and MO, respectively. This is because the membrane surface and pores can be more readily degraded by PAC adsorption on the membrane. PAC also has a higher surface area than MXene, and hence can better adsorb the dyes. However, MXene-UF exhibited high selectivity, because electrostatic interaction is the main mechanism of dye treatment in the hybrid system. Taking into account the advantages of high permeate flux, lower irreversible fouling, and the high selectivity of MXene-UF, this is a promising advanced water treatment technology and a realistic alternative to conventional systems.

REFERENCES

Acero, J. L., F. J. Benitez, F. J. Real and C. Garcia. 2009. Removal of phenyl-urea herbicides in natural waters by UF membranes: Permeate flux, analysis of resistances and rejection coefficients. *Separation and Purification Technology* 65(3): 322-330.

Acero, J. L., F. J. Benitez, F. Teva and A. I. Leal. 2010. Retention of emerging micropollutants from UP water and a municipal secondary effluent by ultrafiltration and nanofiltration. *Chemical Engineering Journal* 163(3): 264-272.

Adams, C., Y. Wang, K. Loftin and M. Meyer. 2002. Removal of antibiotics from surface and distilled water in conventional water treatment processes. *Journal of Environmental Engineering - ASCE*. 128(3): 253-260.

Ahmad, A. L. and K. Y. Tan. 2004. Reverse osmosis of binary organic solute mixtures in the presence of strong solute-membrane affinity. *Desalination* 165(1-3): 193-199.

Ahmad, M., A. U. Rajapaksha, J. E. Lim, M. Zhang, N. Bolan, D. Mohan, M. Vithanage, S. S. Lee and Y. S. Ok. 2014. Biochar as a sorbent for contaminant management in soil and water: a review. *Chemosphere* 99: 19-33.

Al-Hamadani, Y. A. J., K. H. Chu, J. R. V. Flora, D. H. Kim, M. Jang, J. Sohn, W. Joo and Y. Yoon. 2016. Sonocatalytical degradation enhancement for ibuprofen and

sulfamethoxazole in the presence of glass beads and single-walled carbon nanotubes. *Ultrasonics Sonochemistry* 32: 440-448.

Al-Obaidi, M. A., J. P. Li, C. Kara-Zaitri and I. M. Mujtaba. 2017. Optimisation of reverse osmosis based wastewater treatment system for the removal of chlorophenol using genetic algorithms. *Chemical Engineering Journal* 316: 91-100.

Al-Rifai, J. H., H. Khabbaz and A. I. Schafer. 2011. Removal of pharmaceuticals and endocrine disrupting compounds in a water recycling process using reverse osmosis systems. *Separation and Purification Technology* 77(1): 60-67.

Alexy, R., T. Kumpel and K. Kummerer. 2004. Assessment of degradation of 18 antibiotics in the Closed Bottle Test. *Chemosphere* 57(6): 505-512.

Alturki, A. A., N. Tadkaew, J. A. McDonald, S. J. Khan, W. E. Price and L. D. Nghiem. 2010. Combining MBR and NF/RO membrane filtration for the removal of trace organics in indirect potable water reuse applications. *Journal of Membrane Science* 365(1-2): 206-215.

An, A. K., J. Guo, S. Jeong, E.-J. Lee, S. A. A. Tabatabai and T. Leiknes. 2016. High flux and antifouling properties of negatively charged membrane for dyeing wastewater treatment by membrane distillation. *Water Research* 103: 362-371.

Andersen, H., H. Siegrist, B. Halling-Sorensen and T. A. Ternes. 2003. Fate of estrogens in a municipal sewage treatment plant. *Environmental Science & Technology* 37(18): 4021-4026.

Andersen, H. R., M. Lundsbye, H. V. Wedel, E. Eriksson and A. Ledin. 2007. Estrogenic personal care products in a greywater reuse system. *Water Science and Technology* 56(12): 45-49.

Aoustin, E., A. Schäfer, A. G. Fane and T. Waite. 2001. Ultrafiltration of natural organic matter. *Separation and Purification Technology* 22: 63-78.

Aslam, M., P.-H. Lee and J. Kim. 2015. Analysis of membrane fouling with porous membrane filters by microbial suspensions for autotrophic nitrogen transformations. *Separation and Purification Technology* 146: 284-293.

Awwad, M., F. Al-Rimawi, K. J. K. Dajani, M. Khamis, S. Nir and R. Karaman. 2015. Removal of amoxicillin and cefuroxime axetil by advanced membranes technology, activated carbon and micelle-clay complex. *Environmental Technology* 36(16): 2069-2078.

Azais, A., J. Mendret, S. Gassara, E. Petit, A. Deratani and S. Brosillon. 2014. Nanofiltration for wastewater reuse: Counteractive effects of fouling and matrice on the rejection of pharmaceutical active compounds. *Separation and Purification Technology* 133: 313-327.

Bagreev, A., J. Angel Menendez, I. Dukhno, Y. Tarasenko and T. J. Bandosz. 2004. Bituminous coal-based activated carbons modified with nitrogen as adsorbents of hydrogen sulfide. *Carbon* 42(3): 469-476.

Barakat, M. A. and E. Schmidt. 2010. Polymer-enhanced ultrafiltration process for heavy metals removal from industrial wastewater. *Desalination* 256(1-3): 90-93.

Beckett, R., Z. Jue and J. C. Giddings. 1987. Determination of molecular weight distributions of fulvic and humic acids using flow field-flow fractionation. *Environmental Science & Technology* 21(3): 289-295.

Bellona, C. and J. E. Drewes. 2005. The role of membrane surface charge and solute physico-chemical properties in the rejection of organic acids by NF membranes. *Journal of Membrane Science* 249(1-2): 227-234.

Bellona, C., J. E. Drewes, P. Xu and G. Amy. 2004. Factors affecting the rejection of organic solutes during NF/RO treatment - a literature review. *Water Research* 38(12): 2795-2809.

Benotti, M. J., R. A. Trenholm, B. J. Vanderford, J. C. Holady, B. D. Stanford and S. A. Snyder. 2009. Pharmaceuticals and Endocrine Disrupting Compounds in US Drinking Water. *Environmental Science & Technology* 43(3): 597-603.

Bezverkhyy, I., G. Weber and J.-P. Bellat. 2016. Degradation of fluoride-free MIL-100 (Fe) and MIL-53 (Fe) in water: Effect of temperature and pH. *Microporous and Mesoporous Materials* 219: 117-124.

Bhadra, B. N., K. H. Cho, N. A. Khan, D.-Y. Hong and S. H. Jhung. 2015. Liquid-phase adsorption of aromatics over a metal–organic framework and activated carbon: effects of hydrophobicity/hydrophilicity of adsorbents and solvent polarity. *The Journal of Physical Chemistry C* 119(47): 26620-26627.

Blair, B. D., J. P. Crago, C. J. Hedman, R. J. F. Treguer, C. Magruder, L. S. Royer and R. D. Klaper. 2013. Evaluation of a model for the removal of pharmaceuticals,

personal care products, and hormones from wastewater. *Science of the Total Environment* 444: 515-521.

Boerlage, S. F., M. D. Kennedy, M. R. Dickson, D. E. El-Hodali and J. C. Schippers. 2002. The modified fouling index using ultrafiltration membranes (MFI-UF): characterisation, filtration mechanisms and proposed reference membrane. *Journal of Membrane Science* 197(1-2): 1-21.

Boussahel, R., S. Bouland, K. M. Moussaoui and A. Montiel. 2000. Removal of pesticide residues in water using the nanofiltration process. *Desalination* 132(1-3): 205-209.

Bowen, W. and A. Mohammad. 1998. Characterization and prediction of nanofiltration membrane performance - A general assessment. *Chemical Engineering Research and Desalination* 76(A8): 885-893.

Bueno, M. J. M., M. J. Gomez, S. Herrera, M. D. Hernando, A. Aguera and A. R. Fernandez-Alba. 2012. Occurrence and persistence of organic emerging contaminants and priority pollutants in five sewage treatment plants of Spain: Two years pilot survey monitoring. *Environmental Pollution* 164: 267-273.

Buerge, I. J., H. R. Buser, M. Kahle, M. D. Muller and T. Poiger. 2009. Ubiquitous Occurrence of the Artificial Sweetener Acesulfame in the Aquatic Environment: An Ideal Chemical Marker of Domestic Wastewater in Groundwater. *Environmental Science & Technology* 43(12): 4381-4385.

Buser, H. R., T. Poiger and M. D. Muller. 1998. Occurrence and fate of the pharmaceutical drug diclofenac in surface waters: Rapid photodegradation in a lake. *Environmental Science & Technology* 32(22): 3449-3456.

Buser, H. R., T. Poiger and M. D. Muller. 1999. Occurrence and environmental behavior of the chiral pharmaceutical drug ibuprofen in surface waters and in wastewater. *Environmental Science & Technology* 33(15): 2529-2535.

Carballa, M., G. Fink, F. Omil, J. M. Lema and T. Ternes. 2008. Determination of the solid-water distribution coefficient (K-d) for pharmaceuticals, estrogens and musk fragrances in digested sludge. *Water Research* 42(1-2): 287-295.

Cartagena, P., M. El Kaddouri, V. Cases, A. Trapote and D. Prats. 2013. Reduction of emerging micropollutants, organic matter, nutrients and salinity from real wastewater by combined MBR-NF/RO treatment. *Separation and Purification Technology* 110: 132-143.

Cartinella, J. L., T. Y. Cath, M. T. Flynn, G. C. Miller, K. W. Hunter and A. E. Childress. 2006. Removal of natural steroid hormones from wastewater using membrane contactor processes. *Environmental Science & Technology* 40(23): 7381-7386.

Cassano, A., C. Conidi, R. Ruby-Figueroa and R. Castro-Muñoz. 2018. Nanofiltration and tight ultrafiltration membranes for the recovery of polyphenols from agro-food by-products. *International Journal of Molecular Sciences* 19(2): 351.

Castro-Muñoz, R., B. E. Barragán-Huerta, V. Fíla, P. C. Denis and R. Ruby-Figueroa. 2017. Current role of membrane technology: From the treatment of agro-industrial

by-products up to the valorization of valuable compounds. *Waste and Biomass Valorization*: 1-17.

Castro-Muñoz, R., J. Yáñez-Fernández and V. Fíla. 2016. Phenolic compounds recovered from agro-food by-products using membrane technologies: an overview. *Food Chemistry* 213: 753-762.

Chang, E. E., Y. C. Chang, C. H. Liang, C. P. Huang and P. C. Chiang. 2012. Identifying the rejection mechanism for nanofiltration membranes fouled by humic acid and calcium ions exemplified by acetaminophen, sulfamethoxazole, and triclosan. *Journal of Hazardous Materials* 221: 19-27.

Chianese, A., R. Ranauro and N. Verdone. 1999. Treatment of landfill leachate by reverse osmosis. *Water Research* 33(3): 647-652.

Childress, A. E. and M. Elimelech. 2000. Relating nanofiltration membrane performance to membrane charge (electrokinetic) characteristics. *Environmental Science & Technology* 34(17): 3710-3716.

Chin, Y.-P., G. Aiken and E. O'Loughlin. 1994. Molecular weight, polydispersity, and spectroscopic properties of aquatic humic substances. *Environmental Science & Technology* 28(11): 1853-1858.

Chon, K., J. Cho and H. K. Shon. 2013. A pilot-scale hybrid municipal wastewater reclamation system using combined coagulation and disk filtration, ultrafiltration, and reverse osmosis: Removal of nutrients and micropollutants, and characterization of membrane foulants. *Bioresource Technology* 141: 109-116.

Chon, K., S. Sarp, S. Lee, J. H. Lee, J. A. Lopez-Ramirez and J. Cho. 2011. Evaluation of a membrane bioreactor and nanofiltration for municipal wastewater reclamation: Trace contaminant control and fouling mitigation. *Desalination* 272(1-3): 128-134.

Chu, K. H., M. Fathizadeh, M. Yu, J. R. Flora, A. Jang, M. Jang, C. M. Park, S. S. Yoo, N. Her and Y. Yoon. 2017. Evaluation of removal mechanisms in a graphene oxide-coated ceramic ultrafiltration membrane for retention of natural organic matter, pharmaceuticals, and inorganic salts. *ACS Applied Materials & Interfaces* 9(46): 40369-40377.

Chu, K. H., Y. Huang, M. Yu, N. Her, J. R. Flora, C. M. Park, S. Kim, J. Cho and Y. Yoon. 2016. Evaluation of humic acid and tannic acid fouling in graphene oxide-coated ultrafiltration membranes. *ACS Applied Materials & Interfaces* 8(34): 22270-22279.

Chu, K. H., V. Shankar, C. M. Park, J. Sohn, A. Jang and Y. Yoon. 2017. Evaluation of fouling mechanisms for humic acid molecules in an activated biochar-ultrafiltration hybrid system. *Chemical Engineering Journal* 326: 240-248.

Chun, Y., G. Sheng, C. T. Chiou and B. Xing. 2004. Compositions and sorptive properties of crop residue-derived chars. *Environmental Science & Technology* 38(17): 4649-4655.

Clara, M., B. Strenn and N. Kreuzinger. 2004. Carbamazepine as a possible anthropogenic marker in the aquatic environment: investigations on the behaviour of Carbamazepine in wastewater treatment and during groundwater infiltration. *Water Research* 38(4): 947-954.

Coday, B. D., B. G. M. Yaffe, P. Xu and T. Y. Cath. 2014. Rejection of Trace Organic Compounds by Forward Osmosis Membranes: A Literature Review. *Environmental Science & Technology* 48(7): 3612-3624.

Cohen, B. E. 1975. PERMEABILITY OF LIPOSOMES TO NONELECTROLYTES .1. ACTIVATION-ENERGIES FOR PERMEATION. *Journal of Membrane Biology* 20(3-4): 205-234.

Comerton, A. M., R. C. Andrews, D. M. Bagley and P. Yang. 2007. Membrane adsorption of endocrine disrupting compounds and pharmaceutically active compounds. *Journal of Membrane Science* 303(1-2): 267-277.

Comerton, A. M., R. C. Andyews and D. M. Bagley. 2009. The influence of natural organic matter and cations on the rejection of endocrine disrupting and pharmaceutically active compounds by nanofiltration. *Water Research* 43(3): 613-622.

Corzo, B., T. de la Torre, C. Sans, E. Ferrero and J. J. Malfeito. 2017. Evaluation of draw solutions and commercially available forward osmosis membrane modules for wastewater reclamation at pilot scale. *Chemical Engineering Journal* 326: 1-8.

Couarraze, G., B. Leclerc, G. Conrath, F. Falsonrieg and F. Puisieux. 1989. DIFFUSION OF A DISPERSED SOLUTE IN A POLYMERIC MATRIX. *International Journal of Pharmaceutics* 56(3): 197-206.

Crittenden, J. C., R. R. Trussell, D. W. Hand, K. J. Howe and G. Tchobanoglous (2012). MWH's water treatment: principles and design, John Wiley & Sons.

Cui, Y., Q. Ge, X. Y. Liu and T. S. Chung. 2014. Novel forward osmosis process to effectively remove heavy metal ions. *Journal of Membrane Science* 467: 188-194.

D'Haese, A., P. Le-Clech, S. Van Nevel, K. Verbeken, E. R. Cornelissen, S. J. Khan and A. R. D. Verliefde. 2013. Trace organic solutes in closed-loop forward osmosis applications: Influence of membrane fouling and modeling of solute build-up. *Water Research* 47(14): 5232-5244.

Danis, U. and C. Aydiner. 2009. Investigation of process performance and fouling mechanisms in micellar-enhanced ultrafiltration of nickel-contaminated waters. *Journal of Hazardous Materials* 162(2-3): 577-587.

Deblonde, T., C. Cossu-Leguille and P. Hartemann. 2011. Emerging pollutants in wastewater: A review of the literature. *International Journal of Hygiene and Environmental Health* 214(6): 442-448.

Deng, H., L. Yang, G. Tao and J. Dai. 2009. Preparation and characterization of activated carbon from cotton stalk by microwave assisted chemical activation—application in methylene blue adsorption from aqueous solution. *Journal of Hazardous Materials* 166(2-3): 1514-1521.

Devitt, E. C., F. Ducellier, P. Cote and M. R. Wiesner. 1998. Effects of natural organic matter and the raw water matrix on the rejection of atrazine by pressure-driven membranes. *Water Research* 32(9): 2563-2568.

Dhakal, N., S. G. Salinas-Rodriguez, A. Ouda, J. C. Schippers and M. D. Kennedy. 2018. Fouling of ultrafiltration membranes by organic matter generated by marine algal species. *Journal of Membrane Science* 555: 418-428.

Dialynas, E. and E. Diamadopoulos. 2009. Integration of a membrane bioreactor coupled with reverse osmosis for advanced treatment of municipal wastewater. *Desalination* 238(1-3): 302-311.

Dolar, D., M. Gros, S. Rodriguez-Mozaz, J. Moreno, J. Comas, I. Rodriguez-Roda and D. Barcelo. 2012. Removal of emerging contaminants from municipal wastewater with an integrated membrane system, MBR-RO. *Journal of Hazardous Materials* 239: 64-69.

Domenech, X., M. Ribera and J. Peral. 2011. Assessment of Pharmaceuticals Fate in a Model Environment. *Water Air and Soil Pollution* 218(1-4): 413-422.

Essandoh, M., B. Kunwar, C. U. Pittman, D. Mohan and T. Mlsna. 2015. Sorptive removal of salicylic acid and ibuprofen from aqueous solutions using pine wood fast pyrolysis biochar. *Chemical Engineering Journal* 265: 219-227.

Falca, G., V.-E. Musteata, A. R. Behzad, S. Chisca and S. P. Nunes. 2019. Cellulose hollow fibers for organic resistant nanofiltration. *Journal of Membrane Science* 586: 151-161.

Fard, A. K., G. Mckay, R. Chamoun, T. Rhadfi, H. Preud'Homme and M. A. Atieh. 2017. Barium removal from synthetic natural and produced water using MXene as two

dimensional (2-D) nanosheet adsorbent. *Chemical Engineering Journal* 317: 331-342.

Férey, G., C. Mellot-Draznieks, C. Serre, F. Millange, J. Dutour, S. Surblé and I. Margiolaki. 2005. A chromium terephthalate-based solid with unusually large pore volumes and surface area. *Science* 309(5743): 2040-2042.

Fernandez, R. L., J. A. McDonald, S. J. Khan and P. Le-Clech. 2014. Removal of pharmaceuticals and endocrine disrupting chemicals by a submerged membrane photocatalysis reactor (MPR). *Separation and Purification Technology* 127: 131-139.

Freger, V., J. Gilron and S. Belfer. 2002. TFC polyamide membranes modified by grafting of hydrophilic polymers: an FT-IR/AFM/TEM study. *Journal of Membrane Science* 209(1): 283-292.

Galanakis, C. M. 2015. Separation of functional macromolecules and micromolecules: from ultrafiltration to the border of nanofiltration. *Trends in Food Science & Technology* 42(1): 44-63.

Garcia-Vaquero, N., E. Lee, R. J. Castaneda, J. Cho and J. A. Lopez-Ramirez. 2014. Comparison of drinking water pollutant removal using a nanofiltration pilot plant powered by renewable energy and a conventional treatment facility. *Desalination* 347: 94-102.

Gur-Reznik, S., I. Koren-Menashe, L. Heller-Grossman, O. Rufel and C. G. Dosoretz. 2011. Influence of seasonal and operating conditions on the rejection of

pharmaceutical active compounds by RO and NF membranes. *Desalination* 277(1-3): 250-256.

Han, J., Y. S. Liu, N. Singhal, L. Z. Wang and W. Gao. 2012. Comparative photocatalytic degradation of estrone in water by ZnO and TiO2 under artificial UVA and solar irradiation. *Chemical Engineering Journal* 213: 150-162.

Hancock, N. T., W. A. Phillip, M. Elimelech and T. Y. Cath. 2011. Bidirectional Permeation of Electrolytes in Osmotically Driven Membrane Processes. *Environmental Science & Technology* 45(24): 10642-10651.

Hancock, N. T., P. Xu, D. M. Heil, C. Bellona and T. Y. Cath. 2011. Comprehensive Bench- and Pilot-Scale Investigation of Trace Organic Compounds Rejection by Forward Osmosis. *Environmental Science & Technology* 45(19): 8483-8490.

Haque, E., J. E. Lee, I. T. Jang, Y. K. Hwang, J.-S. Chang, J. Jegal and S. H. Jhung. 2010. Adsorptive removal of methyl orange from aqueous solution with metal-organic frameworks, porous chromium-benzenedicarboxylates. *Journal of hazardous materials* 181(1-3): 535-542.

Hasan, Z., J. Jeon and S. H. Jhung. 2012. Adsorptive removal of naproxen and clofibric acid from water using metal-organic frameworks. *Journal of hazardous materials* 209: 151-157.

Hasan, Z., N. A. Khan and S. H. Jhung. 2016. Adsorptive removal of diclofenac sodium from water with Zr-based metal–organic frameworks. *Chemical Engineering Journal* 284: 1406-1413.

He, H., B. Huang, G. Fu, D. Xiong, Z. Xu, X. Wu and X. Pan. 2018. Electrochemically modified dissolved organic matter accelerates the combining photodegradation and biodegradation of 17α-ethinylestradiol in natural aquatic environment. *Water Research* 137(15): 251-261.

Heidler, J., A. Sapkota and R. U. Halden. 2006. Partitioning, persistence, and accumulation in digested sludge of the topical antiseptic triclocarban during wastewater treatment. *Environmental Science & Technology* 40(11): 3634-3639.

Heo, J., L. K. Boateng, J. R. V. Flora, H. Lee, N. Her, Y. G. Park and Y. Yoon. 2013. Comparison of flux behavior and synthetic organic compound removal by forward osmosis and reverse osmosis membranes. *Journal of Membrane Science* 443: 69-82.

Heo, J., J. R. V. Flora, N. Her, Y.-G. Park, J. Cho, A. Son and Y. Yoon. 2012. Removal of bisphenol A and 17β-estradiol in single walled carbon nanotubes–ultrafiltration (SWNTs–UF) membrane systems. *Separation and Purification Technology* 90: 39-52.

Hermia, J. 1982. Constant pressure blocking filtration laws-application to power-law non-Newtonian fluids. *Chemical Engineering Research and Design* 60: 183-187.

Hong, S. K. and M. Elimelech. 1997. Chemical and physical aspects of natural organic matter (NOM) fouling of nanofiltration membranes. *Journal of Membrane Science* 132(2): 159-181.

Horcajada, P., C. Serre, M. Vallet-Regí, M. Sebban, F. Taulelle and G. Férey. 2006. Metal–organic frameworks as efficient materials for drug delivery. *Angewandte Chemie* 118(36): 6120-6124.

Horcajada, P., S. Surblé, C. Serre, D.-Y. Hong, Y.-K. Seo, J.-S. Chang, J.-M. Greneche, I. Margiolaki and G. Férey. 2007. Synthesis and catalytic properties of MIL-100 (Fe), an iron (III) carboxylate with large pores. *Chemical Communications* (27): 2820-2822.

Howe, K. J. and M. M. Clark. 2002. Fouling of microfiltration and ultrafiltration membranes by natural waters. *Environmental Science & Technology* 36(16): 3571-3576.

Hu, J. Y., X. Jin and S. L. Ong. 2007. Rejection of estrone by nanofiltration: Influence of solution chemistry. *Journal of Membrane Science* 302(1-2): 188-196.

Hu, Y., C. Song, J. Liao, Z. Huang and G. Li. 2013. Water stable metal-organic framework packed microcolumn for online sorptive extraction and direct analysis of naproxen and its metabolite from urine sample. *Journal of Chromatography A* 1294: 17-24.

Hu, Z. F., X. R. Si, Z. Y. Zhang and X. H. Wen. 2014. Enhanced EDCs removal by membrane fouling during the UF process. *Desalination* 336: 18-23.

Huang, G., F. Meng, X. Zheng, Y. Wang, Z. Wang, H. Liu and M. Jekel. 2011. Biodegradation behavior of natural organic matter (NOM) in a biological aerated filter (BAF) as a pretreatment for ultrafiltration (UF) of river water. *Applied Microbiology and Biotechnology* 90(5): 1795-1803.

Huang, H. O., H. Cho, K. Schwab and J. G. Jacangelo. 2011. Effects of feedwater pretreatment on the removal of organic microconstituents by a low fouling reverse osmosis membrane. *Desalination* 281: 446-454.

Huang, M. H., Y. S. Chen, C. H. Huang, P. Z. Sun and J. Crittenden. 2015. Rejection and adsorption of trace pharmaceuticals by coating a forward osmosis membrane with TiO_2. *Chemical Engineering Journal* 279: 904-911.

Huang, Y.-B., J. Liang, X.-S. Wang and R. Cao. 2017. Multifunctional metal–organic framework catalysts: synergistic catalysis and tandem reactions. *Chemical Society* Reviews 46(1): 126-157.

Huck, P. M., S. Peldszus, J. Haberkamp and M. Jekel. 2009. Assessing the performance of biological filtration as pretreatment to low pressure membranes for drinking water. *Environmental Science & Technology* 43(10): 3878-3884.

Huerta-Fontela, M., M. T. Galceran and F. Ventura. 2011. Occurrence and removal of pharmaceuticals and hormones through drinking water treatment. *Water Research* 45(3): 1432-1442.

Hughes, Z. E. and J. D. Gale. 2012. Molecular dynamics simulations of the interactions of potential foulant molecules and a reverse osmosis membrane. *Journal of Materials Chemistry* 22(1): 175-184.

Huo, S.-H. and X.-P. Yan. 2012. Metal–organic framework MIL-100 (Fe) for the adsorption of malachite green from aqueous solution. *Journal of Materials Chemistry* 22(15): 7449-7455.

Huq, H. P., J. S. Yang and J. W. Yang. 2007. Removal of perchlorate from groundwater by the polyelectolyte-enhanced ultrafiltration process. *Desalination* 204(1-3): 335-343.

Hyland, K. C., E. R. V. Dickenson, J. E. Drewes and C. P. Higgins. 2012. Sorption of ionized and neutral emerging trace organic compounds onto activated sludge from different wastewater treatment configurations. *Water Research* 46(6): 1958-1968.

Hyung, H. and J.-H. Kim. 2008. Natural organic matter (NOM) adsorption to multi-walled carbon nanotubes: effect of NOM characteristics and water quality parameters. *Environmental* S*cience & Technolo*gy 42(12): 4416-4421.

Ipek, U. 2005. Removal of Ni(II) and Zn(II) from an aqueous solution by reverse osmosis. *Desalination* 174(2): 161-169.

Jeong, M.-G., D. H. Kim, S.-K. Lee, J. H. Lee, S. W. Han, E. J. Park, K. A. Cychosz, M. Thommes, Y. K. Hwang and J.-S. Chang. 2016. Decoration of the internal structure of mesoporous chromium terephthalate MIL-101 with NiO using atomic layer deposition. *Microporous and Mesoporous Materials* 221: 101-107.

Ji, L., F. Liu, Z. Xu, S. Zheng and D. Zhu. 2010. Adsorption of pharmaceutical antibiotics on template-synthesized ordered micro-and mesoporous carbons. *Environmental Science & Technology* 44(8): 3116-3122.

Jia, Y., R. Wang and A. G. Fane. 2009. Hybrid PAC-submerged membrane system for trace organics removal II: System simulation and application study. *Chemical Engineering Journal* 149(1-3): 42-49.

Jiang, C., S. Garg and T. D. Waite. 2017. Iron redox transformations in the presence of natural organic matter: effect of calcium. *Environmental* S*cience* & *Technology* 51(18): 10413-10422.

Jiang, N., R. Shang, S. G. Heijman and L. C. Rietveld. 2018. High-silica zeolites for adsorption of organic micro-pollutants in water treatment: A review. *Water Research* 144: 145-161.

Jin, X., J. Y. Hu and S. L. Ong. 2010. Removal of natural hormone estrone from secondary effluents using nanofiltration and reverse osmosis. *Water Research* 44(2): 638-648.

Jin, X., J. H. Shan, C. Wang, J. Wei and C. Y. Y. Tang. 2012. Rejection of pharmaceuticals by forward osmosis membranes. *Journal of Hazardous Materials* 227: 55-61.

Johnson, D., F. Galiano, S. A. Deowan, J. Hoinkis, A. Figoli and N. Hilal. 2015. Adhesion forces between humic acid functionalized colloidal probes and polymer membranes to assess fouling potential. *Journal of Membrane Science* 484: 35-46.

Joseph, L., B.-M. Jun, M. Jang, C. M. Park, J. C. Muñoz-Senmache, A. J. Hernández-Maldonado, A. Heyden, M. Yu and Y. Yoon. 2019. Removal of contaminants of emerging concern by metal-organic framework nanoadsorbents: A review. *Chemical Engineering Journal* 369:928-946.

Joss, A., C. Baenninger, P. Foa, S. Koepke, M. Krauss, C. S. McArdell, K. Rottermann, Y. S. Wei, A. Zapata and H. Siegrist. 2011. Water reuse: > 90% water yield in MBR/RO through concentrate recycling and CO_2 addition as scaling control. *Water Research* 45(18): 6141-6151.

Ju, Y., I. Hong and S. Hong. 2015. Multiple MFI measurements for the evaluation of organic fouling in SWRO desalination. *Desalination* 365: 136-143.

Jucker, C. and M. M. Clark. 1994. Adsorption of aquatic humic substances on hydrophobic ultrafiltration membranes. *Journal of Membrane Science* 97: 37-52.

Jun, B.-M., S. Kim, J. Heo, C. M. Park, N. Her, M. Jang, Y. Huang, J. Han and Y. Yoon. 2019. Review of MXenes as new nanomaterials for energy storage/delivery and selected environmental applications. *Nano Research* 12(3): 471-487.

Jung, C., J. Park, K. H. Lim, S. Park, J. Heo, N. Her, J. Oh, S. Yun and Y. Yoon. 2013. Adsorption of selected endocrine disrupting compounds and pharmaceuticals on activated biochars. *Journal of Hazardous Materials* 263: 702-710.

Jung, C., J. Park, K. H. Lim, S. Park, J. Heo, N. Her, J. Oh, S. Yun and Y. Yoon. 2013. Adsorption of selected endocrine disrupting compounds and pharmaceuticals on activated biochars. *Journal of Hazardous Materials* 263 Pt 2: 702-710.

Jung, C., N. Phal, J. Oh, K. H. Chu, M. Jang and Y. Yoon. 2015. Removal of humic and tannic acids by adsorption–coagulation combined systems with activated biochar. *Journal of Hazardous Materials* 300: 808-814.

Kasprzyk-Hordern, B., R. M. Dinsdale and A. J. Guwy. 2009. The removal of pharmaceuticals, personal care products, endocrine disruptors and illicit drugs during wastewater treatment and its impact on the quality of receiving waters. *Water Research* 43(2): 363-380.

Ke, F., L.-G. Qiu, Y.-P. Yuan, F.-M. Peng, X. Jiang, A.-J. Xie, Y.-H. Shen and J.-F. Zhu. 2011. Thiol-functionalization of metal-organic framework by a facile coordination-based postsynthetic strategy and enhanced removal of Hg^{2+} from water. *Journal of Hazardous Materials* 196: 36-43.

Khan, N. A., Z. Hasan and S. H. Jhung. 2013. Adsorptive removal of hazardous materials using metal-organic frameworks (MOFs): a review. *Journal of Hazardous Materials* 244: 444-456.

Kim, J. H., P. K. Park, C. H. Lee and H. H. Kwon. 2008. Surface modification of nanofiltration membranes to improve the removal of organic micro-pollutants (EDCs and PhACs) in drinking water treatment: Graft polymerization and cross-linking followed by functional group substitution. *Journal of Membrane Science* 321(2): 190-198.

Kim, J. W., S. M. Yoon, S. J. Lee, M. Narumiya, N. Nakada, I. S. Han and H. Tanaka (2012). Occurrence and fate of PPCPs wastewater treatment plants in Korea. 2012 2nd International Conference on Environment and Industrial Innovation, Singapore, IPCEBEE.

Kim, K., A. Fane, R. B. Aim, M. Liu, G. Jonsson, I. Tessaro, A. Broek and D. Bargeman. 1994. A comparative study of techniques used for porous membrane characterization: pore characterization. *Journal of Membrane Science* 87(1-2): 35-46.

Kim, S., K. H. Chu, Y. A. Al-Hamadani, C. M. Park, M. Jang, D.-H. Kim, M. Yu, J. Heo and Y. Yoon. 2018. Removal of contaminants of emerging concern by membranes in water and wastewater: a review. *Chemical Engineering Journal* 335: 896-914.

Kim, S., K. H. Chu, Y. A. J. Al-Hamadani, C. M. Park, M. Jang, D.-H. Kim, M. Yu, J. Heo and Y. Yoon. 2018. Removal of contaminants of emerging concern by membranes in water and wastewater: A review. *Chemical Engineering Journal* 335: 896-914.

Kim, S., P. Eichhorn, J. N. Jensen, A. S. Weber and D. S. Aga. 2005. Removal of antibiotics in wastewater: Effect of hydraulic and solid retention times on the fate of tetracycline in the activated sludge process. *Environmental Science & Technology* 39(15): 5816-5823.

Kim, S., D. W. Lee and J. Cho. 2016. Application of direct contact membrane distillation process to treat anaerobic digestate. *Journal of membrane science* 511: 20-28.

Kim, S., J. C. Muñoz-Senmache, B.-M. Jun, C. M. Park, A. Jang, M. Yu, A. J. Hernández-Maldonado and Y. Yoon. 2020. A metal organic framework-ultrafiltration hybrid system for removing selected pharmaceuticals and natural organic matter. *Chemical Engineering Journal* 382: 122920.

Kim, S., C. M. Park, A. Jang, M. Jang, A. J. Hernández-Maldonado, M. Yu, J. Heo and Y. Yoon. 2019. Removal of selected pharmaceuticals in an ultrafiltration-activated biochar hybrid system. *Journal of Membrane Science* 570: 77-84.

Kim, S., C. M. Park, M. Jang, A. Son, N. Her, M. Yu, S. Snyder, D.-H. Kim and Y. Yoon. 2018. Aqueous removal of inorganic and organic contaminants by graphene-based nanoadsorbents: A review. *Chemosphere* 212: 1104-1124.

Kim, S. D., J. Cho, I. S. Kim, B. J. Vanderford and S. A. Snyder. 2007. Occurrence and removal of pharmaceuticals and endocrine disruptors in South Korean surface, drinking, and waste waters. *Water Research* 41(5): 1013-1021.

Kimura, K., G. Amy, J. Drewes and Y. Watanabe. 2003. Adsorption of hydrophobic compounds onto NF/RO membranes: an artifact leading to overestimation of rejection. *Journal of Membrane Science* 221(1-2): 89-101.

Kimura, K., T. Iwase, S. Kita and Y. Watanabe. 2009. Influence of residual organic macromolecules produced in biological wastewater treatment processes on removal of pharmaceuticals by NF/RO membranes. *Water Research* 43(15): 3751-3758.

Kimura, K., S. Toshima, G. Amy and Y. Watanabe. 2004. Rejection of neutral endocrine disrupting compounds (EDCs) and pharmaceutical active compounds (PhACs) by RO membranes. *Journal of Membrane Science* 245(1-2): 71-78.

Kirschner, A. Y., Y.-H. Cheng, D. R. Paul, R. W. Field and B. D. Freeman. 2019. Fouling mechanisms in constant flux crossflow ultrafiltration. *Journal of Membrane Science* 574: 65-75.

Kiso, Y., Y. Sugiura, T. Kitao and K. Nishimura. 2001. Effects of hydrophobicity and molecular size on rejection of aromatic pesticides with nanofiltration membranes. *Journal of Membrane Science* 192(1-2): 1-10.

Kong, F. X., H. W. Yang, Y. Q. Wu, X. M. Wang and Y. F. F. Xie. 2015. Rejection of pharmaceuticals during forward osmosis and prediction by using the solution-diffusion model. *Journal of Membrane Science* 476: 410-420.

Kosutic, K., D. Dolar, D. Asperger and B. Kunst. 2007. Removal of antibiotics from a model wastewater by RO/NF membranes. *Separation and Purification Technology* 53(3): 244-249.

Koyuncu, I., O. A. Arikan, M. R. Wiesner and C. Rice. 2008. Removal of hormones and antibiotics by nanofiltration membranes. *Journal of Membrane Science* 309(1-2): 94-101.

Krzeminski, P., C. Schwermer, A. Wennberg, K. Langford and C. Vogelsang. 2017. Occurrence of UV filters, fragrances and organophosphate flame retardants in municipal WWTP effluents and their removal during membrane post-treatment. *Journal of Hazardous Materials* 323: 166-176.

Le Questel, J. Y., G. Boquet, M. Berthelot and C. Laurence. 2000. Hydrogen bonding of progesterone: a combined theoretical, spectroscopic, thermodynamic, and crystallographic database study. *Journal of Physical Chemistry B* 104(49): 11816-11823.

Lee, B.-M., Y.-S. Seo and J. Hur. 2015. Investigation of adsorptive fractionation of humic acid on graphene oxide using fluorescence EEM-PARAFAC. *Water research* 73: 242-251.

Lee, S., J. Cho and M. Elimelech. 2005. Combined influence of natural organic matter (NOM) and colloidal particles on nanofiltration membrane fouling. *Journal of Membrane Science* 262(1-2): 27-41.

Lee, S., M. Ihara, N. Yamashita and H. Tanaka. 2017. Improvement of virus removal by pilot-scale coagulation-ultrafiltration process for wastewater reclamation: Effect of optimization of pH in secondary effluent. *Water Research* 114: 23-30.

Lee, S., N. Quyet, E. Lee, S. Kim, S. Lee, Y. D. Jung, S. H. Choi and J. Cho. 2008. Efficient removals of tris(2-chloroethyl) phosphate (TCEP) and perchlorate using NF membrane filtrations. *Desalination* 221(1-3): 234-237.

Lei, H. X. and S. A. Snyder. 2007. 3D QSPR models for the removal of trace organic contaminants by ozone and free chlorine. *Water Research* 41(18): 4051-4060.

Lew, B., S. Tarre, M. Beliavski, C. Dosoretz and M. Green. 2009. Anaerobic membrane bioreactor (AnMBR) for domestic wastewater treatment. *Desalination* 243(1-3): 251-257.

Liang, R., S. Luo, F. Jing, L. Shen, N. Qin and L. Wu. 2015. A simple strategy for fabrication of Pd@ MIL-100 (Fe) nanocomposite as a visible-light-driven photocatalyst for the treatment of pharmaceuticals and personal care products (PPCPs). *Applied Catalysis B: Environmental* 176: 240-248.

Lin, C.-F., Y.-J. Huang and O. J. Hao. 1999. Ultrafiltration processes for removing humic substances: effect of molecular weight fractions and PAC treatment. *Water research* 33(5): 1252-1264.

Lin, D. and B. Xing. 2008. Tannic acid adsorption and its role for stabilizing carbon nanotube suspensions. *Environmental science & technology* 42(16): 5917-5923.

Lin, J., W. Ye, M.-C. Baltaru, Y. P. Tang, N. J. Bernstein, P. Gao, S. Balta, M. Vlad, A. Volodin and A. Sotto. 2016. Tight ultrafiltration membranes for enhanced separation of dyes and Na_2SO_4 during textile wastewater treatment. *Journal of Membrane Science* 514: 217-228.

Lin, K.-Y. A. and H.-A. Chang. 2015. Ultra-high adsorption capacity of zeolitic imidazole framework-67 (ZIF-67) for removal of malachite green from water. *Chemosphere* 139: 624-631.

Lin, Y. L., J. H. Chiou and C. H. Lee. 2014. Effect of silica fouling on the removal of pharmaceuticals and personal care products by nanofiltration and reverse osmosis membranes. *Journal of Hazardous Materials* 277: 102-109.

Linares, R. V., V. Yangali-Quintanilla, Z. Y. Li and G. Amy. 2011. Rejection of micropollutants by clean and fouled forward osmosis membrane. *Water Research* 45(20): 6737-6744.

Liu, G., J. Zou, Q. Tang, X. Yang, Y. Zhang, Q. Zhang, W. Huang, P. Chen, J. Shao and X. Dong. 2017. Surface modified Ti_3C_2 MXene nanosheets for tumor targeting photothermal/photodynamic/chemo synergistic therapy. *ACS Applied Materials & interfaces* 9(46): 40077-40086.

Liu, P. X., H. M. Zhang, Y. J. Feng, C. Shen and F. L. Yang. 2015. Integrating electrochemical oxidation into forward osmosis process for removal of trace antibiotics in wastewater. *Journal of Hazardous Materials* 296: 248-255.

Lowell, S., J. E. Shields, M. A. Thomas and M. Thommes (2012). Characterization of porous solids and powders: surface area, pore size and density, Springer Science & Business Media.

Lowenberg, J., A. Zenker, M. Baggenstos, G. Koch, C. Kazner and T. Wintgens. 2014. Comparison of two PAC/UF processes for the removal of micropollutants from wastewater treatment plant effluent: Process performance and removal efficiency. *Water Research* 56: 26-36.

Löwenberg, J., A. Zenker, M. Baggenstos, G. Koch, C. Kazner and T. Wintgens. 2014. Comparison of two PAC/UF processes for the removal of micropollutants from wastewater treatment plant effluent: process performance and removal efficiency. *Water Research* 56: 26-36.

Löwenberg, J., A. Zenker, M. Baggenstos, G. Koch, C. Kazner and T. Wintgens. 2014. Comparison of two PAC/UF processes for the removal of micropollutants from wastewater treatment plant effluent: process performance and removal efficiency. *Water Research* 56: 26-36.

Lukatskaya, M. R., O. Mashtalir, C. E. Ren, Y. Dall'Agnese, P. Rozier, P. L. Taberna, M. Naguib, P. Simon, M. W. Barsoum and Y. Gogotsi. 2013. Cation intercalation and high volumetric capacitance of two-dimensional titanium carbide. *Science* 341(6153): 1502-1505.

Ma, J., F. Yu, L. Zhou, L. Jin, M. Yang, J. Luan, Y. Tang, H. Fan, Z. Yuan and J. Chen. 2012. Enhanced adsorptive removal of methyl orange and methylene blue from aqueous solution by alkali-activated multiwalled carbon nanotubes. *ACS Applied Materials & Interfaces* 4(11): 5749-5760.

Ma, L., J. M. Falkowski, C. Abney and W. Lin. 2010. A series of isoreticular chiral metal–organic frameworks as a tunable platform for asymmetric catalysis. *Nature Chemistry* 2(10): 838.

Ma, X., P. Chen, M. Zhou, Z. Zhong, F. Zhang and W. Xing. 2017. Tight ultrafiltration ceramic membrane for separation of dyes and mixed salts (both $NaCl/Na_2SO_4$) in textile wastewater treatment. *Industrial & Engineering Chemistry Research* 56(24): 7070-7079.

Martín-González, M. A., O. González-Díaz, P. Susial, J. Araña, J. A. Herrera-Melián, J. M. Doña-Rodríguez and J. Pérez-Peña. 2014. Reuse of Phoenix canariensis palm frond mulch as biosorbent and as precursor of activated carbons for the adsorption of Imazalil in aqueous phase. *Chemical Engineering Journal* 245: 348-358.

Mashtalir, O., K. M. Cook, V. Mochalin, M. Crowe, M. W. Barsoum and Y. Gogotsi. 2014. Dye adsorption and decomposition on two-dimensional titanium carbide in aqueous media. *Journal of Materials Chemistry A* 2(35): 14334-14338.

Mashtalir, O., K. M. Cook, V. N. Mochalin, M. Crowe, M. W. Barsoum and Y. Gogotsi. 2014. Dye adsorption and decomposition on two-dimensional titanium carbide in aqueous media. *Journal of Materials Chemistry A* 2(35): 14334-14338.

Mawhinney, D. B., R. B. Young, B. J. Vanderford, T. Borch and S. A. Snyder. 2011. Artificial Sweetener Sucralose in U.S. Drinking Water Systems. *Environmental Science & Technology* 45(20): 8716-8722.

Meng, F., M. Seredych, C. Chen, V. Gura, S. Mikhalovsky, S. Sandeman, G. Ingavle, T. Ozulumba, L. Miao and B. Anasori. 2018. MXene sorbents for removal of urea from dialysate: A step toward the wearable artificial kidney. *ACS nano* 12(10): 10518-10528.

Meng, X., W. Tang, L. Wang, X. Wang, D. Huang, H. Chen and N. Zhang. 2015. Mechanism analysis of membrane fouling behavior by humic acid using atomic force microscopy: Effect of solution pH and hydrophilicity of PVDF ultrafiltration membrane interface. *Journal of Membrane Science* 487: 180-188.

Meyer, J. and K. Bester. 2004. Organophosphate flame retardants and plasticisers in wastewater treatment plants. *Journal of Environmental Monitoring* 6(7): 599-605.

Monteagudo, J., A. Durán, R. González and A. Expósito. 2015. In situ chemical oxidation of carbamazepine solutions using persulfate simultaneously activated by heat energy, UV light, Fe^{2+} ions, and H_2O_2. *Applied Catalysis B: Environmental* 176: 120-129.

Mulder, J. (2012). Basic principles of membrane technology, Springer Science & Business Media.

Naguib, M., V. N. Mochalin, M. W. Barsoum and Y. Gogotsi. 2014. 25th anniversary article: MXenes: a new family of two-dimensional materials. *Advanced Materials* 26(7): 992-1005.

Naidu, G., S. Jeong, M. A. H. Johir, A. G. Fane, J. Kandasamy and S. Vigneswaran. 2017. Rubidium extraction from seawater brine by an integrated membrane distillation-selective sorption system. *Water Research* 123: 321-331.

Nam, S.-W., C. Jung, H. Li, M. Yu, J. R. Flora, L. K. Boateng, N. Her, K.-D. Zoh and Y. Yoon. 2015. Adsorption characteristics of diclofenac and sulfamethoxazole to graphene oxide in aqueous solution. *Chemosphere* 136: 20-26.

Neale, P. A. and A. I. Schafer. 2012. Quantification of solute-solute interactions in steroidal hormone removal by ultrafiltration membranes. *Separation and Purification Technology* 90: 31-38.

Ng, H. Y. and M. Elimelech. 2004. Influence of colloidal fouling on rejection of trace organic contaminants by reverse osmosis. *Journal of Membrane Science* 244(1-2): 215-226.

Nghiem, L. D., A. Manis, K. Soldenhoff and A. I. Schafer. 2004. Estrogenic hormone removal from wastewater using NF/RO membranes. *Journal of Membrane Science* 242(1-2): 37-45.

Nghiem, L. D., A. Manis, K. Soldenhoff and A. I. Schafer. 2004. Estrogenic hormone removal from wastewater using NF/RO membranes. *Journal of Membrane Science* 242: 37-45.

Nghiem, L. D., A. I. Schafer and M. Elimelech. 2004. Removal of natural hormones by nanofiltration membranes: Measurement, modeling, and mechanisms. *Environmental Science & Technology* 38(6): 1888-1896.

Nghiem, L. D., A. I. Schafer and M. Elimelech. 2004. Removal of natural hormones by nanofiltration membranes: Measurement, modeling, and mechanisms. *Environmental Science & Technology* 38(6): 1888-1896.

Nghiem, L. D., A. I. Schafer and M. Elimelech. 2005. Pharmaceutical retention mechanisms by nanofiltration membranes. *Environmental Science & Technology* 39(19): 7698-7705.

Nghiem, L. D., A. I. Schafer and M. Elimelech. 2006. Role of electrostatic interactions in the retention of pharmaceutically active contaminants by a loose nanofiltration membrane. *Journal of Membrane Science* 286(1-2): 52-59.

Nghiem, L. D., D. Vogel and S. Khan. 2008. Characterising humic acid fouling of nanofiltration membranes using bisphenol A as a molecular indicator. *Water Research* 42(15): 4049-4058.

Nguyen, T. H., H.-H. Cho, D. L. Poster and W. P. Ball. 2007. Evidence for a pore-filling mechanism in the adsorption of aromatic hydrocarbons to a natural wood char. *Environmental Science & Technology* 41(4): 1212-1217.

Ormad, M. P., N. Miguel, A. Claver, J. M. Matesanz and J. L. Ovelleiro. 2008. Pesticides removal in the process of drinking water production. *Chemosphere* 71(1): 97-106.

Ozaki, H., K. Sharma and W. Saktaywin. 2002. Performance of an ultra-low-pressure reverse osmosis membrane (ULPROM) for separating heavy metal: effects of interference parameters. *Desalination* 144(1-3): 287-294.

Park, C. M., K. H. Chu, N. Her, M. Jang, M. Baalousha, J. Heo and Y. Yoon. 2017. Occurrence and removal of engineered nanoparticles in drinking water treatment and wastewater treatment processes. *Separation and Purification Reviews* 46: 255-2017.

Park, C. M., J. Han, K. H. Chu, Y. A. Al-Hamadani, N. Her, J. Heo and Y. Yoon. 2017. Influence of solution pH, ionic strength, and humic acid on cadmium adsorption onto activated biochar: experiment and modeling. *Journal of industrial and engineering chemistry* 48: 186-193.

Park, G. Y., J. H. Lee, I. S. Kim and J. Cho. 2004. Pharmaceutical rejection by membranes for wastewater reclamation and reuse. *Water Science and Technology* 50(2): 239-244.

Park, J., I. Hung, Z. Gan, O. J. Rojas, K. H. Lim and S. Park. 2013. Activated carbon from biochar: influence of its physicochemical properties on the sorption characteristics of phenanthrene. *Bioresource Technology* 149: 383-389.

Peng, J., X. Chen, W.-J. Ong, X. Zhao and N. Li. 2019. Surface and heterointerface engineering of 2D MXenes and their nanocomposites: insights into electro-and photocatalysis. *Chem* 5(1): 18-50.

Peng, Q., J. Guo, Q. Zhang, J. Xiang, B. Liu, A. Zhou, R. Liu and Y. Tian. 2014. Unique lead adsorption behavior of activated hydroxyl group in two-dimensional titanium carbide. *Journal of the American Chemical Society* 136(11): 4113-4116.

Perreault, F. o., M. E. Tousley and M. Elimelech. 2013. Thin-film composite polyamide membranes functionalized with biocidal graphene oxide nanosheets. *Environmental Science & Technology Letters* 1(1): 71-76.

Petrie, B., R. Barden and B. Kasprzyk-Hordern. 2015. A review on emerging contaminants in wastewaters and the environment: current knowledge, understudied areas and recommendations for future monitoring. *Water Research* 72: 3-27.

Phenrat, T., J. E. Song, C. M. Cisneros, D. P. Schoenfelder, R. D. Tilton and G. V. Lowry. 2010. Estimating attachment of nano-and submicrometer-particles coated with organic macromolecules in porous media: development of an empirical model. *Environmental Science & Technology* 44(12): 4531-4538.

Plakas, K. V., A. J. Karabelas, T. Wintgens and T. Melin. 2006. A study of selected herbicides retention by nanofiltration membranes - The role of organic fouling. *Journal of Membrane Science* 284(1-2): 291-300.

Qin, J. J., M. H. Oo, M. N. Wai and F. S. Wong. 2003. Effect of feed pH on an integrated membrane process for the reclamation of a combined rinse water from electroless nickel plating. *Journal of Membrane Science* 217(1-2): 261-268.

Qin, J. J., M. N. Wai, M. H. Oo and F. S. Wong. 2002. A feasibility study on the treatment and recycling of a wastewater from metal plating. *Journal of Membrane Science* 208(1-2): 213-221.

Radjenovic, J., M. Petrovic, F. Ventura and D. Barcelo. 2008. Rejection of pharmaceuticals in nanofiltration and reverse osmosis membrane drinking water treatment. *Water Research* 42(14): 3601-3610.

Raghunathan, A. V. and N. R. Aluru. 2006. Molecular understanding of osmosis in semipermeable membranes. *Physical Review Letters* 97(2).

Reemtsma, T., U. Miehe, U. Duennbier and M. Jekel. 2010. Polar pollutants in municipal wastewater and the water cycle: Occurrence and removal of benzotriazoles. *Water Research* 44(2): 596-604.

Rege, S. U. and R. T. Yang. 2000. Corrected Horváth-Kawazoe equations for pore-size distribution. *AIChE journal* 46(4): 734-750.

Ren, X., C. Chen, M. Nagatsu and X. Wang. 2011. Carbon nanotubes as adsorbents in environmental pollution management: A review. *Chemical Engineering Journal* 170(2-3): 395-410.

Rodenas, T., I. Luz, G. Prieto, B. Seoane, H. Miro, A. Corma, F. Kapteijn, F. X. L. i Xamena and J. Gascon. 2015. Metal–organic framework nanosheets in polymer composite materials for gas separation. *Nature materials* 14(1): 48-55.

Rodriguez, E., M. Campinas, J. L. Acero and M. J. Rosa. 2016. Investigating PPCP Removal from Wastewater by Powdered Activated Carbon/Ultrafiltration. *Water Air and Soil Pollution* 227(6).

Ryu, J., J. Oh, S. A. Snyder and Y. Yoon. 2014. Determination of micropollutants in combined sewer overflows and their removal in a wastewater treatment plant (Seoul, South Korea). *Environmental Monitoring and Assessment* 186(5): 3239-3251.

Ryu, J., Y. Yoon and J. Oh. 2011. Occurrence of endocrine disrupting compounds and pharmaceuticals in 11 WWTPs in Seoul, Korea. Ksce Journal of Civil Engineering 15(1): 57-64.

Sahar, E., I. David, Y. Gelman, H. Chikurel, A. Aharoni, R. Messalem and A. Brenner. 2011. The use of RO to remove emerging micropollutants following CAS/UF or MBR treatment of municipal wastewater. *Desalination* 273(1): 142-147.

Santamaria, A., N. Yang, E. Eddings and F. Mondragon. 2010. Chemical and morphological characterization of soot and soot precursors generated in an inverse diffusion flame with aromatic and aliphatic fuels. *Combustion and Flame* 157(1): 33-42.

Sanyal, O., A. N. Sommerfeld and I. Lee. 2015. Design of ultrathin nanostructured polyelectrolyte-based membranes with high perchlorate rejection and high permeability. *Separation and Purification Technology* 145: 113-119.

Sarker, M., S. Shin, J. H. Jeong and S. H. Jhung. 2019. Mesoporous metal-organic framework PCN-222 (Fe): Promising adsorbent for removal of big anionic and cationic dyes from water. *Chemical Engineering Journal* 371: 252-259.

Schafer, A. I., L. D. Nghiem and T. D. Waite. 2003. Removal of the natural hormone estrone from aqueous solutions using nanofiltration and reverse osmosis. *Environmental Science & Technology* 37(1): 182-188.

Schlautman, M. A. and J. J. Morgan. 1993. Effects of aqueous chemistry on the binding of polycyclic aromatic-hydrocarbons by dissolved humic materials. *Environmental Science & Technology* 27(5): 961-969.

Secondes, M. F., V. Naddeo, V. Belgiorno and F. Ballesteros, Jr. 2014. Removal of emerging contaminants by simultaneous application of membrane ultrafiltration, activated carbon adsorption, and ultrasound irradiation. *Journal of Hazardous Materials* 264: 342-349.

Seo, J. S., D. Whang, H. Lee, S. Im Jun, J. Oh, Y. J. Jeon and K. Kim. 2000. A homochiral metal–organic porous material for enantioselective separation and catalysis. *Nature* 404(6781): 982-986.

Shankar, V., J. Heo, Y. A. Al-Hamadani, C. M. Park, K. H. Chu and Y. Yoon. 2017. Evaluation of biochar-ultrafiltration membrane processes for humic acid removal under various hydrodynamic, pH, ionic strength, and pressure conditions. *Journal of Environmental Management* 197: 610-618.

Shao, S., L. Cai, K. Li, J. Li, X. Du, G. Li and H. Liang. 2017. Deposition of powdered activated carbon (PAC) on ultrafiltration (UF) membrane surface: influencing factors and mechanisms. *Journal of Membrane Science* 530: 104-111.

Sheng, C. G., A. G. A. Nnanna, Y. H. Liu and J. D. Vargo. 2016. Removal of Trace Pharmaceuticals from Water using coagulation and powdered activated carbon as pretreatment to ultrafiltration membrane system. *Science of the Total Environment* 550: 1075-1083.

Sichel, C., C. Garcia and K. Andre. 2011. Feasibility studies: UV/chlorine advanced oxidation treatment for the removal of emerging contaminants. *Water Research* 45(19): 6371-6380.

Sima, X.-F., Y.-Y. Wang, X.-C. Shen, X.-R. Jing, L.-J. Tian, H.-Q. Yu and H. Jiang. 2017. Robust biochar-assisted alleviation of membrane fouling in MBRs by indirect mechanism. *Separation and Purification Technology* 184: 195-204.

Snyder, S., J. Leising, P. Westerhoff, Y. Yoon, H. Mash and B. Vanderford. 2004. Biological and physical attenuation of endocrine disruptors and pharmaceuticals: Implications for water reuse. *Ground Water Monitoring & Remediation* 24(2): 108-118.

Snyder, S. A., S. Adham, A. M. Redding, F. S. Cannon, J. DeCarolis, J. Oppenheimer, E. C. Wert and Y. Yoon. 2007. Role of membranes and activated carbon in the removal of endocrine disruptors and pharmaceuticals. *Desalination* 202(1-3): 156-181.

Snyder, S. A., P. Westerhoff, Y. Yoon and D. L. Sedlak. 2003. Pharmaceuticals, personal care products, and endocrine disruptors in water: Implications for the water industry. *Environmental Engineering Science* 20(5): 449-469.

Soriano, A., D. Gorri and A. Urtiaga. 2017. Efficient treatment of perfluorohexanoic acid by nanofiltration followed by electrochemical degradation of the NF concentrate. *Water Research* 112: 147-156.

Sourirajan, S. (1970). Reverse Osmosis. London, Logos Press.

Stackelberg, P. E., J. Gibs, E. T. Furlong, M. T. Meyer, S. D. Zaugg and R. L. Lippincott. 2007. Efficiency of conventional drinking-water-treatment processes in removal of pharmaceuticals and other organic compounds. *Science of the Total Environment* 377(2-3): 255-272.

Steinle-Darling, E., M. Zedda, M. H. Plumlee, H. F. Ridgway and M. Reinhard. 2007. Evaluating the impacts of membrane type, coating, fouling, chemical properties and water chemistry on reverse osmosis rejection of seven nitrosoalklyamines, including NDMA. *Water Research* 41(17): 3959-3967.

Stoquart, C., P. Servais, P. R. Bérubé and B. Barbeau. 2012. Hybrid membrane processes using activated carbon treatment for drinking water: a review. *Journal of Membrane Science* 411: 1-12.

Stoquart, C., P. Servais, P. R. Bérubé and B. Barbeau. 2012. Hybrid Membrane Processes using activated carbon treatment for drinking water: A review. *Journal of Membrane Science* 411-412: 1-12.

Stumm-Zollinger, E. and G. M. Fair. 1965. Biodegradation of steroid hormones. *Journal of the Water Pollution Control Federation* 37: 1506-1510.

Sun, C., B. Xiong, Y. Pan and H. Cui. 2017. Adsorption removal of tannic acid from aqueous solution by polyaniline: Analysis of operating parameters and mechanism. *Journal of Colloid and Interface Science* 487: 175-181.

Sun, J., C. Hu, T. Tong, K. Zhao, J. Qu, H. Liu and M. Elimelech. 2017. Performance and mechanisms of ultrafiltration membrane fouling mitigation by coupling coagulation and applied electric field in a novel electrocoagulation membrane reactor. *Environmental Science & Technology* 51(15): 8544-8551.

Susanto, H. and M. Ulbricht. 2008. High-performance thin-layer hydrogel composite membranes for ultrafiltration of natural organic matter. *Water Research* 42(10-11): 2827-2835.

Sutzkover-Gutman, I., D. Hasson and R. Semiat. 2010. Humic substances fouling in ultrafiltration processes. *Desalination* 261(3): 218-231.

Tabak, H. H. and R. L. Bunch. 1970. Steroid hormones as water pollutants. I. Metabolism of natural and synthetic ovulation-inhibiting hormones by microorganisms of activated sludge and primary settled sewage. *Developments in Industrial Microbiology* 11: 367-376.

Tam, L. S., T. W. Tang, G. N. Lau, K. R. Sharma and G. H. Chen. 2007. A pilot study for wastewater reclamation and reuse with MBR/RO and MF/RO systems. *Desalination* 202(1-3): 106-113.

Tang, C. Y., Y.-N. Kwon and J. O. Leckie. 2007. Characterization of humic acid fouled reverse osmosis and nanofiltration membranes by transmission electron microscopy and streaming potential measurements. *Environmental Science & Technology* 41(3): 942-949.

Tariq, A., S. I. Ali, D. Akinwande and S. Rizwan. 2018. Efficient Visible-Light Photocatalysis of 2D-MXene Nanohybrids with Gd^{3+}-and Sn^{4+}-Codoped Bismuth Ferrite. *ACS Omega* 3(10): 13828-13836.

Ternes, T. A., M. Meisenheimer, D. McDowell, F. Sacher, H. J. Brauch, B. H. Gulde, G. Preuss, U. Wilme and N. Z. Seibert. 2002. Removal of pharmaceuticals during drinking water treatment. *Environmental Science & Technology* 36(17): 3855-3863.

Torres, C. I., S. Ramakrishna, C. A. Chiu, K. G. Nelson, P. Westerhoff and R. Krajmalnik-Brown. 2011. Fate of Sucralose During Wastewater Treatment. *Environmental Engineering Science* 28(5): 325-331.

Trivunac, K. and S. Stevanovic. 2006. Removal of heavy metal ions from water by complexation-assisted ultrafiltration. *Chemosphere* 64(3): 486-491.

USEPA (2000). Environmental Protection Agency - Endocrine Disruptor Screening Program. Report to Congress, USEPA, Washington, DC.

USEPA (2016). Contaminant Candidate List (CCL) and Regulatory Determination - CCL4. https://www.epa.gov/ccl/contaminant-candidate-list-4-ccl-4-0.

USFDA (1998). Guidance for Industry Environmental Assessment of Human Durg and Biologics Applications. Food and Drug Administration Report, USA.

Van der Bruggen, B., J. Schaep, W. Maes, D. Wilms and C. Vandecasteele. 1998. Nanofiltration as a treatment method for the removal of pesticides from ground waters. *Desalination* 117(1-3): 139-147.

Van der Bruggen, B., J. Schaep, D. Wilms and C. Vandecasteele. 1999. Influence of molecular size, polarity and charge on the retention of organic molecules by nanofiltration. J*ournal of Membrane Science* 156(1): 29-41.

Verliefde, A. R. D., S. G. Heijman, E. R. Cornelissen, G. Amy, B. Van der Bruggen and J. C. van Dijk. 2007. Influence of electrostatic interactions on the rejection with NF and assessment of the removal efficiency during NF/GAC treatment of pharmaceutically active compounds in surface water. *Water Research* 41(15): 3227-3240.

Visvanathan, C., B. D. Marsono and B. Basu. 1998. Removal of THMP by nanofiltration: effects of interference parameters. *Water research* 32(12): 3527-3538.

Vogel, D., A. Simon, A. A. Alturki, B. Bilitewski, W. E. Price and L. D. Nghiem. 2010. Effects of fouling and scaling on the retention of trace organic contaminants by a nanofiltration membrane: The role of cake-enhanced concentration polarisation. *Separation and Purification Technology* 73(2): 256-263.

Vu, T. A., G. H. Le, C. D. Dao, L. Q. Dang, K. T. Nguyen, P. T. Dang, H. T. Tran, Q. T. Duong, T. V. Nguyen and G. D. Lee. 2014. Isomorphous substitution of Cr by Fe

in MIL-101 framework and its application as a novel heterogeneous photo-Fenton catalyst for reactive dye degradation. *Rsc Advances* 4(78): 41185-41194.

Wang, H., X. Yuan, Y. Wu, G. Zeng, X. Chen, L. Leng and H. Li. 2015. Synthesis and applications of novel graphitic carbon nitride/metal-organic frameworks mesoporous photocatalyst for dyes removal. *Applied Catalysis B: Environmental* 174: 445-454.

Wang, J. and S. Wang. 2018. Activation of persulfate (PS) and peroxymonosulfate (PMS) and application for the degradation of emerging contaminants. *Chemical Engineering Journal* 334: 1502-1517.

Wang, L., H. Song, L. Yuan, Z. Li, P. Zhang, J. K. Gibson, L. Zheng, H. Wang, Z. Chai and W. Shi. 2019. Effective Removal of Anionic Re (VII) by Surface-Modified Ti2CT x MXene Nanocomposites: Implications for Tc (VII) Sequestration. *Environmental Science & Technology* 53(7): 3739-3747.

Wang, P., H. Zhao, H. Sun, H. Yu and X. Quan. 2014. Porous metal–organic framework MIL-100 (Fe) as an efficient catalyst for the selective catalytic reduction of NO x with NH 3. *Rsc Advances* 4(90): 48912-48919.

Wei, Z., Z. Peigen, T. Wubian, Q. Xia, Z. Yamei and S. ZhengMing. 2018. Alkali treated Ti3C2Tx MXenes and their dye adsorption performance. *Materials Chemistry and Physics* 206: 270-276.

Westerhoff, P., Y. Yoon, S. Snyder and E. Wert. 2005. Fate of endocrine-disruptor, pharmaceutical, and personal care product chemicals during simulated drinking

water treatment processes. *Environmental Science & Technology* 39(17): 6649-6663.

Wray, H. E., R. C. Andrews and P. R. Berube. 2014. Surface shear stress and retention of emerging contaminants during ultrafiltration for drinking water treatment. *Separation and Purification Technology* 122: 183-191.

Wu, C. X., A. L. Spongberg, J. D. Witter, M. Fang, K. P. Czajkowski and A. Ames. 2010. Dissipation and Leaching Potential of Selected Pharmaceutically Active Compounds in Soils Amended with Biosolids. *Archives of Environmental Contamination and Toxicology* 59(3): 343-351.

Wu, M. X. and Y. W. Yang. 2017. Metal–organic framework (MOF)-based drug/cargo delivery and cancer therapy. *Advanced Materials* 29(23): 1606134.

Xia, W., A. Mahmood, R. Zou and Q. Xu. 2015. Metal–organic frameworks and their derived nanostructures for electrochemical energy storage and conversion. *Energy & Environmental Science* 8(7): 1837-1866.

Xie, M., L. D. Nghiem, W. E. Price and M. Elimelech. 2012. Comparison of the removal of hydrophobic trace organic contaminants by forward osmosis and reverse osmosis. *Water Research* 46(8): 2683-2692.

Xie, M., L. D. Nghiem, W. E. Price and M. Elimelech. 2013. Impact of humic acid fouling on membrane performance and transport of pharmaceutically active compounds in forward osmosis. *Water Research* 47(13): 4567-4575.

Xie, M., L. D. Nghiem, W. E. Price and M. Elimelech. 2014. Relating rejection of trace organic contaminants to membrane properties in forward osmosis: Measurements, modelling and implications. *Water Research* 49: 265-274.

Xie, Y. H., S. Y. Li, K. Wu, J. Wang and G. L. Liu. 2011. A hybrid adsorption/ultrafiltration process for perchlorate removal. *Journal of Membrane Science* 366(1-2): 237-244.

Xu, G.-R., J.-N. Wang and C.-J. Li. 2013. Strategies for improving the performance of the polyamide thin film composite (PA-TFC) reverse osmosis (RO) membranes: Surface modifications and nanoparticles incorporations. *Desalination* 328: 83-100.

Xu, Y., L. Xu, S. Qi, Y. Dong, Z. u. Rahman, H. Chen and X. Chen. 2013. In situ synthesis of MIL-100 (Fe) in the capillary column for capillary electrochromatographic separation of small organic molecules. *Analytical Chemistry* 85(23): 11369-11375.

Yangali-Quintanilla, V., A. Sadmani, M. McConville, M. Kennedy and G. Amy. 2009. Rejection of pharmaceutically active compounds and endocrine disrupting compounds by clean and fouled nanofiltration membranes. *Water Research* 43(9): 2349-2362.

Yao, Y., B. Gao, H. Chen, L. Jiang, M. Inyang, A. R. Zimmerman, X. Cao, L. Yang, Y. Xue and H. Li. 2012. Adsorption of sulfamethoxazole on biochar and its impact on reclaimed water irrigation. *Journal of Hazardous Materials* 209: 408-413.

Yin, Z., T. Wen, Y. Li, A. Li and C. Long. 2019. Pre-ozonation for the mitigation of reverse osmosis (RO) membrane fouling by biopolymer: The roles of Ca^{2+} and Mg^{2+}. *Water research*: 115437.

Ying, Y., Y. Liu, X. Wang, Y. Mao, W. Cao, P. Hu and X. Peng. 2015. Two-dimensional titanium carbide for efficiently reductive removal of highly toxic chromium (VI) from water. *ACS Applied Materials & Interfaces* 7(3): 1795-1803.

Yoo, D. K., T.-U. Yoon, Y.-S. Bae and S. H. Jhung. 2020. Metal-organic framework MIL-101 loaded with polymethacrylamide with or without further reduction: effective and selective CO2 adsorption with amino or amide functionality. *Chemical Engineering Journal* 380: 122496.

Yoon, J., G. Amy, J. Chung, J. Sohn and Y. Yoon. 2009. Removal of toxic ions (chromate, arsenate, and perchlorate) using reverse osmosis, nanofiltration, and ultrafiltration membranes. *Chemosphere* 77(2): 228-235.

Yoon, J., Y. Yoon, G. Amy, J. Cho, D. Foss and T. H. Kim. 2003. Use of surfactant modified ultrafiltration for perchlorate (ClO4-) removal. *Water Research* 37(9): 2001-2012.

Yoon, Y. and R. Lueptow. 2005. Removal of organic contaminants by RO and NF membranes. *Journal of Membrane Science* 261(1-2): 76-86.

Yoon, Y. and R. M. Lueptow. 2005. Removal of organic contaminants by RO and NF membranes. *Journal of Membrane Science* 261(1-2): 76-86.

Yoon, Y., J. Ryu, J. Oh, B. G. Choi and S. A. Snyder. 2010. Occurrence of endocrine disrupting compounds, pharmaceuticals, and personal care products in the Han River (Seoul, South Korea). *Science of the Total Environment* 408(3): 636-643.

Yoon, Y., P. Westerhoff, S. A. Snyder and M. Esparza. 2003. HPLC-fluorescence detection and adsorption of bisphenol A, 17β-estradiol, and 17α-ethynyl estradiol on powdered activated carbon. *Water Research* 37(14): 3530-3537.

Yoon, Y., P. Westerhoff, S. A. Snyder and M. Esparza. 2003. HPLC-fluorescence detection and adsorption of bisphenol A, 17β-estradiol, and 17α-ethynyl estradiol on powdered activated carbon. *Water Research* 37(14): 3530-3537.

Yoon, Y., P. Westerhoff, S. A. Snyder and E. C. Wert. 2006. Nanofiltration and ultrafiltration of endocrine disrupting compounds, pharmaceuticals and personal care products. *Journal of Membrane Science* 270(1-2): 88-100.

Yoon, Y., P. Westerhoff, S. A. Snyder, E. C. Wert and J. Yoon. 2007. Removal of endocrine disrupting compounds and pharmaceuticals by nanofiltration and ultrafiltration membranes. *Desalination* 202(1-3): 16-23.

Yoon, Y., P. Westerhoff, J. Yoon and S. A. Snyder. 2004. Removal of 17 beta estradiol and fluoranthene by nanofiltration and ultrafiltration. *Journal of Environmental Engineering-ASCE* 130(12): 1460-1467.

Yoon, Y., P. Westerhoff, J. Yoon and S. A. Snyder. 2004. Removal of 17b-estradiol and fluoranthene by nanofiltration and ultrafiltration. *Journal of Environmental Engineering-ASCE* 130(12): 1460-1467.

You, S. J., J. D. Lu, C. Y. Tang and X. H. Wang. 2017. Rejection of heavy metals in acidic wastewater by a novel thin-film inorganic forward osmosis membrane. *Chemical Engineering Journal* 320: 532-538.

Yu, S., X. Wang, H. Pang, R. Zhang, W. Song, D. Fu, T. Hayat and X. Wang. 2018. Boron nitride-based materials for the removal of pollutants from aqueous solutions: a review. *Chemical Engineering Journal* 333: 343-360.

Yu, W., L. Xu, J. Qu and N. Graham. 2014. Investigation of pre-coagulation and powder activate carbon adsorption on ultrafiltration membrane fouling. *Journal of Membrane Science* 459: 157-168.

Yuan, S. H. and X. H. Lu. 2005. Comparison treatment of various chlorophenols by electro-Fenton method: relationship between chlorine content and degradation. *Journal of Hazardous Materials* 118(1-3): 85-92.

Zazouli, M. A., H. Susanto, S. Nasseri and M. Ulbricht. 2009. Influences of solution chemistry and polymeric natural organic matter on the removal of aquatic pharmaceutical residuals by nanofiltration. *Water Research* 43(13): 3270-3280.

Zhang, F., X. Sang, X. Tan, C. Liu, J. Zhang, T. Luo, L. Liu, B. Han, G. Yang and B. P. Binks. 2017. Converting Metal–Organic Framework Particles from Hydrophilic to Hydrophobic by an Interfacial Assembling Route. *Langmuir* 33(43): 12427-12433.

Zhang, F., J. Shi, Y. Jin, Y. Fu, Y. Zhong and W. Zhu. 2015. Facile synthesis of MIL-100 (Fe) under HF-free conditions and its application in the acetalization of aldehydes with diols. *Chemical Engineering Journal* 259: 183-190.

Zhang, N., S. Chen, B. Yang, J. Huo, X. Zhang, J. Bao, X. Ruan and G. He. 2018. Effect of hydrogen-bonding interaction on the arrangement and dynamics of water confined in a polyamide membrane: A molecular dynamics simulation. *The Journal of Physical Chemistry B* 122(17): 4719-4728.

Zhang, Z. F., N. Q. Ren, Y. F. Li, T. Kunisue, D. W. Gao and K. Kannan. 2011. Determination of Benzotriazole and Benzophenone UV Filters in Sediment and Sewage Sludge. *Environmental Science & Technolog*y 45(9): 3909-3916.

Zhao, P., B. Y. Gao, Q. Y. Yue, S. C. Liu and H. K. Shon. 2016. The performance of forward osmosis in treating high-salinity wastewater containing heavy metal Ni^{2+}. *Chemical Engineering Journal* 288: 569-576.

Zheng, H., Y. Zhang, L. Liu, W. Wan, P. Guo, A. M. Nyström and X. Zou. 2016. One-pot synthesis of metal–organic frameworks with encapsulated target molecules and their applications for controlled drug delivery. *Journal of the American chemical society* 138(3): 962-968.

Zhu, B.-J., X.-Y. Yu, Y. Jia, F.-M. Peng, B. Sun, M.-Y. Zhang, T. Luo, J.-H. Liu and X.-J. Huang. 2012. Iron and 1, 3, 5-benzenetricarboxylic metal–organic coordination polymers prepared by solvothermal method and their application in efficient As (V) removal from aqueous solutions. *The Journal of Physical Chemistry C* 116(15): 8601-8607.

Zularisam, A., A. Ismail and R. Salim. 2006. Behaviours of natural organic matter in membrane filtration for surface water treatment—a review. *Desalination* 194(1-3): 211-231

APPENDIX A

PRINTABLE AUTHORSHIP LICENSE

12/16/2020 Rightslink® by Copyright Clearance Center

Copyright Clearance Center RightsLink®

Home | Help | Email Support | sewoon kim

Removal of contaminants of emerging concern by membranes in water and wastewater: A review

Author:
Sewoon Kim,Kyoung Hoon Chu,Yasir A.J. Al-Hamadani,Chang Min Park,Min Jang,Do-Hyung Kim,Miao Yu,Jiyong Heo,Yeomin Yoon

Publication: Chemical Engineering Journal

Publisher: Elsevier

Date: 1 March 2018

© 2017 Elsevier B.V. All rights reserved.

Please note that, as the author of this Elsevier article, you retain the right to include it in a thesis or dissertation, provided it is not published commercially. Permission is not required, but please ensure that you reference the journal as the original source. For more information on this and on your other retained rights, please visit: https://www.elsevier.com/about/our-business/policies/copyright#Author-rights

BACK CLOSE WINDOW

© 2020 Copyright - All Rights Reserved | Copyright Clearance Center, Inc. | Privacy statement | Terms and Conditions
Comments? We would like to hear from you. E-mail us at customercare@copyright.com

Removal of selected pharmaceuticals in an ultrafiltration-activated biochar hybrid system

Author:
Sewoon Kim,Chang Min Park,Am Jang,Min Jang,Arturo J. Hernández-Maldonado,Miao Yu,Jiyong Heo,Yeomin Yoon

Publication: Journal of Membrane Science

Publisher: Elsevier

Date: 15 January 2019

A metal organic framework-ultrafiltration hybrid system for removing selected pharmaceuticals and natural organic matter

Author:
Sewoon Kim,Juan C. Muñoz-Senmache,Byung-Moon Jun,Chang Min Park,Am Jang,Miao Yu,Arturo J. Hernández-Maldonado,Yeomin Yoon

Publication: Chemical Engineering Journal

Publisher: Elsevier

Date: 15 February 2020

ACS Publications
Most Trusted. Most Cited. Most Read.

Fouling and Retention Mechanisms of Selected Cationic and Anionic Dyes in a Ti3C2Tx MXene-Ultrafiltration Hybrid System

Author: Sewoon Kim, Miao Yu, Yeomin Yoon
Publication: Applied Materials
Publisher: American Chemical Society
Date: Apr 1, 2020

PERMISSION/LICENSE IS GRANTED FOR YOUR ORDER AT NO CHARGE

This type of permission/license, instead of the standard Terms & Conditions, is sent to you because no fee is being charged for your order. Please note the following:

- Permission is granted for your request in both print and electronic formats, and translations.
- If figures and/or tables were requested, they may be adapted or used in part.
- Please print this page for your records and send a copy of it to your publisher/graduate school.
- Appropriate credit for the requested material should be given as follows: "Reprinted (adapted) with permission from (COMPLETE REFERENCE CITATION). Copyright (YEAR) American Chemical Society." Insert appropriate information in place of the capitalized words.
- One-time permission is granted only for the use specified in your request. No additional uses are granted (such as derivative works or other editions). For any other uses, please submit a new request.

BACK CLOSE WINDOW